Reply to comments from Referees and Readers

We would like to thank the editor, two anonymous referees and Jörg Kleffmann for their comments and suggestions to help improve our manuscript. Below we give a point-to-point response to address the referees' and Jörg Kleffmann's comments. The original comments are in blue italics and our responses are in black. The corrections are marked as red color in the attached revised manuscript.

1. Response to interactive comments on "High resolution vertical distribution and sources of HONO and NO_2 in the nocturnal boundary layer in urban Beijing, China" by Anonymous Referee #1

This work by Meng et al. presents some of the first vertical profiles of HONO from China, from a tall tower located in urban Beijing. Using two IBBCEAS instruments, the Authors assess nocturnal HONO production and loss from a limited dataset of 3 case study days of HONO and NO_2 observations via established approaches or other measurements for this region. Overall, this manuscript brings very little new information to bear on understanding HONO nocturnal formation in Beijing between clean and haze periods. Much of the analysis is replicated from the literature, but without using those approaches properly to place quantitative constraints on the observations. The presented dataset is frankly too limited to draw very broad conclusions, mainly because the supporting measurements presented in the methods are not being used to clearly account for direct HONO emissions or aerosol surface area, nor for ground surface production. The interpretation of this dataset needs to be pushed further with all available measurements in order to be accepted into Atmospheric Chemistry and Physics.

One potentially productive avenue for this work would be to investigate the contribution of vertical transport of HONO produced at the surface into the nocturnal boundary layer, versus that calculated for aerosol formation. The meteorological data collected over the height of the tower is sufficient to carry out this analysis and would bring the necessary new dimension to this work. It is likely that this work can also close the mass balance of nocturnal HONO production for Beijing, but much more work is required. When combined with a thorough re-analysis of the dataset to satisfy the four major comments below, this work should be reviewed again to determine if it is suitable for acceptance.

Response: We thank the Anonymous Referee #1 for pointing out the shortcomings in our analysis and presentation of the measurement data. We have significantly revised the manuscript to address the referee's comments and concerns. Below we give point-to-point response to address the referee's specific comments.

Major Comments:

1. Direct emissions: There are at least two direct emissions analyses for HONO from the Beijing vehicle fleet that have been previously published, which are cited in this work (Zhang et al 2018 and Tong et al 2016), but not used to build a deeper analysis of the observations. The Authors cite one of these and conclude that the majority of their observed nocturnal HONO comes from direct emissions. However, the Authors state they have the necessary measurements from this campaign to thoroughly quantify the HONO primary emissions (HONO, NO_2, NO, and CO), but they do not use them. This analysis must be completed in full, with a figure added to this manuscript (or the SI) to show how the value stated was determined along with an assessment of its error. A thorough review and comparison to the literature for this emission ratio must also be made. It will also be valuable if the Authors can comment on the traffic patterns in Beijing that result in so much nocturnal HONO coming from direct emissions, as typically these are reported to peak during morning and evening rush hours. Finally, it is not clear if the Authors have accounted for and removed direct HONO emissions from their aerosol conversion analyses, which should be done, as it may otherwise.

Response: As the referee suggested, we have analyzed the correlations of HONO with CO, NO, and BC, which are considered to be the primary pollutants emitted from combustion processes like vehicle emissions (Sun et al., 2014; Zhang et al., 2018). Good correlations of HONO with CO (R^2=0.85), NO (R^2=0.76), and BC (R^2=0.84) at ground level were observed (Figure S5). This indicated the potential impact of direct emissions on the ambient HONO concentrations at night. Following the suggestion by Jörg Kleffmann, we have re-estimated the emission factor based on the field data. Five criteria were applied to ensure as much of freshly emitted air masses as possible: (a) only nighttime data (from 18:00 LT to next 6:00 LT) were included to avoid the fast photolysis of HONO; (b) only sharp peaks during nighttime and the elevations of HONO and NO_x over the background levels were estimated; (c) $\Delta NO/\Delta NO_x > 0.80$; (d) good correlation between HONO and NO_x; (e) short duration of the plume (< 30 min). The typical nocturnal wind speed at measurement site was 1.2 m s^{-1} and the

distance to the roads was less than 1 km. So the duration of fresh air masses should have been less 30 min during transport processes. Criteria (b) and (c) were used as indicators for identifying fresh vehicular emissions. Criteria (d) and (e) further confirmed that the increase in HONO was primarily caused by direct emissions instead of heterogeneous reactions of NO_2.

Two examples of emission plumes based on the preceding selection criteria were showed in Figure 6 in the manuscript. The slopes of HONO to NO_x can be considered as the emission ratios (Rappenglück et al., 2013). For a month field observations, 11 fresh emission plumes satisfied criteria (Table 1). The derived emission factors ranged between 0.78% and 1.73%, with an average value of 1.28% ± 0.36%, which was larger than the 0.53%–0.8% measured in the tunnel in Wuppertal (Kurtenbach et al., 2001) but within the range of previously published results (0.19%–2.1%) (Kirchstetter et al., 1996; Kurtenbach et al., 2001; Su et al., 2008; Rappengluck et al., 2013; Yang et al., 2014; Xu et al., 2015; Liang et al., 2017; Zhang et al., 2018; Li et al., 2018). The minimum ratio of 0.78% approximated the value (0.8%) measured in Wuppertal. The maximum ratio of 1.73% in our study was comparable to the value of 1.7% in Houston, Texas by Rappenglück et al. (2013). Comparisons of the derived HONO/NO_x ratios with the previously reported results are summarized in Table S2 in the supplementary information, as the referee suggested.

The minimum HONO/NO_x ratio of 0.78% was used to minimize the risk of overestimating direct emissions (Su et al., 2008). In this case the risk of overestimating vehicular emissions was minimized, but still could be the potential secondary HONO formation during the transport from emission to the measurement site. The direct emissions contributed an average of 29.3% ± 12.4% to the ambient HONO levels at night, with an average $HONO_{emis}$/HONO value of 35.9% ± 11.8% during the clean episode and an average $HONO_{emis}$/HONO value of 26% ± 11.3% during the haze episode. The lower vehicular emission contributions during haze episode could be caused by an odd-even car ban.

As pointed out by the referee, we have already considered the influence of direct emissions in the aerosol conversion analysis, which has been stated in detailed in section 3.4.2. The discussion in "3.3 Direct emissions" have been significantly revised to address the referee's comments and concerns.

2. Aerosol conversion of NO_2 to HONO: A simple calculation is made to conclude that aerosol surface conversion of NO_2 is not important to the observed HONO in the vertical profiles. The Authors use a single value of aerosol surface area from Beijing to perform this calculation, ignoring that they have

a direct proxy for aerosol surface area from their particulate matter measurements (i.e. total $PM_{1.0}$ mass). While this will also have uncertainty associated with it, the magnitude of potential error will be dramatically reduced. The current analysis is shallow and must be improved. One is left wondering why the aerosol measurements are given in the methods and not used in the data interpretation. The contribution of aerosol surface to HONO nocturnal production as a function of height has been reported infrequently and would be an improved contribution from this dataset. This should, again, include error analysis that spans the range of NO_2 uptake coefficients, not only the highest value reported from the literature. The Authors are encouraged to use the chemical speciation of their aerosol to justify a selected NO_2 uptake coefficient that is likely to be representative of conversion in Beijing and to propagate error based on the full range of quantified uptake coefficients towards a mass balance for HONO nocturnal production.

Further to this, the Authors make a series of confusing statements in their discussion of the importance of NO_2 conversion on aerosols from their calculations. The Authors state that 1.02 ppb of HONO are produced during E3 and that is 'much less' than the measured 3.06 ppb. This is 33 %, which is certainly significant and counter to the conclusion that aerosol conversion is not important. Also here, if direct emissions are not accounted for, then this fraction becomes 1.02/1.53 which is 67 %. These findings need to be clarified as perhaps the time intervals have not been specified, which is leading to the confusion. The same analysis needs to explored and discussed for the other two vertical profiling periods using the measured vertical profile data instead of broad approximations of the necessary species.

Finally, the Authors reproduce the analysis of VandenBoer (2013) to conclude that the data presented in Figure 11 clearly indicates the ground surface is the major HONO source, without quantifying its contribution with their measurements. Based on the presented vertical profiles in the manuscript and the SI, there is only one very clear observation of a vertical gradient that is clearly consistent with ground production (C2, Figure 7). In particular, the analysis of potential temperature to identify the nocturnal boundary layer height in Figure 8 does not show increasing HONO mixing ratios as the surface is approached, but instead there are uniform vertical profiles in the NBL and the residual layer, which indicates either efficient mixing or significant production in the overlying air (i.e. aerosol conversion). The increasing HONO mixing ratios in the residual layer matching those in the NBL over time strongly support aerosol conversion, since this air is disconnected from surface mixing if the

inversion has been properly identified using the Brown et al (2012) approach. This is treated superficially in the analysis and needs to be explored in detail.

Response: We made a deeper analysis in aerosol conversion of NO_2 to HONO, as the referee suggested. The newly obtained aerosol surface areas at ground and at 260 m, which was corrected to ambient aerosol surface area (S_{aw}) for particle hygroscopicity via a growth factor (Liu et al., 2013; Wang et al., 2018), were used to estimate the nocturnal HONO production from heterogeneous reaction of NO_2 on aerosol surface. The time series of S_{aw} at ground level and at 260 m is shown in Figure. S2 in the supplementary information. The surface area information for particles larger than 0.5 μm were not valid at ground level and at 260 m during the measurement periods. Hence, this is a lower limit estimate of the total surface area for the heterogeneous reaction. The vertical profiles of HONO and NO_2, and the aerosol surface area measured at 260 m allowed us to estimate the nocturnal HONO production by heterogeneous uptake of NO_2 on aerosol surface.

As the referee pointed out, the influence of direct HONO emissions have been considered in the aerosol conversion analysis. The CO and BC measured at ground level were independent of the CO and BC observed at 260 m during the haze period (Fig. S10), since it can be expected that air masses in the residual layer were decoupled from the ground-level processes and largely free of NO_2 emissions (Brown et al., 2012; VandenBoer et al., 2013). An estimate of the nocturnal HONO production on aerosol surface was made using the RH corrected aerosol surface area (S_{aw}) and NO_2 observations from the residual layer during E3. The yield of hydrolysis reaction assumes that HONO and HNO_3 are formed by equimolar disproportionation of two NO_2 molecules and immediately release HONO (Finlayson-Pitts et al., 2003; Finlayson-Pitts, 2009). The reactive uptake of NO_2 by the aerosols was assumed to occur on all measured aerosol surface area, regardless of chemical composition. An NO_2 uptake coefficients in the dark of 1×10^{-5} to 1×10^{-6} from the literature, an average S_{aw} of 2314 μm^2 cm^{-3} observed in the residual layer between 22 and 01 h (the vertical measurement periods on December 11th), and the upper limit of the observed NO_2 of 54 ppb from the residual layer were used during E3. The HONO production of 30-300 ppt in an interval of 1.5 h could account for HONO increases of 15-368 ppt between profile measurements. Thus, the production of HONO solely on aerosol surface explained HONO observations during E3. In addition, the data presented in Figure 10 (the original Figure 11) were divided into the clean episode and the haze episodes for re-analysis. The column average concentration of HONO was independent of the HONO

mixing ratio observed from the ground level to 10 m in height (R^2 = 0.27) during E3 (Figure 10a), suggesting that the aerosols presumably dominates the production of HONO aloft by heterogeneous conversion of NO_2 during the haze episode.

The same analysis for HONO production on aerosol surface were also made to the other vertical measurements during C2, as the referee suggested. A high correlations (R^2 = 0.83) between the measured CO and BC at ground level and the CO and BC at 260 m were observed (Figure. S10), which indicated that vehicle emissions affected air masses in the residual layer. The lack of NO vertical profile cannot directly correct the contribution of direct HONO emissions. So we assumed that the contribution of direct emissions was consistent at ground level and in the residual layer, and the relative importance of aerosol and ground surfaces in nocturnal HONO production could be roughly estimated. The average $HONO_{emis}$/HONO ratio of 35.9% ± 11.8% during the clean episode was used as the contribution of direct emissions to ambient HONO levels during C2. This is a higher limit estimate of the contribution of direct emissions to the HONO levels in the residual layer. The average S_{aw} of 791 and 894 $\mu m^2\ cm^{-3}$ from 17 to 24 h (the vertical measurement periods on December 9th and 10th), and the upper limit of NO_2 observations of 36 and 44 ppb from the residual layer were used to estimate HONO production on aerosols on December 9th and 10th. The HONO production of 26–259 ppt in an interval of 5.5 h was lower than the direct emissions corrected HONO increases of 305–608 ppt between the vertical profile measurements on December 9th. The formation of HONO solely on aerosol surface cannot explain the observed HONO increases in the residual layer. The HONO observed in the residual layer was primarily derived from heterogeneous conversion of NO_2 on the ground surface followed by vertical transport throughout the column. The column average concentration of HONO was related to the amounts of HONO observed between the ground level and 10 m (Figure 10b, R^2 = 0.93), which also suggested that the surface source of HONO affected HONO observed throughout the depth of boundary layer. However, the HONO production on aerosols in an interval of 5.35 h is 33–332 ppt on December 10th, which was comparable to the direct emissions corrected HONO increases of 114–369 ppt between the two vertical profile measurements. This could have been due to the formed shallow inversion layer near the surface (Figure 4), which inhibited the vertical transport of nighttime HONO at ground level. Besides the contribution of direct HONO emissions could be even more overestimated, which might also affect the estimated result. All of these may result in the aerosols dominated the heterogeneous production of HONO from NO_2 in the

residual layer on December 10th.

As the referee suggested, we have significantly modified the discussion in this section to make our statements more clearly. The representative uptake coefficient of NO_2 in Beijing derived from the chemical speciation of the aerosol will be further studied in other manuscript. In this study, we primarily focused on estimating the relative importance of aerosol and ground surface in nocturnal HONO production at different pollution levels.

3. Nocturnal surface processes: The Authors evaluate the conversion efficiency of NO_2 on the ground surface by replicating the approaches used in Zhang et al (2018) and Tong et al (2016), to find values of C-HONO that are comparable to other observations in urban environments. While this is a sound approach to interpret NO_2 conversion to HONO, a quantification of the importance of the mechanism is not made. How much of the total column HONO is produced by this mechanism? The Authors have made the measurements, integrated the column HONO quantities, but not performed this analysis. Further to this, the Authors state that they calculated the amount of HONO being deposited on the surface, but do not present any of the values or a sensitivity analysis on the range of deposition velocities reported in the literature. It is concerning that a boundary layer mixing depth of 100 m was used when the mixed layer at the surface was directly measured. This section requires significant revision and expanded analysis to have sufficient quality to be accepted.

Response: Thanks for the comment and suggestion. Following Jörg Kleffmann's suggestion, the slope determined by linear regression will statistically better describe the efficient first order conversion rate constant of NO_2 to HONO. Thus, we re-estimated the conversion frequency and corresponded HONO production rate by NO_2 (P_{NO_2}). Direct HONO emissions have been considered and removed in evaluating the conversion frequency. The conversion frequency during vertical measurements (December 9th, 10th, and 11th) were 0.0082, 0.0060 and 0.0114 h^{-1}, respectively, corresponding to a HONO production rate by NO_2 of 0.25 ± 0.03, 0.28 ± 0.02, and 0.60 ± 0.02 ppb h^{-1}. It is necessary to elaborate that the derived P_{NO_2} is net HONO production, which means sources and sinks of HONO (aerosol and ground surface source, deposition, etc.) have already been taken into account in P_{NO_2}. As the referee suggested, the net contribution of surface production of HONO to the column could be roughly estimated based on the assumption that HONO production on aerosols was insignificant compared to the ground surface during the clean episode, which has been suggested in

other studies of HONO vertical gradient (VandenBoer et al., 2013; Wong et al., 2011; Zhang et al., 2009). The surface production rate of HONO was estimated to be 0.25 ± 0.03 and 0.28 ± 0.02 ppb h^{-1} on December 9th and 10th, respectively, which was an order of magnitude higher than the maximum production rate of HONO on aerosols (0.047 and 0.062 ppb h^{-1}). The agreement supported that ground surface dominated HONO production by heterogeneous conversion of NO_2 during the clean episode. In contrast, the production of HONO on aerosols as an important nighttime HONO source cannot be ignored during the haze episode, as discussed in section 3.4.2. To estimate the contribution of the surface HONO production, a deposition velocity of NO_2 to the surface in the dark, V_{dep,NO_2} of 0.07 cm s^{-1} (VandenBoer et al., 2013), in a measured boundary layer of height, h of 140 m, were used to estimate the HONO production rate ($P_{HONO,ground}$) by heterogeneous conversion of NO_2 on ground surfaces ($P_{HONO,ground} = \frac{1}{2}\frac{V_{dep,NO_2}}{h}\overline{[NO_2]}$). The $P_{HONO,ground}$ of 0.47 ± 0.02 ppb h^{-1} on December 11th (E3) was comparable to the HONO production rate on aerosol surface of 0.2 ppb h^{-1}. This result also suggested that the production of HONO on aerosols is an important nocturnal HONO source during the haze episode.

The calculation and sensitivity analysis of deposition velocity of HONO have been stated in the revised manuscript, as the referee suggested. The temperature-dependent deposition velocity of HONO ($V(HONO)_T = \exp(23920/T - 91.5)$) (Laufs et al., 2017) was used to estimate the deposition velocity of HONO ($V_{dep,HONO}$). The average $V_{dep,HONO}$ calculated from nocturnal measurements (00:00–06:00 LT) was 1.8 cm s^{-1}, with a range of values spanning 0.9 to 3 cm s^{-1}, which was within the range of previously reported values between 0.077 and 3 cm s^{-1} (Harrison and Kitto, 1994; Harrison et al., 1996; Spindler et al., 1998; Stutz et al., 2002; Coe and Gallagher, 1992; Laufs et al., 2017). A mesured boundary layer mixing height of 140 m was also used for analysis as suggested. Following the referree's suggestion, we also made a budget analysis of nighttime HONO, which was utilized to estimate nocturnal sources/sinks of HONO. The average dry deposition rate (L_{dep}) of HONO was estimated to be 0.74 ± 0.31 and 1.55 ± 0.32 ppb h^{-1} during C2 and E3, respectively, implying that significant amounts of HONO were deposited to the ground surface at night. The budget analysis results also suggested that the production rate of HONO on aerosols (0.19 ± 0.01 ppb h^{-1}) was comparable to the surface production rate (0.47 ± 0.03 ppb h^{-1}) during the haze episode.

We have significantly revised the discussion in the manuscript in "3.3 Direct emissions", "3.4.2 Relative importance of aerosol and ground surfaces in nocturnal HONO production" and "3.4.3 Nocturnal HONO production and loss at ground level" to address referee's concerns and to make our argument more clearly.

4. Figures: All measured and calculated quantities should be presented with the relevant error bars.

Figure 2 regression types are not specified in the caption or in the manuscript. The error in the measurements should be depicted on the panels and the appropriate regression for considering significant error in both measurements used (e.g. orthogonal least-distance regression). The uncertainty in the slopes and intercept should then also be reported.

The purpose of Figure 4 is very unclear. Either expand discussion around it in terms of its importance to nocturnal HONO production or remove it from the manuscript.

Figures 5 and 6 do not seem to have much purpose for this work. Figure 5 can be removed entirely as its contents are described clearly with the first and third sentences from Lines 237-240. Figure 6 could be removed entirely or one panel from parts a) and b) moved to the SI as an example since it, again, shows that the atmosphere is well mixed at sunset, which is expected and does not contribute significantly to the analysis of nocturnal sources.

The Figure 7 vertical profiles do not demonstrate that steady state between HONO production and loss has been reached, as the concentration of HONO at the surface has continued to increase. Typically, this observation has been seen after midnight (e.g. see VandenBoer et al (2013)). It does not mean that HONO deposition is not happening, but it does prevent quantifying the deposition term using the observations, which the Authors should be clear about.

Response: Thanks for the comment and suggestion. The relevant error bars have been presented in the revised manuscript as suggested. We have significantly modified Figure 2 and added the regression type to the caption. The orthogonal linear squares regression was utilized to estimate the error of both measurements. The uncertainty of slope and intercept were also added in Figure 2. As the referee pointed out, the measurement uncertainty of IBBCEAS instrument have already been depicted in section 2.2 (line 249–253) of the manuscript. Thus, we did not add the statements of measurement uncertainty of IBBCEAS instrument here.

The purpose of Figure 4 was to identify the variation of wind speed in the overlying air. The

vertical profile data were used for analysis when wind speed less than 6 $m \cdot s^{-1}$ throughout the column. The statements in line 334–338 are sufficient to describe its contents, so we removed it from the manuscript as suggested. Figure 5 has also been removed, and the panel (a) of Figure 6 has been moved to the supplement as an example, as the referee suggested.

We agree that a near-steady state between HONO production and loss has not been reached in Figure 4 (the original Figure 7). A near-steady state plateau in HONO mixing ratio and HONO/NO_2 was observed near midnight during E3 in Figure 5 (the original Figure 8), and the vertical profiles showed an approximate plateau between 23 to 01 h. We have revised the description of Figure 4 and 5 (the original Figure 7 and 8) in section 3.2.2 to make our argument more clearly.

Minor Comments:

1. Line 168: If reported measurements are 15 s, then the associated detection limit should be presented.

Response: The detection limits of HONO and NO_2 at time resolution of 15s are 120 ppt and 200 ppt, respectively, which have been added to the revised manuscript (line 247–248) as suggested.

2. Line 171: The measurement error was 'approximately' assessed as 9 %. How was this done and why is it 'approximately'? This should be used to denote error bars on observations presented in the figures. Have any corrections for NO_2 to HONO conversion on the instrument inlet and cavity surfaces been characterized and corrected for?

Response: The measurement error of 9% is the total relative uncertainty of the IBBCEAS instrument, which is estimated considering the uncertainty in the absorption cross sections (5%), the calibration of mirror reflectivity (5%), spectral fitting (4%), the correction of effective cavity length (3%), the pressure in the cavity (1%), $\Delta I/I_0$ (1%) and sample loss (0.5%). The propagated uncertainties are estimated to be 8.7% which is approximately to be 9%. The relative uncertainty of IBBCEAS instrument and estimated uncertainty of 8.7% have been presented in the revised manuscript.

The inlet and optical cavity made exclusively of PFA Teflon are used to minimize the generation and wall loss of HONO. To investigate any potential secondary HONO formation on the inlet or cavity walls from conversion of NO_2. We measured 80 ppb NO_2 at different RH levels (20% RH, 30% RH, 50% RH and 70% RH) flowing through a 3 m PFA inlet tube into the IBBCEAS instrument for a

long time at typical sampling flow rate (6 L min^{-1}). No significant HONO was observed in the cavity, suggesting that the secondary HONO formation is negligible for IBBCEAS instrument under typical operation condition. A more detailed description of our IBBCEAS instrument can be found in our published article Du et al. (2018).

3. Line 178: The models and detection limits of the supporting gas analyzers need to be given. Why is none of this supporting data shown or used in the analysis?

Response: Instrumental section has been revised including adding the models and detection limits of gas analyzers and giving related references. The auxiliary data was also shown in manuscript Figure 3, which was used in the subsequent analysis as the referee suggested.

4. Lines 180-185: Again, supporting measurements are noted as having been made here, but they are not used to interpret the data. These should be used as noted in the major comments above.

Response: The auxiliary data have been used to interpret the vertical measurements in the subsequent analysis.

5. Lines 191-194: An NO_2 intercept of 750 ppt should be explained. Is it statistically different from zero? See major comment on figure regressions and error analysis above.

Response: We would first like to apologize for our mistake. The NO_2 intercept of 750 ppt in Figure 2 was caused by the mismatch of the timeline of NO_2 data measured by two IBBCEAS in correlation analysis. We have corrected this error and significantly modified Figure 2 as the referee suggested.

References:

Alicke, B., Platt, U., Stutz, J.: Impact of nitrous acid photolysis on the total hydroxyl radical budget during the Limitation of Oxidant Production/Pianura Padana Produzione di Ozono study in Milan, J. Geophys. Res., 107, LOP 9-1-LOP 9-17, https://doi.org/10.1029/2000jd000075, 2002.

Brown, S. S., Dubé, W. P., Osthoff, H. D., Wolfe, D. E., Angevine, W. M., and Ravishankara, A. R.: High resolution vertical distributions of NO_3 and N_2O_5 through the nocturnal boundary layer, Atmos. Chem. Phys., 7, 139-149, https://doi.org/10.5194/acp-7-139-2007, 2007.

Coe, H., and Gallagher, M. W.: Measurements of Dry Deposition of NO_2 to A Dutch Heathland Using the Eddy-Correlation Technique, Q. J. Roy. Meteor. Soc., 118, 767-786, https://doi.org/10.1002/qj.49711850608, 1992.

Duan, J., Qin, M., Ouyang, B., Fang, W., Li, X., Lu, K. D., Tang, K., Liang, S. X., Meng, F. H., Hu, Z. K., Xie, P. H., Liu, W. Q., and Häsler, R.: Development of an incoherent broadband cavity-enhanced absorption spectrometer for in situ measurements of HONO and NO2, Atmos. Meas. Tech., 11, 4531-4543, https://doi.org/10.5194/amt-11-4531-2018, 2018.

Finlayson-Pitts, B. J., Wingen, L. M., Sumner, A. L., Syomin, D., and Ramazan, K. A.: The heterogeneous hydrolysis of NO_2 in laboratory systems and in outdoor and indoor atmospheres: An integrated mechanism, Phys. Chem. Chem. Phys., 5, 223-242, https://doi.org/10.1039/b208564j, 2003.

Finlayson-Pitts, B. J.: Reactions at surfaces in the atmosphere: integration of experiments and theory as necessary (but not necessarily sufficient) for predicting the physical chemistry of aerosols, Phys. Chem. Chem. Phys., 36, 7760-7779, https://doi.org/10.1039/B906540G, 2009.

Harrison, R. M., and Kitto, A. M. N.: Evidence for a surface source of atmospheric nitrous acid, Atmos. Environ., 28, 1089-1094, https://doi.org/10.1016/1352-2310(94)90286-0, 1994.

Harrison, R. M., Peak, J. D., and Collins, G. M.: Tropospheric cycle of nitrous acid, J. Geophys. Res., 101, 14429-14439, https://doi.org/10.1029/96JD00341, 1996.

Kirchstetter, T. W., Harley, R. A., and Littlejohn D.: Measurement of nitrous acid in motor vehicle exhaust, Environ. Sci. Technol., 30, 2843-2849, https://doi.org/10.1021/es960135y, 1996.

Kurtenbach, R., Becker, K. H., Gomes, J. A. G., Kleffmann, J., Lörzer, J., Spittler, M., Wiesen, P., Ackermann, R., Geyer, A., and Platt, U.: Investigations of emission and heterogeneous formation of HONO in a road traffic tunnel, Atmos. Environ., 35, 3385–3394, https://doi.org/10.1016/S1352-2310(01)00138-8, 2001.

Laufs, S., Cazaunau, M., Stella, P., Kurtenbach, R., Cellier, P., Mellouki, A., Loubet, B., and Kleffmann, J.: Diurnal fluxes of HONO above a crop rotation, Atmos. Chem. Phys., 17, 6907-6923, https://doi.org/10.5194/acp-17-6907-2017, 2017.

Li, D. D., Xue, L. K., Wen, L., Wang, X. F., Chen, T. S., Mellouki, A., Chen, J. M., and Wang, W. X.: Characteristics and sources of nitrous acid in an urban atmosphere of northern China: Results from 1-yr continuous observations, Atmos. Environ., 182, 296-306,

https://doi.org/10.1016/j.atmosenv.2018.03.033, 2018.

Liang, Y. T., Zha, Q. Z., Wang, W. H., Cui, L., Lui, K. H., Ho, K. F., Wang, Z., Lee, S. C., and Wang, T.: Revisiting nitrous acid (HONO) emission from on-road vehicles: A tunnel study with a mixed fleet, J. Air Waste Manag., 67, 797-805, https://doi.org/10.1080/10962247.2017.1293573, 2017.

Liu, X., Cheng, Y., Zhang, Y., Jung, J., Sugimoto, N., Chang, S.Y., Kim, Y. J., Fan, S., and Zeng, L.: Influences of relative humidity and particle chemical composition on aerosol scattering properties during the 2006 PRD campaign, Atmos. Environ., 42, 1525–1536, https://doi.org/10.1016/j.atmosenv.2007.10.077, 2008.

Rappenglück, B., Lubertino, G., Alvarez, S., Golovko, J., Czader, B., and Ackermann, L.: Radical precursors and related species from traffic as observed and modeled at an urban highway junction, J. Air Waste Manag. Assoc., 63, 1270-1286, https://doi.org/10.1080/10962247.2013.822438, 2013.

Spindler, G., Brüggemann, E., and Herrmann, H.: Nitrous acid (HNO_2) Concentration Measurements and Estimation of Dry Deposition over Grassland in Eastern Germany, Transactions on Ecology and Environment, 28, 223-227, 1999.

Stutz, J., Alicke, B., Neftel, A.: Nitrous acid formation in the urban atmosphere: Gradient measurements of NO_2 and HONO over grass in Milan, Italy, J. Geophys. Res., 107, LOP 5-1-LOP 5-15, https://doi.org/10.1029/2001JD000390, 2002.

Su, H., Cheng, Y. F., Cheng, P., Zhang, Y. H., Dong, S. F., Zeng, L. M., Wang, X. S., Slanina, J., Shao, M., and Wiedensohler, A.: Observation of nighttime nitrous acid (HONO) formation at a non-urban site during PRIDE-PRD2004 in China, Atmos. Environ., 42, 6219-6232, https://doi.org/10.1016/j.atmosenv.2008.04.006, 2008.

Sun, Y. L., Jiang, Q., Wang, Z. F., Fu, P. Q., Li, J., Yang, T., and Yin, Y.: Investigation of the sources and evolution processes of severe haze pollution in Beijing in January 2013, J. Geophys. Res. Atmos., 119, 4380-4398, https://doi.org/10.1002/2014JD021641, 2014.

VandenBoer, T. C., Brown, S. S., Murphy, J. G., Keene, W. C., Young, C. J., Pszenny, A. A. P., Kim, S., Warneke, C., de Gouw, J. A., Maben, J. R., Wagner, N. L., Riedel, T. P., Thornton, J. A., Wolfe, D. E., Dubé, W. P., Öztürk, F., Brock, C. A., Grossberg, N., Lefer, B., Lerner, B., Middlebrook, A. M., and Roberts, J. M.: Understanding the role of the ground surface in HONO vertical structure: High resolution vertical profiles during NACHTT-11, J. Geophy. Res.- Atmos., 118, 10155-110171, https://doi.org/10.1002/jgrd.50721, 2013.

Wang, H. C., Lu, K. D., Chen, X. R., Zhu, Q. D., Wu, Z. J., Wu, Y. S., and Sun, K.: Fast particulate nitrate formation via N_2O_5 uptake aloft in winter in Beijing, Atmos. Chem. Phys., 18, 10483-10495, https://doi.org/10.5194/acp-18-10483-2018, 2018.

Wong, K. W., Oh, H. -J., Lefer, B. L., Rappenglück, B., and Stutz, J.: Vertical profiles of nitrous acid in the nocturnal urban atmosphere of Houston, TX, Atmos. Chem. Phys., 11, 3595-3609, https://doi.org/10.5194/acp-11-3595-2011, 2011.

Xu, Z., Wang, T., Wu, J. Q., Xue, L. K., Chan, J., Zha, Q., Z., Zhou, S. Z., Louie, P. K. K., and Luk, C. W. Y.: Nitrous acid (HONO) in a polluted subtropical atmosphere: Seasonal variability, direct vehicle emissions and heterogeneous production at ground surface, Atmos. Environ., 106, 100-109, https://doi.org/10.1016/j.atmosenv.2015.01.061, 2015.

Yang, Q., Su, H., Li, X., Cheng, Y. F., Lu, K. D., Cheng, P., Gu, J. W., Guo, S., Hu, M., Zeng, L. M., Zhu, T., and Zhang, Y. H.: Daytime HONO formation in the suburban area of the megacity Beijing, China, Sci. China Chem., 57, 1032-1042, https://doi.org/10.1007/s11426-013-5044-0, 2014.

Zhang, N., Zhou, X. L., Shepson, P. B., Gao, H. L., Alaghmand, M., and Stirm, B.: Aircraft measurement of HONO vertical profiles over a forested region, Geophys. Res. Lett., 36, L15820, https://doi.org/10.1029/2009GL038999, 2009.

Zhang, W. Q., Tong, S. R., Ge, M. F., An, J. L., Shi, Z. B., Hou, S. Q., Xia, K. H., Qu, Y., Zhang, H. X., Chu, B. W., Sun, Y. L., and He, H.: Variations and sources of nitrous acid (HONO) during a severe pollution episode in Beijing in winter 2016, Sci. Total Environ., 648, 253-262, https://doi.org/10.1016/j.scitotenv.2018.08.133, 2018.

2. Response to interactive comments on "High resolution vertical distribution and sources of HONO and NO_2 in the nocturnal boundary layer in urban Beijing, China" by Anonymous Referee #3

Manuscript acp-2019-613 reports results of a nighttime vertical gradient study aimed at determining the sources and sinks of nitrous acid (HONO) in Beijing, China. Measurements were made from an instrumented container capable of ascending and then descending a 325 m tower over an hour, enabling measurements at ground level and up to a height of 240 m. The maximum height achieved means that measurements covered the surface layer, nocturnal boundary layer, and residual layer. Furthermore, the measurement campaign covered three periods of time marked by clean or hazy air masses. The results are then used to draw conclusions about the relative importance of direct (automobile), ground, and aerosol sources of HONO to the airshed.

The analytical measurements appear to be of high quality. The tower experiments are ideal for elucidating HONO sources and sinks, and it was a good idea to operate simultaneous ground-based and vertically transported IBBCEAS systems. It is not the first time that gradient measurements of HONO and related physical/chemical have been made using a tower/elevator and much of the approach to data analysis and interpretation closely follows previous studies (especially, VandenBoer, et al. J. Geophys. Res. 2013, 118, 10,155–10,171, doi:10.1002/jgrd.50721 and Stutz et al. J. Geophys. Res. 2002, 107, doi:10.1029/2001JD000390). Despite the lack of novelty, the data has the potential to provide insights into myriad processes affecting HONO production and loss in Beijing, an area where frequent high aerosol concentrations mean that multiphase chemistry has a large influence on atmospheric composition. However, I do not feel that sufficient analysis of the data was carried out to support the authors' conclusions. Therefore, I feel that the manuscript is not ready for publication; additional work must be carried out to properly analyze the data and extract the information it holds.

Response: We thank Anonymous Referee #3 for the valuable comments. The detailed and insightful comments and suggestions have greatly helped us to revise and improve the manuscript. We would like to point out that the measurement container in our study is lifted on the side wiring of the tower, far away from the steel structure of the tower, thus minimizing potential wall effects, which is different from previous studies (Kleffmann et al., 2003; VandenBoer et al., 2013). To the best of our knowledge, this study is the first high-resolution vertical measurements conducted in China, which has suffered from heavy air pollution for several years. We have significantly revised the manuscript

accordingly to address the referee's comments and concerns. Below are a point-to-point response to address the referee's specific comments.

Specific comments:

One of the most important aims of the manuscript is to determine the relative contribution of direct sources vs. ground and aerosol surfaces to overall HONO production at the site. The conclusions are: (1) direct sources are a major source (~51% of total ambient HONO is from combustion); (2) vertical profiles of HONO concentration do not support heterogeneous NO_2-to-HONO conversion on aerosol surfaces; (3) heterogeneous NO_2-to-HONO conversion on ground surfaces followed by vertical convection dominate HONO production at night. These conclusions are based on interpretation and discussion of results on p. 11-15, which I found to be unclear and not necessarily supportive of the final conclusions. To be suitable for publication I feel the relative contribution of the various HONO processes need to be quantified in more detail for the full data set and the derivations of those calculations more clearly explained in the text.

There was some ambiguity regarding how the contribution of direct emissions to ambient HONO was determined. It seems to be derived from the HONO/NO_x ratio measured on days dominated by fresh vehicle emissions, which were identified when NO > 80 ppb and NO/NO_x > 80%. The ratio was then used to devise a linear relationship between ambient NO_x and direct HONO emissions that is applied over the whole campaign. How this relationship was used to derive the contribution of direct emissions to ambient HONO is not clear. Also, the statement that direct sources constitute 51% of total ambient HONO is generalized for the entire campaign. However, it is clear that the relative contribution of HONO sources will change with time of day, traffic intensity and type of traffic, meteorology. Indeed, it is expected that the HONO mass balance for each nocturnal profile will be different, with each source/sink having a different relative contribution depending on time and meteorology.

Response: Thanks for the comment and suggestion. Considering the differences in the type of vehicles, fuel compositions, etc., the reported emission factors of HONO might not be representative for the Beijing region. The local emission factors of HONO were derived from the field data. Following the suggestions by Jörg Kleffmann, five criteria were applied to ensure as much of the freshly emitted air masses as possible: (a) only nighttime data (from 18:00 LT to next 6:00 LT) were

included to avoid the fast photolysis of HONO; (b) only sharp peaks during nighttime and the elevations of HONO and NO_x over the background levels were estimated; (c) $\Delta NO/\Delta NO_x > 0.80$; (d) good correlation between HONO and NO_x; (e) short duration of the plume (< 30 min). Criteria (b) and (c) were used as indicators for identifying fresh vehicular emissions. Criteria (d) and (e) further confirmed that the increase in HONO was primarily caused by freshly emitted plumes instead of heterogeneous reactions of NO_2.

For a month measurements, 11 fresh plumes satisfied selection criteria (Table 1). Two examples of fresh plumes observed on December 9th to 10th, 2016 based on the preceding selection criteria were shown in Figure 6 in the manuscript. The derived emission factors varied from 0.78% to 1.73%, with an average value of 1.28% ± 0.36%, which was in the range of previously published results (0.19%–2.1%) (Kirchstetter et al., 1996; Kurtenbach et al., 2001; Su et al., 2008; Rappengluck et al., 2013; Yang et al., 2014; Xu et al., 2015; Liang et al., 2017; Zhang et al., 2018; Li et al., 2018). Comparisons of derived HONO/NO_x ratios with the previously reported results were summarized in Table S2 in the supplementary information. To minimize the risk of overestimating direct emissions, the minimum HONO/NO_x ratio was used as an upper limit for the emission factor (Su et al., 2008). The HONO/NOx ratio of 0.78% was used to estimate the direct HONO emissions ($[HONO]_{emis} = 0.0078 \times [NO_x]$). The average $HONO_{emis}$/HONO ratio was used to evaluate the contribution of direct emissions to ambient HONO levels at night. The vehicle emissions contributed 29.3% ± 12.4% to the ambient HONO concentrations at night. As the referee pointed out, we have considered the difference in direct HONO emissions at different pollution levels, the contribution of direct emissions during the clean and haze episodes were estimated respectively. The contributions of direct emissions to ambient HONO levels were estimated to be 35.9% ± 11.8% and 26% ± 11.3% during the clean and the haze episodes, respectively. The lower vehicle emissions contribution during the haze episode could have been caused by an odd-even car ban, which required alternate driving days for cars with even- and odd-numbered license plates.

The measurement site as a typical residential area is surrounded by several main roads, and the nocturnal traffic emission is relatively stable. Because NO was not measured at ground level after 14:00 on December 10th, the direct HONO emissions during the third episode (E3, December 11th to 12th) cannot be directly estimated. The contribution of direct emissions to ambient HONO during the first episode (E1, from December 7th to 10:00 on December 8th) and the second episode (C2, from

10:00 on December 8th to December 11th) were estimated to be 26% ± 5.9% and 32.8% ± 11.8%, respectively, which were comparable to the preceding results. Therefore, we used an average $HONO_{emis}$/HONO ratio to evaluate the relative contribution of direct HONO emissions during E3, which was used to correct observed HONO concentration in the subsequent analysis.

As the referee suggested, the budget analysis of nighttime HONO has been utilized to estimate the sources/sinks of HONO for the nocturnal profiles at different pollution periods. The nocturnal production of HONO on aerosol and ground surfaces have different relative contribution at different pollution periods, as the referee expected. We have significantly revised the discussion in the manuscript in "3.3 Direct emissions", "3.4.2 Relative important of aerosol and ground surfaces in nocturnal HONO production" and "3.4.3 Nocturnal HONO production and loss at ground level" to address the referee's concerns and to make our argument more clearly.

When determining the relative contribution of aerosol surfaces to the HONO budget, the authors attempt to quantify HONO production using an assumed uptake coefficient (for NO_2-to-HONO conversion) and an aerosol surface area-to-volume ratio from a completely different study, which is supposed to be a typical of winter in Beijing. I don't see how one can justify using a single aerosol surface area-to-volume ratio for the entire campaign, especially since this will vary with time, meteorology, and day (see Table 1). Further, it is not clear why a single value was used since a suite of aerosol measurements were made during the current study; measurements of black carbon, non-refractory PM, and AMS measurements at ground and 260 m height are reported. This data should be used to refine the analysis and make it more specific for each ascent/descent period. I encourage the authors to provide a more in-depth analysis of the contribution of aerosol surface area to HONO processes. I believe there may indeed be evidence for an important role for aerosol here under hazy conditions. For example, clear gradients, denoted by decreasing HONO/NO_2 ratio with elevation, were only observed on a few occasions, whereas it was more often the case that the HONO/NO_2 ratio was quite constant over the vertical range. Thus, it is possible that aerosol chemistry may influence this profile, but only a detailed quantitative analysis can tell you this.

Response: As the referee suggested, the newly obtained aerosol surface areas (S_a) at ground level and at 260 m were used to estimate the nocturnal production of HONO by heterogeneous conversion of NO_2 on aerosol surface. A hygroscopic factor was applied to correct S_a to ambient (wet) aerosol

surface area (S_{aw}) for particle hygroscopicity (Liu et al., 2013; Wang et al., 2018). The time series of S_{aw} at ground level and at 260 m was shown in Figure. S2 in the supplementary information. The surface area information for particles larger than 0.5 μm were not valid at ground level and 260 m during the measurement period. Hence, this is a lower limit estimate of the total surface area for the heterogeneous reaction.

An estimate of the nocturnal HONO production on aerosol surface was made using the RH corrected aerosol surface area (S_{aw}) and NO_2 observations from the residual layer. The correlation between CO and BC observed at ground level and the CO and BC at 260 m were analyzed. The CO and BC measured at ground level were independent of CO and BC observed at 260 m during the haze period (Figure. S10), since it can be expected that air masses in the residual layer were decoupled from the ground-level processes and largely free of NO_2 emissions. (Brown et al., 2012; VandenBoer et al., 2013). The vertical profiles of HONO and NO_2, and aerosol surface areas measured at 260 m allowed to estimate the nocturnal HONO production by heterogeneous conversion of NO_2 on aerosol surface. The HONO production from the heterogeneous NO_2 conversion ($2NO_{2(g)}+H_2O_{(ads)} \xrightarrow{surface} HONO_{(g)}+HNO_{3(ads)}$) on aerosol surface would then have become the primary HONO source in the residual layer during E3. The yield of hydrolysis reaction assumes that HONO and HNO_3 are formed by equimolar disproportionation of two NO_2 molecules and immediately release HONO (Finlayson-Pitts et al., 2003; Finlayson-Pitts, 2009). The reactive uptake of NO_2 by the aerosol was assumed to occur on all measured aerosol surface area, regardless of chemical composition. HONO production was calculated using the equation of Ye et al. (2018) modified to account for the disproportionation. The uptake coefficient of NO_2 ranged between 1×10^{-5} to 1×10^{-6} in the dark, an average S_{aw} of 2314 μm^2 cm^{-3} between 22 and 01 h (the vertical measurement periods on Decemebr 11th) and an upper limit of observed NO_2 of 54 ppb from the residual layer were used to estimate the heterogeneous production of HONO on aerosols during E3. The HONO production of 30–300 ppt in an interval of 1.5 h could account for the observed HONO increases of 15–368 ppt in the residual layer between profile measurements. The heterogeneous production of HONO solely on aerosol surface explained the HONO observations during E3. As the referee expected, the aerosol surface plays an important role in nocturnal HONO production during the haze episode. The column average concentration of HONO was independent of the mixing ratio of HONO observed from the

ground level to 10 m in height (R^2 = 0.27) during E3 (Figure 10a), which suggested that aerosols presumably dominated the production of HONO aloft by heterogeneous uptake of NO_2.

The production of HONO on aerosols were also discussed to the other vertical measurements during C2, as the referee #1 suggested. The column average HONO concentration was related to the mixing ratio of HONO observed from the ground level to 10 m (Figure 10b, R^2 = 0.93), suggesting that the surface HONO source affected the HONO observed throughout the depth of boundary layer during C2. A high correlations (R^2 = 0.83) between measured CO and BC at ground level and the CO and BC at 260 m were observed (Figure. S10), which indicated that vehicle emissions affected air masses in the residual layer. The lack of NO vertical profile cannot directly correct the influence of direct HONO emissions. If it is assumed that the contribution of direct HONO emissions (35.9% ± 11.8%) was consistent at ground level and in the residual layer, the relative importance of aerosol and ground surface in nocturnal HONO production could be roughly estimated. It is necessary to elaborate that the contribution of direct emissions to HONO levels in the residual layer is a higher limit estimate. The production of HONO on aerosol surface was estimated during vertical measurements on December 9th and 10th. The HONO increases of 305–608 ppt between the vertical profile measurements, which have the contribution from direct HONO emissions subtracted, were higher than the production of HONO (26–259 ppt) on aerosols in an interval of 5.5 h on December 9th. The production of HONO solely on aerosol surface cannot explain the observed HONO increases in the residual layer, suggesting that the observed HONO throughout the depth of boundary layer was primarily derived from the heterogeneous NO_2 conversion on the ground surface followed by vertical transport throughout the column. The HONO production from the aerosol surface in an interval of 5.35 h was 33–332 ppt in the residual layer on December 10th, which was comparable to the corrected HONO increases of 114–369 ppt between profile measurements. This could have been due to a shallow inversion layer formed near the surface (Figure 4), which inhibited the vertical transport of nighttime HONO at ground level. Besides the contribution of direct HONO emissions could be even more overestimated, which might also affect the estimated result. All of these may result in the aerosols dominated the heterogeneous production of HONO from NO_2 in the residual layer on December 10th.

As the referee expected, the aerosol chemistry plays an important role under hazy conditions. The production of HONO solely on aerosol surface explained the HONO observations during the haze

episode. However, the ground surface was still the dominant nocturnal surface on which HONO was formed from the heterogeneous conversion of NO_2 during the clean episode. We have significantly revised the discussion in section 3.4.2 as suggested, adding more detailed quantitative analysis to draw broad conclusions.

Finally, the authors state that ground level HONO production has been corrected for the influence of direct emissions from automobiles. Has this correction been carried out for the production on aerosol surfaces as well? I had a difficult time understanding the rationale of going through all the calculations in section 3.4.3 on the topic of ground level HONO production. It was not clear how equation 4 and 5 were derived. The purpose of these equations is to estimate a HONO conversion frequency, which appears to be the pseudo-first order rate constant associated with the conversion of NO_2-to-HONO. These values should then be used to compare to the other HONO sources and sinks to evaluate the relative importance of all the various HONO sources/sinks. However, this comparison is not clearly carried out at the end of the paper as I would expect. Instead, starting with line 410 the text veers off subject by deriving a HONO yield from deposited NO_2. While this may be a useful calculation to carry out, I don't see how it helps the authors reach their research objectives and main conclusions.

In closing, I feel the interpretation of the vertical profiles relies on highly generalized 'back of the envelope' calculations. Such calculations can be very useful in certain cases; however, the quality and quantity of the data provided by this study should allow for a more elaborate analyses. I recommend the authors revisit their data to devise a mass balance for HONO processes where they quantify the sources and sinks for each vertical profile. I expect this approach will provide valuable insights that are not clear from the current presentation of the data.

Response: Thanks for the comment and suggestion. The influence of direct HONO emissions was taken into account in evaluating the heterogeneous production of HONO on aerosol surface, which has been discussed in section 3.4.2 of the revised manuscript. Equation 4 and 5 were derived by Su et al. (2008) to correct for the effects of source and diffusion, which was derived from the equation ($[Y]_t^{Xscaled} = \overline{[X]}\frac{[Y]_t}{[X]_t}$), in which the mixing ratio of *Y* at time *t* was scaled with species *X* at the same time (Lammel, 1999). As the referee suggested, the slope determined by linear regression will

statistically better describe the efficient first order conversion rate constant of NO_2 to HONO. Thus the conversion frequency was re-estimated following the method by Alicke et al. (2002). The conversion frequencies (k_{HONO}) on December 9th, 10th, and 11th were 0.0082, 0.0060 and 0.0114 h^{-1}, respectively, corresponding to a HONO production rate by NO_2 (P_{NO_2}) of 0.25 ± 0.03, 0.28 ± 0.02 and 0.60 ± 0.02 ppb h^{-1} (i.e. $C_{HONO} \times \overline{[NO_2]}$). It is necessary to elaborate that the derived P_{NO_2} is net HONO production, which means sources and sinks of HONO (aerosol and ground surface source, deposition, etc.) have already been taken into account in P_{NO_2}.

As the referee suggested, the surface production rate of HONO was used to compare to the production rate on aerosols based on the assumption that the production of HONO on aerosols was insignificant compared to the ground surface during the clean episode, which has been suggested in other studies of HONO vertical gradient (VandenBoer et al., 2013; Wong et al., 2011; Zhang et al., 2009). The P_{NO_2} could be approximately considered as the net contribution of surface HONO production to the column during C2. The production rate of HONO on the ground surface (0.25 ± 0.03 and 0.28 ± 0.02 ppb h^{-1}) was an order of magnitude higher than the maximum production rate on aerosol surface (0.047 and 0.062 ppb h^{-1}), which suggested that the HONO observed throughout the column was primarily derived from the heterogeneous conversion of NO_2 on the ground surface followed by vertical transport throughout the column during the clean episode. This result was consistent with the result in section 3.4.2. In contrast, the production of HONO on aerosols as an important nighttime HONO source cannot be ignored during the haze episode, as discussed in section 3.4.2. To compare the production of HONO on aerosol and ground surfaces, the production rate of HONO on the ground surface was estimated by equation (Eq. 8) with a deposition velocity (V_{dep,NO_2}) of 0.07 cm s^{-1} (VandenBoer et al., 2013) and a boundary layer height of 140 m. The derived production rate of HONO ($P_{HONO,ground}$) on the ground surface was 0.47 ± 0.02 ppb h^{-1} on December 11th (E3), which was comparable to the production rate on aerosol surface of 0.2 ppb h^{-1}. This result also suggests that production of HONO on aerosols is an important nocturnal source of HONO during the haze episode.

A budget analysis of nighttime HONO was utilized to evaluate the contributions of various HONO sources/sinks, as the referee suggested. The derived a net HONO yield from the ground surface conversion of NO_2 have been removed in the revised manuscript. The nocturnal HONO budget from 18:00 to 06:00 LT on December 9th (C2) and 10th (E3) were shown in Figure 11 in the

revised manuscript. The average production rate of HONO on aerosols (0.04 ± 0.01 ppb h^{-1}) was insignificant compared to the surface production rate of 0.28 ± 0.03 ppb h^{-1} during the clean episode. However, the average $P_{aerosol}$ of 0.19 ± 0.01 ppb h^{-1} was comparable to the surface production rate of HONO (P_{ground}, 0.47 ± 0.03 ppb h^{-1}) during the haze episode. Direct HONO emissions just contributed a small portion of HONO at a rate of 0.06 ± 0.07 and 0.10 ± 0.10 ppb h^{-1} during C2 and E3, respectively. The dry deposition of HONO contributed 0.74 ± 0.31 and 1.55 ± 0.32 ppb h^{-1} to the nocturnal loss of HONO during C2 and E3, respectively, implying that significant quantities of HONO were deposited to the ground surface at night. This had been suggested in another study on the vertical gradient of HONO (VandenBoer et al., 2013).

Specific comments by line number:

Lines 45-133: I feel that the introduction lacks an explicit statement of the study's research objective(s). The authors provide a [somewhat long] background section reviewing aspects of HONO chemistry that ends with a summary of what they did in their study. The introduction would be far stronger if the authors include a focused discussion of what research objective they hope to achieve. This could be accomplished by stating a hypothesis, following by a plan for how they hoped to test the hypothesis. At the moment, it is only in the second to last sentence of the introduction that one finally learns that a comparison of HONO heterogeneous chemistry on ground vs. aerosol surfaces is the major aim of the work.

Response: We have significantly revised the discussion in the introduction section. The background introduction of HONO chemistry and vertical observations have been revised as suggested, and more explicit statements of research objective have been added to the introduction section.

64-66: The authors state that hydrolysis of NO_2 on humid surfaces via R2 is considered the most likely explanation for observed HONO concentrations. The authors should be aware that this is not a viable mechanism under atmospherically relevant concentrations of NO_2. Reaction R2 is too slow and only becomes important when the NO_2 concentration is high enough to promote N_2O_4 formation. Initial mechanistic studies of this mechanism had to use high NO_2 concentrations due to high instrument detection limits. More recent laboratory studies of this process using state-of-the-science sensitive field-grade instrumentation do not report this chemistry occurring under lower concentrations (50

ppb or less). One can refer to numerous lab studies over the past 10-15 years aimed at studying NO_2 conversion on surfaces containing humic acid reactive sites to learn more about this. It is notable that these studies often include control experiments aimed at quantifying background levels of HONO derived from NO_2 hydrolysis on their experimental system (i.e., in the absence of redox active substrates). These studies consistently show that NO_2-to-HONO conversion on organic matter and other redox active surfaces produce orders of magnitude more HONO than does R2.

Response: We would like to thank the referee for the constructive suggestion. The introduction has been significantly revised as suggested. This statements have been revised as below,

Line 86–92

"The heterogeneous reduction of NO_2 with organic substrates is proposed to be another effective pathway to generate HONO (Brigante et al., 2008; Stemmler et al., 2006; George et al., 2005). However, extrapolation of lab results to real surfaces remains challenging. The nocturnal production of HONO has been considered to be dominated by the NO_2 heterogeneous reaction (R2). Although the heterogeneous reaction (R2) of HONO formation is first-order in NO_2, the mechanism for the conversion of NO_2 on surfaces remains unclear (Finlayson-Pitts et al., 2003; Finlayson-Pitts, 2009)."

81: The colon after the references should be deleted.

Response: Revision has made as the referee suggested.

349: The authors attribute a decrease in HONO/NO_2 ratio at RH above 70% to enhanced HONO deposition. While RH does impact HONO uptake (see Donaldson et al. Environ. Sci. Technol. 2014, 48, 375), it would affect NO_2-to-HONO conversion as well (by enhancing to a point); so there are competing effects here. The abovementioned Donaldson et al. paper suggests that the uptake coefficient for HONO actually decreases with increasing RH.

Response: Thanks for the comment and suggestion. We have revised the description in this paragraph, as below.

Line 548–558:

"A previous observation at ground level also reported that the HONO/NO_2 ratio increased with an increase in RH when the RH was less than 70%. A further increase in RH would lead to a decrease in the HONO/NO_2 ratio, which was considered to be caused by the number of water monolayers that

formed on the surface leading to an efficient uptake of HONO (Li et al., 2012; Yu et al., 2009; Liu et al., 2019). However, a decreased uptake coefficient of HONO with increasing RH from 0% to 80% was observed in a laboratory study (Donaldson et al., 2014). The NO_2 to HONO conversion efficiency depended negatively on RH at an RH above 70%, which was presumably caused by the relative humidity affecting both HONO uptake onto the surface and the NO_2-to-HONO conversion."

372: The number listed having unit of h^{-1} is not a formation rate as stated. Those are units of a first-order rate constant. Rather, units of ppb h^{-1} are appropriate for a formation rate.

Response: The unit of the NO_2-normalized HONO production over time, $\Delta\frac{[HONO]}{[NO_2]}/\Delta t$, is h^{-1} according to the equation (Eq. 5). The unit of its equivalent HONO production rate at constant NO_2 concentration is ppb h^{-1}. We have revised the statements in this paragraph to make it clearer.

405: It would be beneficial to provide a visual comparison of all the production rates (calculated in units of mixing ratio per hour). See for example Fig. 11 from Vandenboer et al. JGR, 2013, 118, 10,155.

Response: As the referee suggested, the comparison of the production and loss rate of HONO have been added in section 3.4.3. Figure 11 shows the production and loss rate of nighttime HONO on December 9th and 10th.

413: I recommend that the authors choose another symbol to represent the compensation point, which they call the HONO yield from deposited NO_2; the greek letter phi is reserved for the photolysis quantum yield. The symbol "H" used for mixing depth is also confusing. Some readers may mistake this for the Henry's law constant without reading further into the text. Consider using "d" (for depth) or lower case "h" or "z", all of which have been used in the past to represent height.

Response: Following the referee's suggestion in the specific comments above, the derived a net HONO yield from ground surface conversion of NO_2 have been removed in the revised manuscript. The symbol "*H*" used for mixing height has been modified to symbol "h" as the referee suggested.

421: Why choose a deposition velocity from the literature, which is derived from completely different

studies. Isn't the point here to model the vertical profile to derive a deposition velocity and the uptake coefficients for NO_2, HONO, etc. that are specific for the current sampling site?

Response: As the referee suggested, the temperature-dependent deposition velocity of HONO ($V(HONO)_T = \exp(23920/T - 91.5)$), which was adjusted to value of 2 cm s^{-1} at 0 °C decreasing exponentially to non-significant values at 40 °C (Laufs et al., 2017), was used to derive the dry deposition velocity of HONO. The $V_{dep,HONO}$ calculated from nocturnal observations (00:00–06:00 LT) ranged between 0.9 and 3 cm s^{-1}, with an average value of 1.8 cm s^{-1}, which was within the range of previously reported values (0.077–3 cm s^{-1}) (Harrison and Kitto, 1994; Harrison et al., 1996; Spindler et al., 1998; Stutz et al., 2002; Coe and Gallagher, 1992; Laufs et al., 2017). However, the limited vertical profile data in this study restricted the estimaton of the uptake coefficients for NO_2 and HONO. Thus we used the uptake coefficients and the deposition velocity from the literature to estimate the heterogeneous production of HONO on aerosol and ground surfaces, which have also been used in other studies of HONO vertical structure (VandenBoer et al., 2013; Wong et al., 2011; Ye et al., 2018).

More general remarks:

More general remarks: More work should be devoted to providing error analysis. For example, error bars on data and errors in reported values derived from their analyses. This will be especially important when comparing quantitatively the relative contribution of sources/sinks to ambient HONO. I felt there were too many figures in the text. For example, what is the purpose of showing Figure 5, where the information is more useful plotted in the format shown in Fig. 6, etc. The manuscript could benefit from editing by a native English speaker. Grammatical errors start on the first line of the abstract and persist throughout the manuscript. Lastly, I note that the authors are comparing their IBBCEAS results to data collected on an instrument from Cambridge University. Does this contribution need to be acknowledged in some way (e.g., in the acknowledgement section or author list)?

Response: Thanks for the comment and suggestion. The error analysis have been taken into account in data analysis, and error bars have been presented in the revised manuscript. Figures 5 have been removed from the manuscript as suggested, and the panel (a) of Figure 6 has been moved to the supplementary information. As the referee suggested, the revised manuscript was edited by a native

English speaker. We also acknowledged Bin Ouyang from Cambridge University for providing HONO comparison data in the acknowledgement section.

References:

Alicke, B., Platt, U., Stutz, J.: Impact of nitrous acid photolysis on the total hydroxyl radical budget during the Limitation of Oxidant Production/Pianura Padana Produzione di Ozono study in Milan, J. Geophys. Res., 107, LOP 9-1-LOP 9-17, https://doi.org/10.1029/2000jd000075, 2002.

Brown, S. S., Dubé, W. P., Osthoff, H. D., Wolfe, D. E., Angevine, W. M., and Ravishankara, A. R.: High resolution vertical distributions of NO_3 and N_2O_5 through the nocturnal boundary layer, Atmos. Chem. Phys., 7, 139-149, https://doi.org/10.5194/acp-7-139-2007, 2007.

Coe, H., and Gallagher, M. W.: Measurements of Dry Deposition of NO_2 to A Dutch Heathland Using the Eddy-Correlation Technique, Q. J. Roy. Meteor. Soc., 118, 767-786, https://doi.org/10.1002/qj.49711850608, 1992.

Finlayson-Pitts, B. J., Wingen, L. M., Sumner, A. L., Syomin, D., and Ramazan, K. A.: The heterogeneous hydrolysis of NO_2 in laboratory systems and in outdoor and indoor atmospheres: An integrated mechanism, Phys. Chem. Chem. Phys., 5, 223-242, https://doi.org/10.1039/b208564j, 2003.

Finlayson-Pitts, B. J.: Reactions at surfaces in the atmosphere: integration of experiments and theory as necessary (but not necessarily sufficient) for predicting the physical chemistry of aerosols, Phys. Chem. Chem. Phys., 36, 7760-7779, https://doi.org/10.1039/B906540G, 2009.

Harrison, R. M., and Kitto, A. M. N.: Evidence for a surface source of atmospheric nitrous acid, Atmos. Environ., 28, 1089-1094, https://doi.org/10.1016/1352-2310(94)90286-0, 1994.

Harrison, R. M., Peak, J. D., and Collins, G. M.: Tropospheric cycle of nitrous acid, J. Geophys. Res., 101, 14429-14439, https://doi.org/10.1029/96JD00341, 1996.

Kleffmann, J., Kurtenbach, R., Lörzer, J., Wiesen, P., Kalthoff, N., Vogel, B., and Vogel, H.: Measured and simulated vertical profiles of nitrous acid—Part I: Field measurements, Atmos. Environ., 37, 2949-2955, https://doi.org/10.1016/s1352-2310(03)00242-5, 2003.

Kirchstetter, T. W., Harley, R. A., and Littlejohn D.: Measurement of nitrous acid in motor vehicle exhaust, Environ. Sci. Technol., 30, 2843-2849, https://doi.org/10.1021/es960135y, 1996.

Kurtenbach, R., Becker, K. H., Gomes, J. A. G., Kleffmann, J., Lörzer, J., Spittler, M., Wiesen, P., Ackermann, R., Geyer, A., and Platt, U.: Investigations of emission and heterogeneous formation of HONO in a road traffic tunnel, Atmos. Environ., 35, 3385–3394, https://doi.org/10.1016/S1352-2310(01)00138-8, 2001.

Lammel, G.: Formation of Nitrous acid: Parameterisation and comparison with observatins, Techical Report, MaxPlank-Inst. fuer Meteorol., Hamburg, Germany.

Laufs, S., Cazaunau, M., Stella, P., Kurtenbach, R., Cellier, P., Mellouki, A., Loubet, B., and Kleffmann, J.: Diurnal fluxes of HONO above a crop rotation, Atmos. Chem. Phys., 17, 6907-6923, https://doi.org/10.5194/acp-17-6907-2017, 2017.

Li, D. D., Xue, L. K., Wen, L., Wang, X. F., Chen, T. S., Mellouki, A., Chen, J. M., and Wang, W. X.: Characteristics and sources of nitrous acid in an urban atmosphere of northern China: Results from 1-yr continuous observations, Atmos. Environ., 182, 296-306, https://doi.org/10.1016/j.atmosenv.2018.03.033, 2018.

Li, X., Brauers, T., Häseler, R., Bohn, B., Fuchs, H., Hofzumahaus, A., Holland, F., Lou, S., Lu, K. D., Rohrer, F., Hu, M., Zeng, L. M., Zhang, Y. H., Garland, R. M., Su, H., Nowak, A., Wiedensohler, A., Takegawa, N., Shao, M., and Wahner, A.: Exploring the atmospheric chemistry of nitrous acid (HONO) at a rural site in Southern China, Atmos. Chem. Phys., 12, 1497-1513, https://doi.org/10.5194/acp-12-1497-2012, 2012.

Liang, Y. T., Zha, Q. Z., Wang, W. H., Cui, L., Lui, K. H., Ho, K. F., Wang, Z., Lee, S. C., and Wang, T.: Revisiting nitrous acid (HONO) emission from on-road vehicles: A tunnel study with a mixed fleet, J. Air Waste Manag., 67, 797-805, https://doi.org/10.1080/10962247.2017.1293573, 2017.

Liu, X., Cheng, Y., Zhang, Y., Jung, J., Sugimoto, N., Chang, S.Y., Kim, Y. J., Fan, S., and Zeng, L.: Influences of relative humidity and particle chemical composition on aerosol scattering properties during the 2006 PRD campaign, Atmos. Environ., 42, 1525–1536, https://doi.org/10.1016/j.atmosenv.2007.10.077, 2008.

Rappenglück, B., Lubertino, G., Alvarez, S., Golovko, J., Czader, B., and Ackermann, L.: Radical precursors and related species from traffic as observed and modeled at an urban highway junction, J. Air Waste Manag. Assoc., 63, 1270-1286, https://doi.org/10.1080/10962247.2013.822438, 2013.

Spindler, G., Brüggemann, E., and Herrmann, H.: Nitrous acid (HNO_2) Concentration Measurements and Estimation of Dry Deposition over Grassland in Eastern Germany, Transactions on Ecology and

Environment, 28, 223-227, 1999.

Stutz, J., Alicke, B., Neftel, A.: Nitrous acid formation in the urban atmosphere: Gradient measurements of NO_2 and HONO over grass in Milan, Italy, J. Geophys. Res., 107, LOP 5-1-LOP 5-15, https://doi.org/10.1029/2001JD000390, 2002.

Su, H., Cheng, Y. F., Cheng, P., Zhang, Y. H., Dong, S. F., Zeng, L. M., Wang, X. S., Slanina, J., Shao, M., and Wiedensohler, A.: Observation of nighttime nitrous acid (HONO) formation at a non-urban site during PRIDE-PRD2004 in China, Atmos. Environ., 42, 6219-6232, https://doi.org/10.1016/j.atmosenv.2008.04.006, 2008.

Tong, S. R., Hou, S. Q., Zhang, Y., Chu, B. W., Liu, Y. C., He, H., Zhao, P. S., and Ge, M. F.: Exploring the nitrous acid (HONO) formation mechanism in winter Beijing: direct emissions and heterogeneous production in urban and suburban areas, Faraday Discuss., 189, 213-230, https://doi.org/10.1039/c5fd00163c, 2016.

VandenBoer, T. C., Brown, S. S., Murphy, J. G., Keene, W. C., Young, C. J., Pszenny, A. A. P., Kim, S., Warneke, C., de Gouw, J. A., Maben, J. R., Wagner, N. L., Riedel, T. P., Thornton, J. A., Wolfe, D. E., Dubé, W. P., Öztürk, F., Brock, C. A., Grossberg, N., Lefer, B., Lerner, B., Middlebrook, A. M., and Roberts, J. M.: Understanding the role of the ground surface in HONO vertical structure: High resolution vertical profiles during NACHTT-11, J. Geophy. Res.- Atmos., 118, 10155-110171, https://doi.org/10.1002/jgrd.50721, 2013.

Wang, H. C., Lu, K. D., Chen, X. R., Zhu, Q. D., Wu, Z. J., Wu, Y. S., and Sun, K.: Fast particulate nitrate formation via N_2O_5 uptake aloft in winter in Beijing, Atmos. Chem. Phys., 18, 10483-10495, https://doi.org/10.5194/acp-18-10483-2018, 2018.

Wong, K. W., Oh, H. -J., Lefer, B. L., Rappenglück, B., and Stutz, J.: Vertical profiles of nitrous acid in the nocturnal urban atmosphere of Houston, TX, Atmos. Chem. Phys., 11, 3595-3609, https://doi.org/10.5194/acp-11-3595-2011, 2011.

Xu, Z., Wang, T., Wu, J. Q., Xue, L. K., Chan, J., Zha, Q., Z., Zhou, S. Z., Louie, P. K. K., and Luk, C. W. Y.: Nitrous acid (HONO) in a polluted subtropical atmosphere: Seasonal variability, direct vehicle emissions and heterogeneous production at ground surface, Atmos. Environ., 106, 100-109, https://doi.org/10.1016/j.atmosenv.2015.01.061, 2015.

Yang, Q., Su, H., Li, X., Cheng, Y. F., Lu, K. D., Cheng, P., Gu, J. W., Guo, S., Hu, M., Zeng, L. M., Zhu, T., and Zhang, Y. H.: Daytime HONO formation in the suburban area of the megacity Beijing,

China, Sci. China Chem., 57, 1032-1042, https://doi.org/10.1007/s11426-013-5044-0, 2014.

Ye, C. X., Zhou, X. L., Pu, D., Stutz, J., Festa, J., Spolaor, M., Tsai, C., Cantrell, C., Mauldin III, R. L., Weinheimer, A., Hornbrook, R. S., Apel, E. C., Guenther, A., Kaser, L., Yuan, B., Karl, T., Haggerty, J., Hall, S., Ullmann, K., Smith, J., and Ortega, J.: Tropospheric HONO distribution and chemistry in the southeastern US, Atmos. Chem. Phys., 18, 9107-9120, https://doi.org/10.5194/acp-18-9107-2018, 2018.

Zhang, N., Zhou, X. L., Shepson, P. B., Gao, H. L., Alaghmand, M., and Stirm, B.: Aircraft measurement of HONO vertical profiles over a forested region, Geophys. Res. Lett., 36, L15820, https://doi.org/10.1029/2009GL038999, 2009.

Zhang, W. Q., Tong, S. R., Ge, M. F., An, J. L., Shi, Z. B., Hou, S. Q., Xia, K. H., Qu, Y., Zhang, H. X., Chu, B. W., Sun, Y. L., and He, H.: Variations and sources of nitrous acid (HONO) during a severe pollution episode in Beijing in winter 2016, Sci. Total Environ., 648, 253-262, https://doi.org/10.1016/j.scitotenv.2018.08.133, 2018.

3. Response to interactive comments on "High resolution vertical distribution and sources of HONO and NO_2 in the nocturnal boundary layer in urban Beijing, China" by Jörg Kleffmann

The gradient study presented in Meng et al. is a nice piece of work showing night-time gradient data on a meteorological tower up to 250 m altitude similar to our former study (Kleffmann et al., 2003). Here a measurement container is lifted on the side wiring of the tower, far away from the open steel construction of the tower, thus minimizing potential wall effects, which is a nice idea. I strongly encourage the authors to extent these measurements including other important species for the future.

Response: We would like to thank Jörg Kleffmann for his time and efforts in preparing this detailed and constructive comments. We have revised the manuscript accordingly to address his concerns. Here are our point-to-point response to Jörg Kleffmann's specific comments.

Major Comments:

1. Direct HONO emissions (section 3.3):

The authors determined the HONO/NO_x emission ratio from the minimum HONO/NO_x ratio, which by definition will only result in an upper limit value, since always some secondary HONO is included in ambient measurement data. If emission ratios should be derived from field data, the authors should look for sharp peaks during night-time and should evaluate only the elevations of HONO and NO_x over the background levels (DHONO/DNO_x). In this case the risk overestimating direct emissions is minimized but still even this peak data presents an upper limit caused by potential secondary HONO formation during transport from the emission to the measurement site (will be short for sharp concentration peaks). I expect that the HONO/NO_x emission ratio derived by the peak method will be considerably lower, closer to direct emission data (see test stands and tunnel data: <1%). The use of correct HONO emission data is important for the whole study, since emission corrected HONO data (considerable ca. 50% contribution, typically emissions have 10-20 % contribution) is used later for the evaluation of the other HONO sources.

Response: Thank you very much for your valuable comments and suggestions. The emission factors have been derived from tunnel measurements in previous studies (Kirchstetter et al., 1996; Kurtenbach et al., 2001; Laing et al., 2017). However, considering the differences in vehicle types, fuel compositions, and other factors, the previously reported emission ratios might not be representative for Beijing region. In order to obtain the local emission factor, the HONO/NO_x ratio

was derived from field data. Following Jörg Kleffmann's suggestion, five criteria were applied to ensure as much of the freshly emitted air masses as possible: (a) only nighttime data (from 18:00 LT to next 6:00 LT) were included to avoid the fast photolysis of HONO; (b) only sharp peaks during nighttime and the elevations of HONO and NO_x over the background levels were estimated; (c) $\Delta NO/\Delta NO_x > 0.80$; (d) good correlation between HONO and NO_x; (d) short duration of the plume (< 30 min). The typical nocturnal wind speed at measurement site was 1.2 m s^{-1}, thus the duration for fresh air masses should have been less 30 min during transport from the emission to the measurement site. Criteria (b), (c), (d) and (e) were used as indicators for identifying fresh vehicular emissions.

For a month field observation, 11 fresh plumes satisfied selection criteria (Table 1). Two examples of emission plumes selected based on the preceding criteria are shown in Fig. R1.

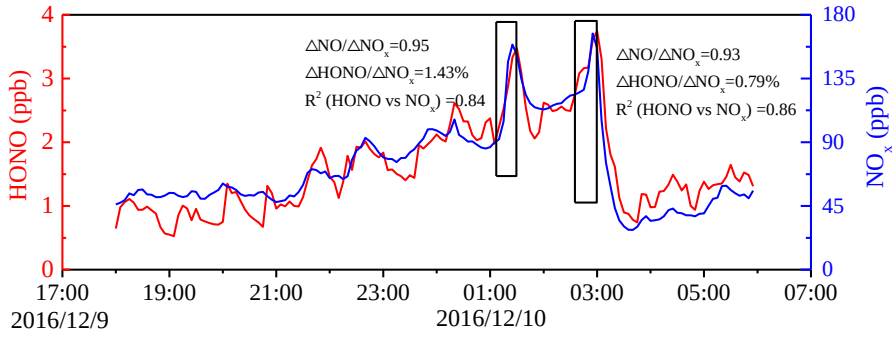

Figure R1. Temporal variation of nocturnal HONO and NO_x on December 9th to 10th, 2016. The HONO emission ratios were estimated using data collected in the black frame.

The derived $HONO/NO_x$ ratios vary from 0.78% to 1.73%, with an average value of 1.28% ± 0.36%, which was larger than the 0.53%–0.8% measured in the tunnel in Wuppertal (Kurtenbach et al., 2001), but in the range of 0.19%–2.1% reported by previous studies (Kirchstetter et al., 1996; Kurtenbach et al., 2001; Su et al., 2008; Rappengluck et al., 2013; Yang et al., 2014; Xu et al., 2015; Liang et al., 2017; Zhang et al., 2018; Li et al., 2018). Comparison of derived $HONO/NO_x$ ratios with previously reported results are summarized Table S2 in the supplementary information. To minimize the risk of overestimating the direct HONO emissions, the minimum $HONO/NO_x$ ratio of 0.78% was used as an upper limit for the emission factor (Su et al., 2008). The direct emissions contributed an average of 29.3% ± 12.4% to the ambient HONO levels at night, with an average $HONO_{emis}$/HONO value of 35.9% ± 11.8% during the clean episode and an average $HONO_{emis}$/HONO value of 26% ± 11.3% during the haze episode. The lower vehicle emissions contribution during haze episode could be

caused by an odd-even car ban, which required alternate driving days for cars with even- and odd-numbered license plates.

2. HONO formation on aerosol surfaces (section 3.4.2).

The authors used heterogeneous uptake data for NO_2 derived in the laboratory to calculate potential HONO formation during night-time. However some studies cited/considered focus on the daytime production of HONO by photosensitized conversion (George et al., Sremmler et al.), leading to overestimation of the night-time conversion. Here references to other dark studies are recommended and it should be mentioned that the used value of 10^-5 represents really the upper limit night-time kinetics (typically 10^-6 is used in the dark). In addition, the authors should explain that they considered a 100 % yield for the NO_2 conversion (see factor $\frac{1}{4}$ in eq. (1)), which is also the upper limit, e.g. when using the typically considered night-time reaction R1: $2NO_2+H_2O=>HONO+HNO_3$ (see the first reference used in line 370) for which the maximum yield is 50 %. So please define that a redox reaction ($NO_2+X=>HONO$) is considered here. But all this will even further decrease the low contribution of particle surfaces to the night-time HONO production, which is in line with my own point of view.

Response: Thanks for the comment and suggestion. The references (George et al., 2005; Stemmler et al., 2007) have been changed to the following one:

Saastad, O. W., Ellermann, T., and Nielsen, C., J.: On the adsorption of NO and NO_2 on cold H2O/H2SO4 surfaces, Geophys. Res. Lett., 20, 1191-1193, https://doi.org/10.1029/93GL01621, 1993.

Following the referee #1's suggestion, the NO_2 uptake coefficient of 1×10^{-5} to 1×10^{-6} in the dark were used to estimate the nighttime production of HONO from heterogeneous conversion of NO_2 on aerosol surface. The yield for the NO_2 conversion and night-time reaction have been stated in the revised manuscript as suggested. A typical heterogeneous reaction ($2NO_{2(g)}+H_2O_{(ads)} \xrightarrow{surface} HONO_{(g)}+HNO_{3(ads)}$) and the maximum yield of 50% were considered in evaluating the HONO production on aerosols, the yield of hydrolysis reaction assumes that HONO and HNO_3 are formed by equimolar disproportionation of two NO_2 molecules and immediately release HONO (Finlayson-Pitts et al., 2003; Finlayson-Pitts, 2009). The reactive uptake of NO_2 by the aerosol was assumed to occur on all measured aerosol surface area, regardless of chemical composition. The

production of HONO on aerosol surface can be estimated using the equation of Ye et al. (2018) modified to account for the disproportionation.

The newly obtained aerosol surface areas at ground and at 260 m, which was corrected to ambient aerosol surface area (S_{aw}) for particle hygroscopicity via a growth factor (Liu et al., 2013; Wang et al., 2018), were used to estimate the nocturnal HONO production from heterogeneous reaction of NO_2 on aerosol surface. An estimate of HONO production on aerosols was made using an average observed S_{aw} of 2314 μm^2 cm^{-3} between 22 and 01 h (the vertical measurement periods on December 11th) and an upper limit of observed NO_2 of 54 ppb from the residual layer. The HONO production of 30-300 ppt in an interval of 1.5 h could account for HONO increases of 15-368 ppt in the residual layer between profile measurements during E3. Therefore, the production of HONO solely on aerosols can explain the HONO observations during the haze episode, implying that the aerosols plays an important role in nocturnal production of HONO during the haze episode. The same analysis was discussed for other vertical measurements during C2. The results indicated that the ground surface dominated HONO production by the heterogeneous uptake of NO_2 during the clean episode.

3. Nocturnal HONO production on the ground (section 3.4.3):

Instead of using the "two-point" equation (4), simply plot the night-time HONO/NO_2 ratio as a function of the time. In this case the slope determined by linear regression will statistically better describe the efficient first order NO_2=>HONO conversion rate constant. Since this is a rate coefficient, it should be better termed by e.g. "k(het)" and not by the term "C" (C: concentration?), which I often found in recent Chinese HONO papers? Since HONO(corr.) will be significantly higher (see point 1) also the efficient conversion rate coefficient will increase.

In this section the authors also determine a net HONO yield from the ground surface conversion of NO_2 of the order of 10 % by using deposition velocities for HONO and NO_2. The value for HONO is to my opinion too low and will be more of the order of 2 cm/s (see cited studies and others). In addition please specify the value used for NO_2. The HONO yield determined is quite high and our recent gradient study (Laufs et al., Atmos. Chem. Phys., 17, 6907–6923, 2017) could be also cited, where we determined lower values in the range of 0.02-0.044 by a more direct approach in good agreement with the gradient study by Stutz et al., 2002 (0.03). In addition you will find there also data

for the deposition velocity of HONO, confirming a higher value, at least at the low temperatures of the present study.

Response: The term "*C*" is first letter of the conversion, and we used the term "k_{HONO}" for conversion frequency as suggested. The conversion frequency (k_{HONO}) has been recalculated following the method introduced by Alicke et al. (2002). The local emission factor of 0.78% derived from field data was used to correct HONO concentration (i.e. $[HONO]_{corr} = [HONO] - [NO_x] \times 0.0078$). Since NO was not measured at ground level after 14:00 on December 10th, the average $HONO_{emis}$/HONO ratio of 35.9% ± 11.8% and 26% ± 11.3% were used to correct HONO observations during the clean and the haze episodes, respectively (i.e. $[HONO]_{corr} = [HONO] - [HONO]_{emis}$). The conversion frequencies, k_{HONO}, on December 9th, 10th, and 11th were 0.0082 h^{-1}, 0.0060 h^{-1}, and 0.0114 h^{-1}, respectively.

As Jörg Kleffmann suggested, the temperature-dependent deposition velocity of HONO ($V(HONO)_T = \exp(23920/T - 91.5)$) was used to estimate the dry deposition velocity of HONO (Laufs et al., 2017). The average $V_{dep,HONO}$ calculated from nocturnal observations (00:00–06:00 LT) was 1.8 cm s^{-1}, with a range of values spanning 0.9 to 3 cm s^{-1}, which was within the range of previously reported values between 0.077 and 3 cm s^{-1} (Harrison and Kitto, 1994; Harrison et al., 1996; Spindler et al., 1998; Stutz et al., 2002; Coe and Gallagher, 1992; Laufs et al., 2017). The NO_2 deposition velocity (V_{dep,NO_2}) of 0.07 cm s^{-1} (VandenBoer et al., 2013) used in calculation has been specified in the revised manuscript. Following the suggestion by the referee #1 and #3, we have significantly revised the discussion in section 3.4.3. A net HONO yield from the surface heterogeneous conversion of NO_2 has been removed in the revised manuscript. The surface production rate of HONO was calculated to compare with other HONO sources.

4. Concept used:

The authors tried to distinguish between heterogeneous night-time formation of HONO on particle surfaces and on the ground, which is an important question with respect to the decades long discussion on the sources of HONO in the atmosphere. Here first, I am missing a more focused introduction of the basic problem. There are ground level studies, which found a nice correlation of HONO/NO_2 with the particle surface area and which propose HONO formation on particles. On the other hand there are gradient studies of HONO (and NO_2) which typically determine a negative

gradient, pointing to the ground as most important surface. However, none of these studies can answer the question! The correlation with particles could be also explained by the variation of the vertical mixing and the fact that both, HONO and particles are emitted/formed near the ground. Here pioneering studies by A. Febo found nice correlation of HONO with Radon during night-time and there is clearly no chemical link between both species. On the other hand the gradients could be also explained by formation on particle surfaces, if there is also a negative gradient in the particle surface area density (S/V). So what we need are gradient measurements over a few hundred meters (like the present study) but including besides HONO and its precursors (most probably NO_2) also the surface area density (see our former study Kleffmann et al., 2003). Only if there is no gradient in the particles, a negative gradient of the HONO/NO_2 ratio will show HONO formation on the ground. Thus, second, I strongly recommend that the authors use this nice tower set-up and include in future campaigns also fast particles and NO measurements!

The later is important since the titration reaction of NO+O_3 may mask the observation leading e.g. to artificial gradients of the HONO/NO_2 ratio not resulting by any HONO processes, but simply by a changing NO_2/NO_x ratio. For example, the decreasing HONO/NO_2 ratio shown in Figure S4 (see first two gradients near the ground) is not plausible since the HONO/NO_x ratio is expected to increase during the night. Most probably NO was converted into NO_2 leading to lower HONO/NO_2 ratio.

Response: We would like to thank Jörg Kleffmann for his introduction to the basic problem of heterogeneous nighttime formation of HONO and his constructive suggestions. The primary reaction surfaces for the nocturnal heterogeneous production of HONO is still controversial, and the role of the aerosols in the heterogeneous production of HONO remains an open question. In this study, we try to explain this problem by investigating the high-resolution vertical profiles of HONO at night. The aerosols as an important nocturnal source of HONO during haze episode was observed. However, this campaign only includes the limited vertical measurement data (only HONO and NO_2 vertical profiles). As Jörg Kleffmann said, the vertical measurements including besides HONO and NO_2 also the aerosol surface areas and NO are needed to investigate the HONO chemistry, while the gradient measurement based on the nice tower set-up provides the basis for our future research. A more comprehensive vertical measurement campaign will performed in the future, including not only the vertical profiles of HONO and NO_2, but also the aerosol surface area and NO measurement.

Minor Comments:

1. There are numerous errors in the references, please check, examples: Line 60: Vogel et al.; missing blanks between the references (throughout the whole manuscript). Line 68: Bröske et al., etc.

Response: As suggested, we have checked and corrected the references in the revised manuscript.

2. Line 76: the photocatalytic conversion of NO_2 on TiO_2 ("mineral dust") is not a redox reaction.

Response: Following the suggestion by the referee #3, the introduction section has been revised. This statement has been removed in the revised manuscript.

3. Line 77-82, R2: This reaction is not a photosensitized conversion.

Response: Thanks for the comment. This reaction (R2) is a heterogeneous reaction, and we adjusted it to a more suitable position (line 95).

4. Lines 84-88: In the cited studies neither all used a DOAS, nor was the DOAS installed on an elevator.

Response: The statements and cited references have been revised in this paragraph, as below:

Lines 122–128:

"Vertical gradient observations provide evidence regarding surfaces and in situ HONO formation, which can help to understand the nighttime HONO sources. Methods of long-path differential optical absorption spectroscopy (LP-DOAS) (Stutz et al., 2002; Wong et al., 2011; Wong et al., 2012), instruments mounted on a movable elevator of a tall tower or a fixed height on a building (Kleffmann et al., 2003; VandenBoer et al., 2013; Villena et al., 2011) and aircraft measurements (Zhang et al., 2009; Li et al., 2014; Ye et al., 2018) have been applied for HONO vertical gradient observations in Europe and the America."

5. Line 93-94: In our gradient study in Chile the measurement frequency was very high, only the vertical resolution was low (should be "or").

Response: Revision has made as Jörg Kleffmann suggested.

6. Line 106-110: Please add our recent flux study Laufs et al., 2017 (see above).

Response: The introduction section of the manuscript has been revised accordingly to address the referee's comments. This paragraph (lines 163–170) have been removed in the revised manuscript, but the flux literature has been added to other parts of the manuscript.

7. Lines 381-384, Fig.11: I do not understand that statement. The figure shows only the column average HONO concentration is near (81%) to the ground level. That could be also explained by a particle source?

Response: Correlation between the column average HONO concentration and HONO measured from the ground level to 10 m in height have been reanalyzed during the clean and the haze episodes, respectively. The production of HONO on aerosols explained the HONO observations in the residual layer during E3. If the production of HONO was indeed dominated by heterogeneous reaction of NO_2 on aerosol and ground surfaces, the column average HONO concentration is expected to be irrelevant or relevant to the mixing ratio of HONO observed from the ground level to 10 m. Figure 10a showed that column average concentration of HONO is irrelevant to the amounts of HONO observed between the ground level and 10 m in height (R^2 = 0.27), which suggested that the aerosols dominated the production of HONO aloft by the heterogeneous reaction of NO_2 during the haze episode. However, a high correlation (R^2 = 0.93) between the column average HONO concentration and HONO measured from the ground level to 10 m was observed during C2 (Figure 10b), which suggested a surface HONO source at night during the clean episode. The HONO observed throughout the depth of the boundary layer was primarily derived from heterogeneous conversion of NO_2 on the ground followed by vertical transport throughout the column. The statements of Figure 10 (the original Figure 11) have been significantly revised in the manuscript to make our argument more clearly.

8. Figures 7+8: The concentrations in the residual layer typically represent daytime levels (in the absence of a volume source of HONO). Here HONO levels of 1-2 ppb are observed, which should be discussed. Such high HONO levels at 250 m altitude are really exceptional!

Response: We sincerely thank the Jörg Kleffmann for his constructive advice. We completely agree with Jörg Kleffmann that high HONO levels in the residual layer (typically represents HONO daytime levels) are well worth studying. However, this study primarily focused on the investigation of the vertical distribution of nocturnal HONO and relative importance of aerosol and ground surfaces in nocturnal HONO production at different pollution levels. The limited vertical measurement and

ancillary data restricted the analysis on daytime HONO levels. In the future, we plan to conduct further in-depth research on the daytime HONO. Combined with more comprehensive vertical measurements, the vertical distribution and sources/sinks of daytime HONO will be studied.

References:

Alicke, B., Platt, U., Stutz, J.: Impact of nitrous acid photolysis on the total hydroxyl radical budget during the Limitation of Oxidant Production/Pianura Padana Produzione di Ozono study in Milan, J. Geophys. Res., 107, LOP 9-1-LOP 9-17, https://doi.org/10.1029/2000jd000075, 2002.

Brown, S. S., Dubé, W. P., Osthoff, H. D., Wolfe, D. E., Angevine, W. M., and Ravishankara, A. R.: High resolution vertical distributions of NO_3 and N_2O_5 through the nocturnal boundary layer, Atmos. Chem. Phys., 7, 139-149, https://doi.org/10.5194/acp-7-139-2007, 2007.

George, C., Strekowski, R. S., Kleffmann, J., Stemmler, K., and Ammann, M.: Photoenhanced uptake of gaseous NO_2 on solid organic compounds: a photochemical source of HONO?, Faraday Discuss., 130, 195-210, https://doi.org/10.1039/b417888m, 2005.

Coe, H., and Gallagher, M. W.: Measurements of Dry Deposition of NO_2 to A Dutch Heathland Using the Eddy-Correlation Technique, Q. J. Roy. Meteor. Soc., 118, 767-786, https://doi.org/10.1002/qj.49711850608, 1992.

Finlayson-Pitts, B. J., Wingen, L. M., Sumner, A. L., Syomin, D., and Ramazan, K. A.: The heterogeneous hydrolysis of NO_2 in laboratory systems and in outdoor and indoor atmospheres: An integrated mechanism, Phys. Chem. Chem. Phys., 5, 223-242, https://doi.org/10.1039/b208564j, 2003.

Finlayson-Pitts, B. J.: Reactions at surfaces in the atmosphere: integration of experiments and theory as necessary (but not necessarily sufficient) for predicting the physical chemistry of aerosols, Phys. Chem. Chem. Phys., 36, 7760-7779, https://doi.org/10.1039/B906540G, 2009.

Harrison, R. M., and Kitto, A. M. N.: Evidence for a surface source of atmospheric nitrous acid, Atmos. Environ., 28, 1089-1094, https://doi.org/10.1016/1352-2310(94)90286-0, 1994.

Harrison, R. M., Peak, J. D., and Collins, G. M.: Tropospheric cycle of nitrous acid, J. Geophys. Res., 101, 14429-14439, https://doi.org/10.1029/96JD00341, 1996.

Kirchstetter, T. W., Harley, R. A., and Littlejohn D.: Measurement of nitrous acid in motor vehicle

exhaust, Environ. Sci. Technol., 30, 2843-2849, https://doi.org/10.1021/es960135y, 1996.

Kurtenbach, R., Becker, K. H., Gomes, J. A. G., Kleffmann, J., Lörzer, J., Spittler, M., Wiesen, P., Ackermann, R., Geyer, A., and Platt, U.: Investigations of emission and heterogeneous formation of HONO in a road traffic tunnel, Atmos. Environ., 35, 3385–3394, https://doi.org/10.1016/S1352-2310(01)00138-8, 2001.

Laufs, S., Cazaunau, M., Stella, P., Kurtenbach, R., Cellier, P., Mellouki, A., Loubet, B., and Kleffmann, J.: Diurnal fluxes of HONO above a crop rotation, Atmos. Chem. Phys., 17, 6907-6923, https://doi.org/10.5194/acp-17-6907-2017, 2017.

Li, D. D., Xue, L. K., Wen, L., Wang, X. F., Chen, T. S., Mellouki, A., Chen, J. M., and Wang, W. X.: Characteristics and sources of nitrous acid in an urban atmosphere of northern China: Results from 1-yr continuous observations, Atmos. Environ., 182, 296-306, https://doi.org/10.1016/j.atmosenv.2018.03.033, 2018.

Liang, Y. T., Zha, Q. Z., Wang, W. H., Cui, L., Lui, K. H., Ho, K. F., Wang, Z., Lee, S. C., and Wang, T.: Revisiting nitrous acid (HONO) emission from on-road vehicles: A tunnel study with a mixed fleet, J. Air Waste Manag., 67, 797-805, https://doi.org/10.1080/10962247.2017.1293573, 2017.

Liu, X., Cheng, Y., Zhang, Y., Jung, J., Sugimoto, N., Chang, S.Y., Kim, Y. J., Fan, S., and Zeng, L.: Influences of relative humidity and particle chemical composition on aerosol scattering properties during the 2006 PRD campaign, Atmos. Environ., 42, 1525–1536, https://doi.org/10.1016/j.atmosenv.2007.10.077, 2008.

Rappenglück, B., Lubertino, G., Alvarez, S., Golovko, J., Czader, B., and Ackermann, L.: Radical precursors and related species from traffic as observed and modeled at an urban highway junction, J. Air Waste Manag. Assoc., 63, 1270-1286, https://doi.org/10.1080/10962247.2013.822438, 2013.

Spindler, G., Brüggemann, E., and Herrmann, H.: Nitrous acid (HNO_2) Concentration Measurements and Estimation of Dry Deposition over Grassland in Eastern Germany, Transactions on Ecology and Environment, 28, 223-227, 1999.

Stemmler, K., Ndour, M., Elshorbany, Y., Kleffmann, J., D'Anna, B., George, C., Bohn, B., and Ammann, M.: Light induced conversion of nitrogen dioxide into nitrous acid on submicron humic acid aerosol, Atmos. Chem. Phys., 7, 4237-4248, https://doi.org/10.5194/acp-7-4237-2007, 2007.

Stutz, J., Alicke, B., Neftel, A.: Nitrous acid formation in the urban atmosphere: Gradient measurements of NO_2 and HONO over grass in Milan, Italy, J. Geophys. Res., 107, LOP 5-1-LOP

5-15, https://doi.org/10.1029/2001JD000390, 2002.

Su, H., Cheng, Y. F., Cheng, P., Zhang, Y. H., Dong, S. F., Zeng, L. M., Wang, X. S., Slanina, J., Shao, M., and Wiedensohler, A.: Observation of nighttime nitrous acid (HONO) formation at a non-urban site during PRIDE-PRD2004 in China, Atmos. Environ., 42, 6219-6232, https://doi.org/10.1016/j.atmosenv.2008.04.006, 2008.

VandenBoer, T. C., Brown, S. S., Murphy, J. G., Keene, W. C., Young, C. J., Pszenny, A. A. P., Kim, S., Warneke, C., de Gouw, J. A., Maben, J. R., Wagner, N. L., Riedel, T. P., Thornton, J. A., Wolfe, D. E., Dubé, W. P., Öztürk, F., Brock, C. A., Grossberg, N., Lefer, B., Lerner, B., Middlebrook, A. M., and Roberts, J. M.: Understanding the role of the ground surface in HONO vertical structure: High resolution vertical profiles during NACHTT-11, J. Geophy. Res.- Atmos., 118, 10155-110171, https://doi.org/10.1002/jgrd.50721, 2013.

Wang, H. C., Lu, K. D., Chen, X. R., Zhu, Q. D., Wu, Z. J., Wu, Y. S., and Sun, K.: Fast particulate nitrate formation via N_2O_5 uptake aloft in winter in Beijing, Atmos. Chem. Phys., 18, 10483-10495, https://doi.org/10.5194/acp-18-10483-2018, 2018.

Xu, Z., Wang, T., Wu, J. Q., Xue, L. K., Chan, J., Zha, Q., Z., Zhou, S. Z., Louie, P. K. K., and Luk, C. W. Y.: Nitrous acid (HONO) in a polluted subtropical atmosphere: Seasonal variability, direct vehicle emissions and heterogeneous production at ground surface, Atmos. Environ., 106, 100-109, https://doi.org/10.1016/j.atmosenv.2015.01.061, 2015.

Yang, Q., Su, H., Li, X., Cheng, Y. F., Lu, K. D., Cheng, P., Gu, J. W., Guo, S., Hu, M., Zeng, L. M., Zhu, T., and Zhang, Y. H.: Daytime HONO formation in the suburban area of the megacity Beijing, China, Sci. China Chem., 57, 1032-1042, https://doi.org/10.1007/s11426-013-5044-0, 2014.

Ye, C. X., Zhou, X. L., Pu, D., Stutz, J., Festa, J., Spolaor, M., Tsai, C., Cantrell, C., Mauldin III, R. L., Weinheimer, A., Hornbrook, R. S., Apel, E. C., Guenther, A., Kaser, L., Yuan, B., Karl, T., Haggerty, J., Hall, S., Ullmann, K., Smith, J., and Ortega, J.: Tropospheric HONO distribution and chemistry in the southeastern US, Atmos. Chem. Phys., 18, 9107-9120, https://doi.org/10.5194/acp-18-9107-2018, 2018.

Zhang, W. Q., Tong, S. R., Ge, M. F., An, J. L., Shi, Z. B., Hou, S. Q., Xia, K. H., Qu, Y., Zhang, H. X., Chu, B. W., Sun, Y. L., and He, H.: Variations and sources of nitrous acid (HONO) during a severe pollution episode in Beijing in winter 2016, Sci. Total Environ., 648, 253-262, https://doi.org/10.1016/j.scitotenv.2018.08.133, 2018.

High resolution vertical distribution and sources of HONO and NO_2 in the nocturnal boundary layer in urban Beijing, China

Fanhao Meng[1,2], Min Qin[1], Ke Tang[1,2], Jun Duan[1], Wu Fang[1], Shuaixi Liang[1,2], Kaidi Ye[1,2], Pinhua Xie[1,2,3,5], Yele Sun[3,4,5], Conghui Xie[4], Chunxiang Ye[6], Pingqing Fu[4,*], Jianguo Liu[1,2,3], Wenqing Liu[1,2,3]

[1]Key Laboratory of Environmental Optics and Technology, Anhui Institute of Optics and Fine Mechanics, Chinese Academy of Sciences, Hefei, 230031, China

[2]University of Science and Technology of China, Hefei, 230027, China

[3]Center for Excellence in Regional Atmospheric Environment, Institute of Urban Environment, Chinese Academy of Sciences, Xiamen, 361021, China

[4]State Key Laboratory of Atmospheric Boundary Layer Physics and Atmospheric Chemistry, Institute of Atmospheric Physics, Chinese Academy of Sciences, Beijing, 100029, China

[5]University of Chinese Academy of Sciences, Beijing, 100049, China

[6]State Key Joint Laboratory of Environmental Simulation and Pollution Control, College of Environmental Sciences and Engineering, Peking University, Beijing, China

[*]now at: Institute of Surface-Earth System Science, Tianjing University, Tianjing, 300072, China

Correspondence: Min Qin (mqin@aiofm.ac.cn)

Abstract. Nitrous acid (HONO), an important precursor of the hydroxyl radical (OH), plays a key role in atmospheric chemistry, but its sources are still debated. The production of HONO on aerosol surface ~~and~~ or on ground surface in nocturnal ~~urban~~ atmospheres ~~is of interests~~ remains controversial. ~~However, ground surface measurement commonly in our society is not able to distinguish these two parts. Here, for the first time, we reported~~ The vertical profile provides vertical information on HONO and NO_2 to understand the nocturnal HONO production and loss. In this study, we report the first high-resolution (<2.5 m) nocturnal vertical profiles ~~measurements~~ of HONO and NO_2 ~~in urban Beijing at night using an incoherent broadband cavity enhanced absorption spectrometer (IBBCEAS) amounted~~ measured from in-suit instruments on a movable container ~~which~~ that was ~~attached to~~ lifted on the side wiring of a 325-m meteorological tower in Beijing, China. ~~of 325-m high~~. ~~The mixing ratios of HONO during one a haze episode (E1), the a clean episode (C2), and another haze episode (E3) were 4.26 ± 2.08,~~

~~0.83 ± 0.65 and 3.54 ± 0.91 ppb, respectively. High-resolution vertical profiles revealed that the vertical distribution of HONO is consistent with stratification and layering in the nocturnal urban atmosphere below 250 m.~~ High-resolution vertical profiles revealed the negative gradients of HONO and NO_2 in nocturnal boundary layers, and a shallow inversion layer affected the vertical distribution of HONO. The vertical distribution of HONO was consistent with stratification and layering in the nocturnal urban atmosphere below 250 m. The increase of HONO/NO_2 ratio was observed throughout the column from the clean episode to the haze episode, and a relatively constant HONO/NO_2 ratios in the residual layer were observed during the haze episode. Direct HONO emissions from ~~combustion processes~~ traffic contributed ~~51.1%~~ 29.3% ± 12.4% to the ambient HONO concentrations at night. ~~The HONO production from the heterogeneous conversion of NO_2 on the aerosol surfaces cannot explain HONO vertical measurements at night, indicating that the heterogeneous reaction of NO_2 on ground surfaces dominated the nocturnal HONO production. The nocturnal HONO in the boundary layer is primarily derived from the heterogeneous conversion of NO_2 at ground level and direct emissions; it is then transported throughout the column by vertical convection. $\phi_{NO_2 \to HONO}$, the HONO yield from deposited NO_2, is used to evaluate HONO production from the heterogeneous conversion of NO_2 at night. The derived $\phi_{NO_2 \to HONO}$ $\eta_{NO_2 \to HONO}$ values on 9 (C2), 10 (C2) and 11 December (E3) were 0.10, 0.08, and 0.09 0.04, 0.046 and 0.039, respectively, indicating a significant production of HONO from heterogeneous reaction of NO_2 at ground level. The similar $\phi_{NO_2 \to HONO}$ values measured during clean and haze episodes suggest that the heterogeneous conversion potential of NO_2 at ground level is consistent at night. Furthermore, the dry deposition loss of HONO to the ground surface and vertical mixing effects associated with convection reached a near steady state at midnight on 11–12 December, indicating that significant quantities of HONO are deposited to the ground surface at night, and the ground surface is the source and sink of HONO at night.~~ The ground surface dominates HONO production by heterogeneous uptake of NO_2 during the clean episode. In contrast, the HONO production solely on aerosols (30–300 ppt) explained the observed HONO increases (15–368 ppt) in the residual layer, suggesting that the aerosol surface was the location where the HONO was formed, which could presumably dominate the production of HONO aloft during the haze episode. Average dry deposition rates of 0.74 ± 0.31 and 1.55 ± 0.32 ppb h^{-1} were estimated during the clean and haze episodes, implying that significant quantities of HONO could be deposited to the ground surface at night. Our results highlight ever-changing contributions of aerosol and ground surfaces in nocturnal

HONO production at different pollution levels and encourage more vertical gradient observations to evaluate the contributions from varied HONO sources.

1 Introduction

It is well known that the rapid photolysis of nitrous acid (HONO) (R1) after sunrise is the most important hydroxyl radical (OH) source. 25%~~–90%~~60% of daytime OH production was accounted ~~by~~ for due to HONO photolysis, according to previously reported (Lu et al., 2012; Ma et al., 2017; Tong et al., 2016; Su et al., 2008b; Huang et al., 2017; ~~Hendrick et al., 2014;~~ Spataro et al., 2013). OH initiates daytime photochemistry and promotes the formation of secondary products (including ozone (O_3)~~,~~ and peroxyacetyl nitrate (PAN)) and secondary aerosols (Alicke and Platt, 2002; Tang et al., 2015; Kleffmann, 2007; An et al., 2012). In addition, HONO as a nitrosating agent forms carcinogenic nitrosamines (Sleiman et al., 2010; Bartolomei et al., 2015; Gómez Alvarez et al., 2014), and its health effects have attracted increasing amounts of concern (Hanst et al., 1977; Pitts et al., 1978). ~~there is a growing concern about the possible health effects of the formation of nitrosamines (Hanst et al., 1977; Pitts et al., 1978), in which HONO acts as a nitrosating agent to form carcinogenic nitrosamines (Sleiman et al., 2010; Bartolomei et al., 2015; Gómez Alvarez et al., 2014).~~

$$\mathrm{HONO}+h\nu\left(320\mathrm{nm}<\lambda<405\mathrm{nm}\right)\rightarrow\mathrm{NO}+\mathrm{OH} \quad \text{(R1)}$$

Despite the importance of HONO, the details of the formation processes of HONO in the atmosphere ~~remain unclear.~~ are debated for decades. New~~ly~~ ~~available~~ state-of-the-art science instruments have observed much higher daytime HONO concentrations than simulated values from atmospheric chemical models in both rural and urban areas, implying missing HONO sources (Li et al., 2012; Wang et al., 2017; Oswald et al., 2015; Wong et al., 2012; Li et al., 2014; Liu et al., 2019; Karamchandani et al., 2015; Kleffmann, 2007; Mendez et al., 2017; Michoud et al., 2014; Michoud et al., 2015; Tang et al., 2015; Vogela et al., 2003; Sörgel et al., 2011). Several homogeneous reaction mechanisms for HONO have been proposed, but the latter have been considered as irrelevant ~~in real~~ under actual atmospheric conditions, including photolysis of ortho-substituted nitroaromatics (Bejan et al., 2006) and the reaction of photoexcited NO_2 with H_2O (Li et al., 2008). The heterogeneous reduction of NO_2 with organic substrates is proposed to be another effective pathway to generate HONO (Brigante et al., 2008; Stemmler et al., 2006; George et al., 2005). However, extrapolation of lab results to real surfaces remains challenging. The nocturnal production of HONO has been

considered to be dominated by the NO_2 heterogeneous reaction (R2). Although the heterogeneous reaction (R2) of HONO formation is first-order in NO_2, the mechanism for the conversion of NO_2 on surfaces remains unclear (Finlayson-Pitts et al., 2003; Finlayson-Pitts, 2009). ~~In contrast to the homogeneous formation of HONO, the heterogeneous conversion from NO_2 to HONO on humid surfaces (R2) is considered the most likely explanation for the observed HONO concentrations.~~

$$2NO_{2(g)}+H_2O_{(ads)} \xrightarrow{surface} HONO_{(g)}+HNO_{3(ads)} \quad (R2)$$

A few studies have evaluated the relative importance of aerosol and ground surfaces in the nocturnal production of HONO via reaction (R2). The heterogeneous reaction on ground surface have been suggested as the primary nocturnal HONO source based on vertical measurements and fluxes in HONO (Harrison and Kitto, 1994; Harrison et al., 1996; Laufs et al., 2017; Kleffmann et al., 2003; Su et al., 2008b; VandenBoer et al., 2013; Villena et al., 2011; Wong et al., 2011; Wong et al., 2013; Stutz et al., 2002; Ye et al., 2017; Zhang et al., 2009). ~~However, whether the conversion processes primarily occurs on the ground surface or on aerosol surface remains controversial. (Kleffmann et al., 2003; Su et al., 2008a; Cui et al., 2018; R. Br¨oske et al., 2003; Acker et al., 2006; VandenBoer et al., 2013; Bao et al., 2018; Liu et al., 2014; Meusel et al., 2016; Reisinger, 2000; Tong et al., 2016; Ye et al., 2017).~~ However, ~~A lot of~~ other ground ~~measurements~~ level studies have found significantly positive correlations between HONO/NO_2 and aerosol surface areas, ~~suggesting~~ which suggests that the aerosols ~~surfaces~~ play an important role in the heterogeneous conversion ~~from~~ of NO_2 to HONO (Reisinger, 2000; Cui et al., 2018; Zhang et al., 2018; Hou et al., 2016; Tong et al., 2016; An et al., 2012; Bao et al., 2018; Liu et al., 2014; Reisinger, 2000). Therefore, the primary reaction surfaces for the nighttime HONO formation is still controversial, and the role of the aerosols in the heterogeneous production of HONO remains an open question. ~~Various chemical compositions both in the soil and on aerosol particles are reactive towards HONO production. Recent laboratory studies have found that reaction of NO_2 and H_2O adsorbed on mineral dust, glass and buildings can produce HONO (Finlayson-Pitts et al., 2003; Ma et al., 2017; Mendez et al., 2017). And the redox reaction of NO_2 has been extensively investigated on the surfaces of soot, mineral dust soil, and humic acid (Kleffmann et al., 1999; Aubin and Abbatt, 2007; Scharko et al., 2017; Ma et al., 2017). The photosensitized conversion of NO_2 on organic surfaces and emission from biological processes have also been suggested to be a potentially important source of HONO in forested and agricultural region (Gómez~~

~~Alvarez et al., 2014; Stemmler et al., 2006; Monge et al., 2010; Han et al., 2016; Han et al., 2017; Su et al., 2011; Oswald et al., 2013; Tang et al., 2019; Laufs et al., 2017):.~~

~~$2NO_{2(g)}+H_2O_{(ads)} \rightarrow HONO_{(g)}+HNO_{3(ads)}$ (R2)~~

~~While~~ Vertical gradient observations provide ~~direct~~ evidence ~~about the~~ regarding ~~ground~~ surfaces and in situ HONO formation, which can help to understand the nighttime HONO sources. ~~The~~ Methods of long-path differential optical absorption spectroscopy (LP-DOAS) (Stutz et al., 2002; Wong et al., 2011; Wong et al., 2012), instruments mounted on ~~the~~ a movable elevator of a tall tower or ~~the~~ a fixed height ~~of~~ on a building (Kleffmann et al., 2003; VandenBoer et al., 2013; Villena et al., 2011) and aircraft measurements (Zhang et al., 2009; Li et al., 2014; Ye et al., 2018) ~~are the primary~~ have been applied for HONO vertical gradient observations in Europe and the America. ~~measurement methods (Kleffmann et al., 2003; Stutz et al., 2002; VandenBoer et al., 2013; Villena et al., 2011; Wong et al., 2011; Wong et al., 2012; Zhang et al., 2009; Li X et al., 2017; Ye et al., 2018; Li et al., 2014; Oswald et al., 2015; Kleffmann, 2007)~~. ~~Wong et al. (2011) measured the vertical gradients of HONO using LP-DOAS instrument in downtown Houston. The observations showed that NO_2 to HONO conversion on the ground was the dominant source of HONO, and vertical transport was found to be the primary source of HONO aloft. Similar results were found by Villena et al. (2011), who conducted HONO vertical gradient measurements on the 3rd and 21st floor of the high rise building (6 and 53 m above ground level) in Santiago de Chile.~~ To determine the surface responsible for nocturnal HONO formation, Kleffmann et al. (2003) and Wong et al. (2011) measured the HONO vertical gradient between 10 and 190 m altitude in a semi-rural area in Germany and at three different height intervals (lower: 20–70 m, middle: 70–130 m and upper: 130–300 m) in downtown Houston. Their consistent conclusion was that the reaction on the ground surfaces dominated the nocturnal formation of HONO. However, these ~~that have been conducted~~ types of measurements are limited by the measurement frequency ~~and~~ or vertical resolution between the surface and the planetary boundary layer (PBL). VandenBoer et al. (2013) performed ~~carried out~~ measurements of high resolution vertical profiles (vertical resolution ~10 m ~~over 250m~~) of HONO on a 300-m ~~triangular open frame~~ tower. ~~They found that the ground surface HONO production was dominated by heterogeneous uptake of NO_2, and nocturnally deposited HONO may form a conservative surface reservoir which is released on the following day.~~ The total column observations of HONO also showed the ground as the dominant nocturnal surface on which HONO was generated from the heterogeneous reaction of NO_2. The vertical

information of HONO were interpreted in conjunction with a chemical model. The results suggested a conservative surface reservoir that was formed by the deposition of HONO could be a significant fraction of the unknown daytime source. ~~However, the above HONO vertical gradient observations were predominantly conducted in the lower PBL. In order to understand the important role of HONO photochemistry in troposphere, Zhang et al. (2009) measured HONO vertical profiles using aircraft in the PBL and the lower free troposphere (FT) over a forested region in northern Michigan. The study also found that the ground surface was a major source of HONO in the lower PBL, and the HONO emitted from ground surfaces accounted for 16-27% of the overall HONO in the PBL, most of which was distributed in the lower PBL.~~ Furthermore, in an attempt to understand the importance of HONO photochemistry in the troposphere, HONO gradients were measured in the PBL and the lower free troposphere (FT) over a forested region in Michigan (Zhang et al., 2009). An evaluation of the relative importance of aerosol and ground surfaces for the heterogeneous production of HONO also suggested that the ground surface was a major HONO source in the lower boundary layer. In addition, a substantial amount of daytime HONO existed in the FT (~8 ppt).

~~Based on the measurements of vertical gradient and HONO flux, most studies suggests the dominate role of HONO formation on the ground surface that the heterogeneous reaction on ground surface dominated the HONO formation (Kleffmann et al., 2003; Oswald et al., 2015; VandenBoer et al., 2013; Villena et al., 2011; Wong et al., 2011; Wong et al., 2013; Stutz et al., 2002; Zhang et al., 2009; Meusel et al., 2016; Neuman et al., 2016; Harrison and Kitto, 1994; Harrison et al., 1996; Laufs et al., 2017), but Cui et al. (2018) also reported evidence for the important role of HONO formation on aerosol particle surfaces. The aerosol mass loading and its chemical composition seem to be a key parameter influencing the relative importance of HONO formation on aerosol particle surfaces.~~

Beijing, as the largest and the most densely populated city in China, has suffered from severe haze pollution for several years due to rapid economic development and urbanization. ~~The aerosol surface area has been reported to be 2-3 orders of magnitude higher than typical background area (Cai et al., 2017; Liu et al., 2012; Zhang et al., 2015). And several studies indicated that the increase of secondary aerosols were caused by high levels of OH from photolysis of HONO, which resulted in frequent occurrence of haze pollution (Fu et al., 2019; An et al., 2012; Huang et al., 2014).~~ Several ground-based observations of HONO have been conducted in urban and suburban areas of Beijing in recent years (Tong et al., 2016; Zhang et al., 2018; Hou et al., 2016; Wang et al., 2017; Lu et al., 2012; Hendrick et

al., 2014). Higher levels of HONO have been observed (up to 9.71 ppb) in Beijing ~~in~~ during winter (Spataro et al., 2013). ~~and the contribution of HONO photolysis to OH budget at noon can reach 90% in Beijing in winter (Hendrick et al., 2014).~~ ~~However, most of studies that have been conducted at ground level, while the vertical measurements are very limited in Beijing.~~ Although few near real-time HONO vertical gradients have been made, and they have suggested that the reaction at the ground surface is the most important nighttime HONO source (Kleffmann et al., 2003; VandenBoer et al., 2013; Wong et al., 2012; Zhang et al., 2009). The relative importance of aerosol and ground surface in the production of nocturnal HONO may be different in the Beijing region. First, as the primary precursor of nighttime HONO, NO_2 has a much higher concentration during winter in Beijing due to the burning of fossil fuels and vehicle emissions. Second, the aerosol surface area has been reported to be two to three orders of magnitude higher than the typical background area (Cai et al., 2017; Liu et al., 2012; Zhang et al., 2015). High aerosol surface area levels favor heterogeneous reactions on aerosol surfaces (haze period: 3000 μm^2 cm^{-3}; Wang et al., 2018), which presumably makes aerosol surfaces to play a more important role in the production of nighttime HONO. Third, there is more stable nocturnal stratification during the haze period in winter in Beijing, which may have influenced the vertical distribution of HONO. The contribution of the surface production of HONO to HONO levels aloft may be overestimated.

~~Here, we report~~ In this study, the first high-resolution vertical profile measurements of HONO and NO_2 in the megacity of Beijing at different pollution levels (following the transition from ~~the~~ a clean episode to a haze episode) are reported. The vertical profiles of HONO and NO_2 ~~were~~ are measured at high vertical resolution (< 2.5 m over 240 m height) between the surface, the nocturnal boundary layer, and the residual layer. Although the vertical profile measurements are rather limited in scope, including only four nights in December 2016, with limited ancillary data, ~~it~~ this study is unique ~~both because of its~~ due to the high vertical resolution obtained and ~~because of~~ due to the continuous HONO and NO_2 vertical measurements ~~of HONO and NO_2~~ obtained at different stages of pollution. ~~Based on the dataset, the heterogeneous formation of HONO on the ground surfaces and aerosol surfaces is investigated.~~ ~~Evidences also suggest HONO deposition at certain atmospheric conditions.~~ The vertical profiles are then interpreted to evaluate the aerosol and ground surfaces responsible for the nighttime HONO formation during different pollution periods. The vertical measurements and simultaneous observations at ground level are then used to identify and quantify nighttime HONO sources.

2 Experimental ~~M~~methods

2.1 Measurement site

Vertical profile measurements were conducted from ~~7 to 12~~ December 7th to 12th of 2016 at the Tower Branch of the Institute of Atmospheric Physics (IAP), Chinese Academy of Science (39°58'N, 116°23'E) as part of the "In-depth study of air pollution sources and processes within Beijing and its surrounding region (APHH-Beijing)" winter campaign. The site is a typical urban residential area located between the 3rd and 4th Ring Road in the north of Beijing. It is approximately 1 km from the 3rd Ring Road~~;~~, 200 m from the Beijing-Tibet Expressway, and 50 m from the Beitucheng West Road (Fig. S1). The ~~main~~ primary sampling platform ~~is~~ was the Beijing 325-m meteorological tower (BMT), equipped with an external container that was lifted on the side wiring of the tower, which ~~can~~ could ascend and descend at a relatively constant rate of ~ 9 m min^{-1}. A single vertical ascent or descent ~~takes~~ required less than 30 min. After reaching the top, the container stopped and data were measured continuously for 5–20 min of each cycle. For security reasons, the container reached a maximum height limit of 260 m during the daytime and 240 m at night (Fig. 1). The container instruments ~~include~~ included the following: a global position system (GPS), an altimeter, and an incoherent broadband cavity enhanced absorption spectrometer (IBBCEAS) for measurements of HONO and NO_2. In addition, another IBBCEAS was mounted in temperature-stabilized lab containers for the measurement of HONO and NO_2 at ground level.

2.2 Instrumentation

HONO and NO_2 were simultaneously measured ~~by~~ using a home-made IBBCEAS. A detailed description of the IBBCEAS instrument can ~~be found in~~ refer to Duan et al (2018)~~;~~, and its application to the measurement made during this study is described below. IBBCEAS is a spectroscopic technique that combines broad-band light source (UV-LED) with the principle of time-integrated cavity output spectroscopy. The HONO was sampled into an inlet tube (1.5 m length~~,~~ with a 4 mm outside diameter (OD)) before entering ~~the~~ an optical cavity (550 mm in length~~,~~ and 25.4 mm OD)~~, which~~ that utilized PFA to minimize the HONO loss. The sampling gas flow rate was controlled at ~~6~~ six standard liters per minute (SLPM) ~~(Standard Liters per Minute)~~ by a gas pump (KNF). ~~The light emitted by the ultraviolet light emitting diode (UV-LED) was collimated by using an achromatic lens and coupled into the optical cavity.~~ In the optical cavity, light was reflected between the two highly reflective mirrors (R =

99.980% @368 nm, CRD Optics, California, USA) to obtain a long optical absorption length. ~~Then the light through the cavity was coupled into an optical fiber by another achromatic lens before being received by a charge coupled device (CCD) spectrometer (QE65000, Ocean Optics, Florida, USA).~~ To protect the highly reflective mirrors, pure N_2 was used to continuously purge the mirrors to prevent contact between the mirrors and the sample airflow. The purge flow rate was controlled at 0.1 SLPM ~~by~~ using mass flow controllers (MFCs, CS200A, Sevenstar, Beijing, China). The typical time resolution of the IBBCEAS instrument ~~is~~ was 30 s, and the 1 σ detection limits for HONO and NO_2 ~~are~~ were 90 ppt and 170 ppt, respectively. In this study, the IBBCEAS instrument was mounted in ~~the~~ a movable container of the BMT for vertical profile measurements, and this made measurements with a time resolution of 15 s (vertical resolution of 2.4 m). The detection limits for HONO and NO_2 were 120 ppt and 200 ppt, respectively. Another IBBCEAS instrument was mounted in temperature-stabilized lab containers at ground level, and it collected data with a time resolution of 30 s. The total relative ~~measurement error~~ uncertainty of the IBBCEAS instrument was ~~approximately 9%~~ 8.7%, and it considered the uncertainty in the cross section (5%), the calibration of reflectivity (5%), spectral fitting (4%), the effective cavity length (3%), the pressure in the cavity (1%), $\Delta I/I_0$ (1%), and sample loss (0.5%). Correction of the light intensity was performed every hour, and the mirror reflectivity was calibrated ~~every day~~ daily.

Meteorological parameters~~, including~~ that included wind speed (WS), wind direction (WD), temperature (*T*), and relative humidity (RH) were obtained using a 15-level meteorological gradient observation system installed at fixed intervals along the meteorological tower (at heights of 8, 15, 32, 47, 65, 80, 100, 120, 140, 160, 180, 200, 240, 280, and 320 m). The gaseous species, including nitrogen monoxide (NO), ozone (O_3), and carbon monoxide (CO)~~, and sulfur dioxide (SO_2),~~ were measured using a commercial gas analyzer from Thermo Scientific (Waltham, Massachusetts, USA) (Tan et al., 2017). NO was detected using NO-O_3 chemiluminescence (Model 42iTL, Thermo Scientific), with a detection limit of 50 ppt. O_3 and CO were measured by an O_3 analyzer (Model 49i, Thermo Scientific) and a CO analyzer (Model 48iTLE, Thermo Scientific), with the detection limits of 0.50 ppb and 0.04 ppm, respectively. Measurements of NO, O_3 and CO agreed well within the instrumental accuracies. The 7-wavelength aethalometer (AE33, Magee Scientific Corp, Berkeley, California, USA) was deployed to measure the black carbon (BC) ~~mass concentration~~ at a time resolution of 1 min (Xie et al., 2019). Aerosol particles were continuously collected onto a quartz filter in the instrument to measure

their light attenuation at 370, 470, 520, 590, 660, 880, and 950 nm. Trace gas (CO and O_3) ~~CO, O_3, SO_2,~~ and aerosol parameters (BC, NR-PM_1 and aerosol surface area) ~~BC~~ were measured simultaneously at ground level and at 260 m on the tower. The non-refractory submicron aerosol (NR-PM_1) species were ~~also~~ measured simultaneously at ground level and at 260 m ~~on the tower with~~ using an aerodyne high-resolution time-of-flight aerosol mass spectrometer (AMS) and an aerosol chemical speciation monitor (ACSM), respectively. The detailed sampling setup and calibration of the AMS and ACMS, as well as data analysis, have been described ~~in~~ by Xu et al. (2019) and Sun et al. (2013). The dry-state particle number size distributions were measured at ground level and at 260 m using a scanning mobility particle sizer (SMPS) (Du et al., 2017). The particle number size distributions of 15-500 nm was used to calculate the aerosol surface area (S_a) by assuming the particles are in spherical shape. A hygroscopic factor f(RH) was applied to correct S_a to the aerosol surface area in the real atmosphere (S_{aw}) (Li et al., 2012). The S_{aw} was calculated using following equations:

$$f(RH) = 1 + a\left(\frac{RH}{100}\right)^b \quad (1)$$

$$S_{aw} = S_a \times f(RH) \quad (2)$$

where a and b are the empirical parameters used to estimate f(RH), which were set to 2.06 and 3.6, respectively (Liu et al., 2008). The uncertainty of S_{aw} was estimated to be ~30%, which was associated with the uncertainty from the S_a measurement (~20%) and the growth factor (~20%).

2.3 Inter-comparison

In the present study, the measurements of HONO and NO_2 were conducted simultaneously in the container and at ground level. Therefore, the calibration and inter-comparison of the two IBBCEAS instruments were crucial. Comparison experiments were ~~carried out~~ conducted in a temperature-stabilized laboratory. The sampling unit and sampling flow rate of the two instruments were identical to minimize ~~the~~ measured deviations. Figure. 2 shows ~~significantly positive correlations~~ the excellent agreement between the two IBBCEAS instruments (HONO: R^2 = 0.99, NO_2: R^2 = ~~0.95~~ 0.99), with a slope of ~~0.99~~ 1.00 ± 0.01 (NO_2), ~~1.03~~ 1.02 ± 0.01 (HONO) and ~~an~~ a small intercept of ~~750~~ 180 ± 90 ppt (NO_2) and ~~-4~~ -30 ± 10 ppt (HONO). The difference was approximately ~~3%~~ 2%, within the measurement error range of the instruments.

To verify the accuracy of the IBBCEAS instrument, an inter-comparison between the IBBCEAS of this study and the IBBCEAS of Cambridge University was conducted. The HONO measurements

297 from the two different instruments were highly ~~correlated~~ consistent (R^2 = ~~0.95~~ 0.97, Fig. 2c), with a
298 small intercept and a slope close to 1. In addition, the IBBCEAS instrument was also compared with
299 the long optical path absorption photometer (LOPAP) and the stripping coil ion chromatography
300 (SC-IC) ~~in~~ from our previous studies (Tang et al., 2019;Duan et al., 2018)~~, which~~. This also showed
301 good ~~correlations for~~ agreements of the HONO measurements (LOPAP: R^2 = 0.894, SC-IC: R^2 = 0.98).

302 **3 Results and discussion**

303 **3.1 General observations and vertical measurements**

304 The time-series of meteorological parameters, ~~NR-PM$_1$ mass concentration, HONO, NO$_x$ and~~
305 ~~other relevant species~~ trace gases, and aerosol parameters are shown in Fig. 3. Based on the NR-PM$_1$
306 mass concentration level, three different meteorological conditions were characterized during the
307 measurement periods (Table 1). The first episode (E1) from ~~7~~ December 7th to 10:00 on ~~8~~ December 8th
308 was a haze event. The NR-PM$_1$ mass concentration increased rapidly from 30 to ~150 μg·m^{-3} at ground
309 level and at 260 m on the tower due to a low wind speed (0.78 ± 0.42 m·s^{-1}) and a high RH (51% ±
310 13%).

311 The second episode (~~8~~ 11 December 8-11, C2) was a clean event with low NR-PM$_1$ mass loading
312 (mean: 24 ± 19 μg·m^{-3})~~,~~ and a high wind speed (> 5 m·s^{-1}), ~~dominantly~~ primarily from northwest. The
313 third episode (E3) from ~~11~~ December 11th to ~~12~~ December 12th was another haze event. During this
314 period, the atmosphere was characterized by stagnant weather, lower wind speeds (an average of 0.77 ±
315 0.4 m·s^{-1})~~,~~ and a high RH (55% ± 5%). The mass concentration of the NR-PM$_1$ gradually increased and
316 then remained at relatively constant levels at ground level and 260 m on the tower, and ranging from 69
317 to 218 μg·m^{-3} with ~~the~~ a mean value of 154 ± 35 μg·m^{-3}.

318 Throughout the entire measurement periods, HONO concentrations ranged from 0.05 to 7.59 ppb.
319 The mean HONO mixing ratios during E1, C2, and E3 were 4.26 ± 2.08, 0.83 ± 0.65, and 3.54 ± 0.91
320 ppb, respectively. The maximum HONO concentration ~~of HONO~~ was 7.59 ppb, which was observed
321 during E1 (at 08:10 on ~~8~~ December 8th). From ~~11 to 12~~ December 11th to 12th ~~, with stagnant weather,~~
322 the pollutants continuously increased with the stagnant weather. The HONO concentrations remained ~~a~~
323 at high levels, and the daytime mean HONO mixing ratio even reached 3.1 ± 0.92 ppb. Figure 3 also
324 ~~presents~~ shows the time series of simultaneously measured other relevant species. The mean NO$_2$
325 mixing ratios during E1, C2, and E3 were 51.98 ± 8.41, 23.30 ± 11.91, and 51.88 ± 5.97 ppb,

respectively. Because NO and O_3 were not measured at ground level after 14:00 on ~~10~~ December 10th, the mean concentrations of NO and O_3 during E1 and C2 were 90.99 ± 67.98~~,~~ and 14.66 ± 21.79 ppb, respectively, and 4.04 ± 1.81~~,~~ and 14.37 ± 10.65 ppb, respectively. After sunset, the concentration of O_3 at the surface was rapidly titrated ~~by~~ due to the elevated NO and increased with ~~the~~ an increase ~~of~~ in height. The mixing ratio of O_3 below 260 m was less than 9 ppb during the vertical measurements. The BC, NR-PM_1, and aerosol surface area showed very similar patterns both at ground level and at 260 m. The RH corrected aerosol surface area (S_{aw}) is shown in Fig. S2. Higher BC, NR-PM_1 and S_{aw} levels were observed at ground level during the haze periods (E1 and E3).

Nocturnal stable surface layers of air ~~are~~ generally form~~ed~~ at low wind speeds (< 6 $m \cdot s^{-1}$) (VandenBoer et al., 2013). Hence, the vertical profile data ~~are adopted~~ were used when the wind speeds ~~was~~ were less than 6 $m \cdot s^{-1}$, except on ~~7~~ December 7th ~~(Fig. 4)~~. Vertical measurements ~~with~~ during low wind events were successfully conducted ~~in~~ on three occasions (December 9–10, 10–11, and 11–12 ~~December~~) and ~~would~~ will be discussed below. The near-continuous vertical measurements avoided the observation bias from prolonged fixed sampling. The date and time of the measurement for each vertical profile is detailed in Table S1 in the supplementary information.

3.2 Nocturnal HONO vertical profiles

3.2.1 Vertical measurements after sunset

Vertical measurements were conducted from ground level to 240 m after sunset. ~~Figure 5 show the temporal and spatial variations of HONO and NO_2 during the clean episode (C2) and the haze episode (E3).~~ The mixing ratios of HONO and NO_2 at ground level were consistent with those measured in the container. The mixing ratios of HONO and NO_2 showed nearly flat profiles throughout the column during C2 and E3 (Fig. S3), indicating that HONO and NO_2 were relatively well mixed after sunset ~~during these two episodes~~. ~~The vertical profiles of HONO, NO_2, and △HONO just after sunset are shown in Fig. 6. During C2 and E3, The mixing ratios of HONO and NO_2 (Fig. 6a) showed nearly flat profiles throughout the column.~~ The vertical variations of △HONO ~~(Fig. 6b)~~, which is the difference ~~of~~ in the HONO concentrations between measured in the container and at ground level, centered around 0 ppb and varied between -0.4 and 0.4 ppb~~,~~. ~~confirming~~ This result also indicated the relatively uniform vertical distribution of ~~both~~ HONO ~~and NO_2~~. The vertical variations ~~of~~ in *T* and RH during these three vertical measurements were similar (Fig. ~~S2~~ S4). While *T* decreased gradually ~~as the~~

~~increase~~ with increasing height, RH increased gradually with increasing height~~, and~~. In addition, RH was relatively higher during the haze episode. Also, there ~~were~~ was no *T* inversion just after sunset, and the consistent variations ~~of~~ in the HONO and NO_2 at ground level and in the vertical measurements all supported a relatively well-mixed boundary layer, which explain~~s~~ed the uniform vertical distribution of HONO and NO_2.

3.2.2 Nocturnal vertical profiles

Nocturnal small-scale stratification and layering was determined according to the method of Brown et al. (2012), who used the potential temperature profile as an indicator of atmospheric static stability. According to the vertical variations in the potential temperature, the stable layer was divided into the "surface layer", the "nocturnal boundary layer (NBL)", the "top of the nocturnal boundary layer", and the "residual layer (RL)".

Figure ~~7~~ 4 depicts the nocturnal vertical profiles of HONO, NO_2, and potential temperature during C2 ~~the clean episode~~. The orthogonal linear least squares regression slope and correlation coefficients of HONO and NO_2 to altitude were applied to estimate the nocturnal gradient of HONO and NO_2 (Table 2). On the night of ~~9~~ December 9th (~~C2~~ Fig. 4a), negative profiles of both HONO and NO_2 were clearly seen. When the container ascended during 22:42–23:06, the potential temperature profile showed distinct stratification. The surface layer extended to 10–20 m and the NBL extended to ~140 m. ~~There was a significant negative gradient of HONO (-4.49 ± 0.31 ppt m^{-1}) and NO_2 (-14.38 ± 1.62 ppt m^{-1}) within NBL~~ The obviously negative gradient of HONO (-4.49 ± 0.31 ppt m^{-1}) and NO_2 (-14.38 ± 1.62 ppt m^{-1}) were observed throughout the heights from 0 to 240 m. ~~Above the NBL,~~ A negative gradient of HONO was ~~also~~ observed in the RL, but was not consistently observed in other measurements (see below). ~~When~~ During the descent of the container ~~during~~ from 23:15–23:40, the potential temperature profile showed that a shallow *T* inversion ~~was~~ had rapidly formed between 130 and 200 m. The obvious vertical variation in RH during 23:15–23:40 (Fig. S3) also indicated the different layers at different heights, which was due to the influence of a shallow inversion layer. Within the shallow inversion layer, ~~the~~ vertical convection and transport ~~was~~ were inhibited, and ~~the~~ a remarkable negative gradient was observed there. However, within the NBL, the negative gradient of HONO and NO_2~~, however,~~ disappeared. This might have been due to the continuous vertical mixing below the shallow inversion layer from 23:06 to 23:40. ~~By the way~~ Additionally, the surface source of

HONO ~~is~~ was obvious, as ~~seen from~~ evidenced by the ~~apparent accumulation~~ apparently negative gradient of HONO ~~within NBL~~ in Table 2. ~~In addition, the obviously vertical variation in RH during 23:15-23:40 (Fig. S3) indicated the different layers at different height, which was due to the influence of the shallow inversion layer.~~

The vertical profile of potential temperature on ~~10~~ December 10th (~~C2~~ Fig. 4b) ~~shows~~ showed that a shallow inversion layer formed between the surface layer and the NBL. In the shallow inversion layer, the mixing ratios of HONO decreased rapidly with increasing height, and a significant negative gradient was observed within the shallow inversion layer and surface layer. With the attenuation of the shallow inversion layer during the descent of the container from 23:01 to 23:25, the inhibition of vertical transport and mixing gradually weakened. ~~and the negative gradient of HONO disappeared below ~100 m, which indicated the surface source of HONO or the interaction of different air masses due to the change of WD (Fig. S3-S5). The And~~ The increase in the negative gradient of HONO and NO_2 and the correlation coefficients of HONO and NO_2 to altitude from 22:36 to 23:25 also showed the weakened shallow inversion layer near the surface, which suggested the nighttime HONO surface source. The attenuation event of the shallow inversion layer may have also ~~be~~ been the result of ~~the~~ an increase ~~of~~ in the wind speed and the interaction of different air masses that changed from the west to southeast between 15 and 100 m (Fig. S5). Above the 100 m height, the mixing ratio of HONO decreased with increasing height, and the fluctuation ~~of~~ in HONO was likely due to the interaction of different air masses. In contrast, the vertical profiles of NO_2 ~~shows~~ showed that NO_2 rapidly decreased towards the ground~~:~~, and a significant positive gradient was observed near the surface~~, which~~ that was caused by several factors. ~~The~~ Nocturnal NO_2 is produced by the reaction of O_3 with NO, which ~~mainly~~ primarily occurs near the surface, resulting in a negative gradient in NO_2. However, this effect was counteracted by the dry deposition of NO_2, which by itself would result in a positive gradient (Stutz et al., 2004b). ~~Meanwhile~~ Additionally, the mixing ratio of NO_2 was also affected by local traffic emission sources, ~~All of these lead to the positive gradient of NO_2 near the surface. Compared to the vertical profiles collected on 9 December,~~ and a near-surface shallow inversion layer was formed on ~~10~~ December 10th. All of these presumably led to a clearly positive gradient for the near-surface NO_2. ~~resulting in the clearly positive gradient of near-surface NO_2. Moreover, the increase of the positive gradient NO_2 indicated the formation of near-surface shallow inversion layer likely caused the increase of dry deposition, which affects~~. In contrast to the vertical profiles measured on December 9th, a

positive gradient observed in near-surface NO_2 on December 10th indicated that the shallow inversion layer affected the vertical distribution of HONO and NO_2 at night.

Although the surface layer was a common feature in the potential temperature profiles, it was absent ~~on the night of 11-12 December (E3)~~ during E3, and the NBL extended downward to the lowest measurement height (8 m above the ground~~; Fig. 8~~). As shown in Fig. 5, the vertical profile of HONO showed a significant negative gradient as the container ascended during 22:35–23:00, and higher HONO mixing ratio was observed at ground level. With the development of the boundary layer, the negative gradient of HONO ~~and NO_2 gradually~~ continued to decrease from 6.91 ± 0.33 ppt m^{-1} during 22:35–23:00 to 1.79 ± 0.28 ppt m^{-1} during 00:45–01:09 and even disappeared between 00:00 and 00:26. ~~during 22:35-23:29, which was similar to the vertical profile on 9 December. As shown in Fig. 8, the vertical profile of HONO showed a significant negative gradient as the container ascent during 22:35-23:00, and higher HONO mixing ratios were observed at ground level.~~ Moreover, the consistent $HONO/NO_2$ ratios (~5.6% ± 0.3%) were observed throughout the depth of the NBL between 23 and 01 h (Fig. S6). ~~However, the mixing ratios of HONO and NO_2 approached a steady state plateau within NBL around midnight.~~ A near-steady state plateau of the HONO mixing ratio and $HONO/NO_2$ was established near midnight with the NBL. ~~A possible physical and chemical process, the loss of HONO to the ground surface by dry deposition and vertical convection could account for approaching a near steady states in the HONO mixing ratio and $HONO/NO_2$ (Fig. S4-S6).~~ Similar vertical measurements were reported by VandenBoer et al (2013), who also observed a near-steady state in the HONO mixing ratio and $HONO/NO_2$, and an approximate balance between the production and loss of HONO late in the night. A possible physical and chemical process, the loss of HONO to the ground surface due to dry deposition could account for the buildup and near-steady state observed in the HONO mixing ratio and $HONO/NO_2$. This implied that significant quantities of HONO were deposited to the ground surface at night. ~~Dry deposition loss of HONO to the ground surface and vertical mixing effects associated with vertical convection reached a near-steady state around midnight, which indicated that significant quantities of HONO are deposited to the ground surface at night, and deposition of HONO at ground surface is an important sink of HONO at night.~~

The utility of the orthogonal linear least squares regression slope of HONO to altitude to estimate the vertical gradient of HONO at night implies that the potential nocturnal HONO production from the heterogeneous reaction of NO_2 on aerosol surface. A positive gradient of HONO (0.23 ± 0.36) between

00:00 and 00:26 was observed during E3. The aerosol surface area (S_{aw}) in the residual layer was greater than 1500 μm^2 cm^{-3} throughout the night (range: 1592-2655 μm^2 cm^{-3}). The S_{aw} was 2314 μm^2 cm^{-3} from 22 to 01 h on December 11th and reached a maximum of 2569 μm^2 cm^{-3} in the residual layer. These aerosol surface areas are a factor of 14-38 greater than that observed in previous studies of HONO vertical gradient, which ranged between 60 and 158 μm^2 cm^{-3} (Kleffmann et al., 2003; VandenBoer et al., 2013). Such high aerosol surface areas may provide a sufficient surface for the heterogeneous reaction. The vertical profiles also showed an enhanced HONO/NO_2 ratios from C2 to E3 (Fig. S7). Moreover, a relatively constant HONO mixing ratio and HONO/NO_2 ratio above 160 m were observed from 22:35 to 01:09 during E3. Both of these observations are indicative of a potential aerosol surface source of HONO aloft during the haze episode. Assuming that aerosol surface production dominated the observed HONO mixing ratio in the overlying air during the haze episode, the mixing ratios of HONO and NO_2 observed at 240 m and the aerosol surface area measured at 260 m were parameterized to estimate the nocturnal production of HONO on aerosol surface, which is explored in more detail in section 3.4.2.

3.3 Direct emissions

In the present study, the measurement site ~~is~~ was surrounded by several main roads, and thus might ~~be~~ have been affected by ~~substantial~~ vehicle emissions ~~at night nighttime~~. CO and NO, as the primary pollutants, are emitted from combustion processes like the burning of fossil fuels as well as vehicle emissions (Sun et al., 2014; Tong et al., 2016; Bond et al., 2013). BC is another primary pollutant typically emitted from diesel engines and residential solid fuels (Zhang et al., 2018). Good correlations of the nocturnal HONO with CO (R^2=0.85), NO (R^2=0.76) and BC (R^2=0.84) at ground level were observed (Fig. S8), indicating the potential effect of direct emissions on the observed HONO at night. The emission ratio of HONO/NO_x have been determined from tunnel measurements in California (Kirchstetter et al., 1996), Germany (Kurtenbach et al., 2001), and Hong Kong (Laing et al., 2017). However, considering the differences in the type of vehicles, fuel compositions, and other factors, the reported emission factor of HONO/NO_x might not be representative for the Beijing region. ~~To~~ To evaluate the influence of direct emissions, the local emission ~~ratios of HONO/NO_x~~ factor of HONO was derived from ~~our~~ ambient measurements. Since NO was not measured at ground level after ~~10~~ December 10th, the ~~nocturnal~~ nighttime measurement data of HONO and NO_x ~~(from 18:00 LT to~~

~~next 6:00 LT)~~ from ~~9~~ November 9th to ~~10~~ December 10th were used to evaluate the local HONO emission factor. ~~Considering the differences in the type of vehicles, fuel compositions, etc., the reported emission factor of HONO/NO_x might not be representative for Beijing region. In order to evaluate the influence of direct emission, the local emission factor of HONO was estimated from the ambient measurements.~~

~~As an air mass becomes aged, the conversion of NO_2 to HONO will result in the increase of HONO/NO_x, freshly emitted air masses are characterized by the lowest HONO/NO_x.~~ Considering the potential secondary HONO formation with air mass aging during the transport process, five criteria were applied to ensure as much of the freshly emitted air masses as possible: (a) only nighttime data (from 18:00 LT to next 6:00 LT) were included to avoid the fast photolysis of HONO; (b) only sharp peaks during nighttime and the elevations of HONO and NO_x over the background levels were estimated; (c) $\Delta NO/\Delta NO_x > 0.80$; (d) good correlation between HONO and NO_x; (e) short duration of the plume (< 30 min). The typical nighttime wind speed at measurement site was 1.2 m s^{-1}, thus the duration for fresh air masses should have been less than 30 min during transport from the emission to the measurement site. Criteria (b) and (c) were used as indicators for identifying fresh vehicular emissions. Criteria (d) and (e) further confirmed that the increase in HONO was primarily caused by freshly emitted plumes instead of heterogeneous reactions of NO_2.

Figure 6 shows two emission plumes observed on December 9th to 10th, 2016 based on the preceding selection criteria. The slopes of HONO to NO_x can be considered as the emission ratios (Rappenglück et al., 2013). The HONO/NO_x emission ratios were estimated for the 11 fresh emission plumes that satisfied the preceding criteria (see Table 3). The derived emission factors of 0.78%–1.73% had an average value of 1.28% ± 0.36%, which was larger than the 0.53%–0.8% measured in the tunnel in Wuppertal (Kurtenbach et al., 2001). The minimum ratio of 0.78% approximated the value (0.8%) measured in Wuppertal. It is worth mentioning that the value of 0.8% is widely used as the upper limit of the HONO/NO_x emission ratio from road traffic in interpreting field observations and modeling HONO emissions (Stutz et al., 2002; Su et al., 2008a; Tong et al., 2016). The maximum ratio of 1.73% in this study is comparable to the value of 1.7% in Houston, Texas, observed by Rappenglück et al. (2013). The derived emission ratios were within the range of other published results (0.19%–2.1%) (Kirchstetter et al., 1996; Kurtenbach et al., 2001; Su et al., 2008a; Rappengluck et al., 2013; Yang et al., 2014; Xu et al., 2015; Liang et al., 2017; Zhang et al., 2018; Li et al., 2018; Liu et al., 2019).

Comparisons of the derived HONO/NO_x ratios with the results obtained previously are summarized in Table S2. ~~Thus, the observed~~ To minimize the risk of overestimating the direct emissions, the minimum HONO/NO_x ratio was used as an upper limit for the emission factor (Su et al., 2008a). ~~In order to capture as much of the freshly emitted air mass as possible, two criteria were chosen to ensure that the air mass was dominated by fresh vehicle emission: (a) NO≥80 ppb; and (b) NO/NO_x≥80% (Xu et al., 2015).~~ ~~The derived HONO/NO_x emission factor of 1.41% 1.03% is comparable to the value of 1.24% reported by Liang et al. (2017), who measured HONO emission factor in a road tunnel in Hong Kong.~~ The minimum HONO/NO_x ratio of 0.78% was used to evaluate the contribution of vehicle emissions to the ambient HONO levels at night (Eq. (3)). In this case, the risk of overestimating direct emissions was minimized, but there was still the effect of potential secondary HONO formation. ~~$HONO_{emis}$ was calculated by the following equation: $[HONO]_{emis} = 0.0141 \times [NO_x]$~~

$$[HONO]_{emis} = 0.0078 \times [NO_x] \quad (3)$$

where $[HONO]_{emis}$ and $[NO_x]$ are the HONO mixing ratios from vehicle emissions and the observed NO_x mixing ratios, respectively. The direct emissions contributed an average of 29.3% ± 12.4% to the ambient HONO concentrations at night, with an average $HONO_{emis}$/HONO value of 35.9% ± 11.8% during the clean episode and an average $HONO_{emis}$/HONO value of 26% ± 11.3% during the haze episode. The frequency distribution of $HONO_{emis~~sion~~}$/HONO during ~~the measurement period~~ ~~is~~ the clean and the haze episodes are shown in ~~Fig. S5~~ Fig. 7. ~~The contribution of direct emissions to ambient HONO was estimated to be 51.1% 36% ± 15%, suggesting that the vehicle emissions is an important nocturnal HONO source in Beijing (Zhang et al., 2018).~~ The lower vehicle emissions contribution during the haze episode could have been caused by an odd-even car ban, which required alternate driving days for cars with even- and odd-numbered license plates.

3.4 Nocturnal HONO chemistry

3.4.1 Correlation studies

The heterogeneous conversion of NO_2 is an important pathway ~~of~~ for HONO formation during the nighttime, as many field ~~measurements~~ observations have ~~also~~ found a ~~strong~~ good correlation between HONO and NO_2 (Zhou et al., 2006; Su et al., 2008a; Wang et al., 2013; Huang et al., 2017). However, the use of a correlation analysis to interpret the heterogeneous conversion of NO_2 should be treated carefully ~~treated~~, as physical transport and source emissions also contribute to the correlation. In this

study, the correlations of vertical ~~measurements~~ profiles between HONO and NO_2 were analyzed. Vertical profile data without horizontal transport were used to avoid the influence of physical transport. As shown in Fig. ~~9~~ 8, ~~HONO and NO_2~~ the linear least squares regression correlations of HONO to NO_2 exhibited moderate but significant correlations (C2: R^2 = 0.72, E3: R^2 = 0.69), ~~indicating~~ supporting that NO_2 participated in the formation of HONO. The column of HONO and NO_2 showed a significantly positive correlation during the haze episode. However, the negative correlation between HONO and NO_2 was observed at ground level during the haze episode (Fig. S9), which was also observed in the previous ground-based observations (Hou et al., 2016; Zhang et al., 2018). The observed significant correlation between the HONO column and NO_2 column could be due to: (1) emissions and vertical mixing of HONO and NO_2, and (2) a possible heterogeneous reaction of NO_2 on aerosol surface.

~~The~~ Adsorbed water on ~~the~~ a surface ~~affects~~ has been shown to affect the heterogeneous formation of HONO (Stutz et al., 2004a). The relationship between HONO/NO_2 and RH is illustrated in Fig. ~~10~~ 9. Following the method introduced by Stutz et al (2004a), ~~we analyzed~~ the average of the five highest HONO/NO_2 values in each 10% RH interval was evaluated to eliminate much of the influence of factors like the time of night, advection, the surface density, etc. An increase in the HONO/NO_2 ratio along with RH was observed at each height interval when the RH was less than 70%. A previous observation at ground level also reported that the HONO/NO_2 ratio increased with ~~the~~ an increase ~~of~~ in RH when the RH was less than 70%~~.~~. ~~while the~~ A further increase ~~of~~ in RH would lead to a decrease in the HONO/NO_2 ratio, which was considered to be caused by the number of water monolayers that formed on the surface leading to an efficient uptake of HONO (Li et al., 2012; Yu et al., 2009; Liu et al., 2019). ~~which may be caused by an increase in the number of water layers formed on the surface with the increase of RH, resulting in the more efficient uptake of HONO (Li et al., 2012; Wang et al., 2013b; Yu et al., 2009).~~ However, a decreased uptake coefficient of HONO with increasing RH from 0% to 80% was observed in a laboratory study (Donaldson et al., 2014). The NO_2 to HONO conversion efficiency depended negatively on RH at an RH above 70%, which was presumably caused by the relative humidity affecting both HONO uptake onto the surface and the NO_2-to-HONO conversion. ~~The HONO/NO_2 ratio decreased with the increase of height at similar RH level for both C2 and E3, which implied that the ground surface was the main heterogeneous reaction surface at night.~~ A decrease in the HONO/NO_2 ratio with an increase in height at a similar RH level were observed during C2 and E3. A

higher conversion efficiency of NO_2 to HONO was observed near the surface, and the HONO/NO_2 ratios at different heights were significantly different during C2. However, this differences decreased, and similar HONO/NO_2 ratios were observed at different heights during E3. This observation implied a possible heterogeneous conversion of NO_2 on aerosol surface in the overlying air. It is ~~important~~ necessary to note that the limited vertical measurements resulted in ~~the~~ a limited variation range ~~of~~ in the RH, which limits ~~the~~ this analysis. Additional efforts are needed to conduct more comprehensive vertical measurements to interpret the HONO/NO_2 ratios versus RH for different heights in the future.

3.4.2 ~~Influence of aerosol surface on nocturnal HONO production~~ Relative importance of aerosol and ground surfaces in nocturnal HONO production

The observed positive HONO gradient implied a potential heterogeneous conversion of NO_2 on aerosol surface. The aerosol surface area observed during the haze episode was an order of magnitude higher than in other studies of HONO vertical gradient (Kleffmann et al., 2003; VandenBoer et al., 2013), which presumably provided sufficient aerosol surface area to account for the observed nighttime HONO production (Liu et al., 2019). ~~The relative importance of aerosol surfaces and ground surfaces in nocturnal HONO production has been widely investigated in the field (Kleffmann et al., 2003; Oswald et al., 2015; VandenBoer et al., 2013; Stutz et al., 2002; Wong et al., 2011; Ye et al., 2018; Li et al., 2012; Su et al., 2008a). An estimate of the contribution of nocturnal HONO production from aerosol surfaces,~~ The surface area information for particles larger than 0.5 μm were not valid at ground level and 260 m during the measurement periods. Hence, this is a lower limit estimate of the total surface area for the heterogeneous reaction.

An estimate of the nocturnal HONO production on aerosol surface was made using the RH corrected aerosol surface area (S_{aw}) and NO_2 observations from the residual layer. The CO and BC measured at ground level were independent of the CO and BC observed at 260 m during the haze period (Fig. S10), since ~~we~~ it can be expected that air masses in the residual layer ~~RL (above 200 m) is less affected by~~ were decoupled from the ground-level processes and largely free of NO_2 emissions. (Brown et al., 2012; VandenBoer et al., 2013). ~~It can be approximately considered that~~ The HONO production ~~was primarily derived~~ from the heterogeneous NO_2 conversion (Reaction R1) ~~of NO_2~~ on aerosol surface would then have become the primary HONO source in the residual layer during E3. The yield of the hydrolysis reaction assumes that HONO and HNO_3 are formed by equimolar disproportionation of two NO_2 molecules and immediately release HONO (Finlayson-Pitts et al., 2003;

Finlayson-Pitts, 2009). The reactive uptake of NO_2 by the aerosols was assumed to occur on all measured aerosol surface areas, regardless of their chemical composition. HONO production (*P(HONO)*) can then be expressed using the ~~following~~ equation of Ye et al. (2018) modified to account for the disproportionation:

~~$$\frac{P(HONO)}{[NO_2]} = \frac{1}{4} \times \left[\frac{S}{V}\right] \times \sqrt{\frac{8RT}{\pi M}} \times \gamma \quad (1)$$~~

$$\frac{P(HONO)}{[NO_2]} = \frac{1}{8} \times S_{aw} \times \sqrt{\frac{8RT}{\pi M}} \times \gamma_{NO_2} \quad (4)$$

where ~~γ~~ γ_{NO_2} is the uptake coefficient ~~of NO_2~~, *R* is the gas constant, *T* is the absolute temperature (K), *M* is the molecular mass of NO_2 (M=4.6×10^{-2} kg mol^{-1}), and ~~$\left[\frac{S}{V}\right]$~~ S_{aw} is the RH corrected aerosol surface area ~~density (m^{-1})~~ (μm^2 cm^{-3}). The NO_2-normalized HONO production over time, $\Delta\frac{[HONO]}{[NO_2]}/\Delta t$, can be calculated using ~~Eq. (2)~~ the following Eq. (5):

~~$$\Delta\frac{[HONO]}{[NO_2]}/\Delta t \sim \frac{1}{4} \times \left[\frac{S}{V}\right] \times \sqrt{\frac{8RT}{\pi M}} \times \gamma \quad (2)$$~~

$$\Delta\frac{[HONO]}{[NO_2]}/\Delta t \sim \frac{1}{8} \times S_{aw} \times \sqrt{\frac{8RT}{\pi M}} \times \gamma_{NO_2} \quad (5)$$

~~Assuming that the~~ Assume an NO_2 uptake coefficient of ~~NO_2 is~~ 1×10^{-5} to 1×10^{-6} in the dark, which ~~fitted~~ fits the NO_2 uptake coefficient values ~~of 1×10^{-6} 1×10^{-5} in the dark from those~~ observed in relevant studies (J.Kleffmanna et al., 1998; Kurtenbach et al., 2001; ~~George et al., 2005; Stemmler et al., 2007~~ Saastad et al., 1993; Bröske et al., 2003)~~, with a $\left[\frac{S}{V}\right]$ value of ~10^{-3} m^{-1} (Wang et al., 2018)~~ A representative temperature of 273 K, and an average observed S_{aw} of 2314 μm^2 cm^{-3} in the residual layer between 22 and 01 h during E3 were used. A relative HONO ~~formation~~ accumulation rate of $\Delta\frac{[HONO]}{[NO_2]}/\Delta t$ ~~is ~0.0032 h^{-1}~~ ranged between 0.00037 and 0.0037 h^{-1}, ~~which is~~ equivalent to the HONO production of ~~0.17 ppb h^{-1}~~ 0.02 to 0.2 ppb h^{-1} at a constant NO_2 concentration of 54 ppb, which was ~~when the~~ the upper limit of the observed nocturnal NO_2 ~~above 200 m was 52.9 54 ppb~~ in the residual layer during E3. ~~The nocturnal accumulation of HONO (18:00–00:00) in the RL (above 200 m) is 1.02 ppb during E3, which is much less than the HONO vertical measurements of 3.06 ppb.~~ The produced HONO amount of 30–300 ppt in an interval of 1.5 h could account for the HONO increases of 15–368 ppt in the residual layer between the two vertical profile measurements. ~~It is necessary to elaborate that (1) the typical $\left[\frac{S}{V}\right]$ is ~10^{-3} m^{-1} during the pollution period in winter in Beijing (NO_2 = 45 ppb, temperature = 273 K); (2) the upper limit of NO_2 uptake coefficient and the upper limit of~~

~~observed nocturnal NO_2 in the RL are used to calculate the HONO production on aerosol. The HONO production could be actually overestimated in our study. As described,~~ Thus, ~~HONO~~ production from the heterogeneous conversion of NO_2 solely on ~~the~~ aerosol surface~~s cannot~~ can explain the HONO ~~vertical measurements at night~~ observations during E3. In addition, if the HONO production aloft was indeed dominated by reactions on aerosol surface, the column average concentration of HONO would be expected to be independent of the amount of HONO observed at ground level. Figure 10a shows that the column of HONO is independent of the mixing ratio of HONO observed from the ground level to 10 m in height (R^2 = 0.27), which is consistent with the hypothesis that the aerosol surface presumably dominates HONO production aloft by heterogeneous uptake of NO_2 during the haze episode, and the production of HONO at ground level is not transported to the overlying air. ~~In addition, the integrated column of HONO ($HONO_{column}$) and the mixing ratios of HONO observed from ground level to 10 m height ($HONO_{ground}$) show a significant correlation (R^2 = 0.85) (Fig. 11), which also indicates that the ground surface is the primary reaction surface on which HONO is formed, and then transported throughout the column.~~ This result was contrary to previous observations that the production of HONO on aerosol surface was insignificant compared to the ground surface (Kleffmann et al., 2003; Wong et al., 2011; VandenBoer et al., 2013), which could have been due to the higher aerosol surface area observed in this study. An order of magnitude higher aerosol surface area in the residual layer than in previous vertical observations (<160 μm^2 cm^{-3}) was observed, which could provide sufficient aerosol surface area for the heterogeneous formation of HONO.

An estimate of HONO production from the heterogeneous conversion of NO_2 on aerosols was also made during C2 using S_{aw} and NO_2 observations from the residual layer. The column of the average HONO concentration was related to the amount of HONO observed between ground level and 10 m (Fig. 10b, R^2 = 0.93), suggesting that the surface HONO sources affected the HONO observed throughout the depth of boundary layer during C2. A high correlation (R^2 = 0.83) between the measured CO and BC at ground level and the CO and BC at 260 m was also observed (Fig. S10), which indicated that vehicle emissions affected air masses in the residual layer. The lack of the NO vertical profile cannot directly correct the influence of direct HONO emissions. If it is assumed that the contribution of direct HONO emissions was consistent at ground level and in the residual layer, the relative contribution of the aerosol and ground surfaces to nocturnal HONO production in the residual layer could be roughly estimated during C2. The direct emissions contribution of 35.9% ± 11.8% during C2

is a higher limit estimate of the contribution of direct emissions to the HONO levels in the residual layer.

The averages S_{aw} of 791 and 894 μm^2 cm^{-3} from 17 to 24 h, and an upper limit of NO_2 observations of 36 and 44 ppb from the residual layer were used to estimate HONO production on aerosol surface on December 9th and 10th. The formation rates of HONO on aerosol surface were 0.0047–0.047 ppb h^{-1} on the 9th and 0.0062–0.062 ppb h^{-1} on the 10th. The HONO increased by 305–608 ppt between profile measurements, which have the contributions from direct HONO emissions subtracted, were higher than the production of HONO (26–259 ppt) in the interval of 5.5 h on December 9th. The formation of HONO on aerosol surface cannot explain the observed HONO increases in the residual layer, which suggests that the HONO observed in the residual layer was primarily derived from the heterogeneous conversion of NO_2 on the ground surface followed by vertical transport throughout the column. The HONO production from the aerosol surface in the interval of 5.35 h was 33–332 ppt in the residual layer on December 10th, which was comparable to the corrected HONO increases of 114–369 ppt between profile measurements. A shallow inversion layer formed near the surface might account for the aerosols dominated HONO production in the residual layer, and this could have been due to the following: (1) the inhibition of vertical transport of nighttime HONO source at ground level, and/or (2) an overestimation of the contribution from direct HONO emissions to HONO concentrations in the residual layer.

In conclusion, HONO production solely on aerosol surface accounted for the HONO observations during E3. The ground surface dominated HONO production by heterogeneous conversion of NO_2 during the clean episode, which was then transported throughout the column. With the increases in the NO_2 mixing ratio and aerosol surface areas from the clean episode to the haze episode, the aerosol surface production became an important nocturnal source of HONO and presumably dominated the heterogeneous production of HONO aloft from NO_2 during the haze episode.

3.4.3 Nocturnal HONO production and loss at ground level

~~The nocturnal HONO in the boundary layer is primarily derived from the heterogeneous conversion from NO_2 to HONO on the ground surface, which is consistent with the results of other studies in vertical gradient of HONO (Kleffmann et al., 2003; Wong et al., 2011; Zhang et al., 2009; Ye et al., 2018).~~ The nocturnal HONO observed throughout the depth of the boundary layer is primarily

from the heterogeneous conversion of NO_2 on the ground surface during the clean episode. The HONO conversion frequency can be estimated using the data from the nocturnal measurements at ground level (18:00–06:00 LT). ~~The conversion rate of NO_2 can be evaluated using the HONO conversion frequency. However, real atmospheric components are affected by physical processes, chemical processes, and direct emissions. To reduce the uncertainties associated with transport process and source emissions, the HONO conversion frequency was calculated using the scaling method proposed by Su et al (2008) and adopting NO_2 and BC as reference species.~~ The heterogeneous formation of HONO in reaction (R2) is first order in NO_2, and the HONO formation is proportional to the NO_2 concentration. The conversion frequency was derived using the method proposed by Alicke et al. (2002). ~~Before calculation, the HONO concentration was corrected by direct emission (Eq. (3)).~~ The emission ratio of HONO/NO_x derived in section 3.3 was used to correct the HONO concentration by Eq. (6). Because NO was not measured at ground level after 14:00 on ~~10~~ December 10th, the NO_x data ~~of NO_x~~ was not available during the nocturnal vertical measurements ~~at night~~ on ~~10 and 11~~ December 10th and 11th. The ~~monthly~~ average $HONO_{emis}$/HONO ratio of ~~38.7%~~ 35.9% ± 11.8% and 26% ± 11.3% ~~was calculated~~ were used to correct the observed HONO concentrations ~~($HONO_{corr}$)~~ (i.e. $[HONO]_{corr} = [HONO] - [HONO]_{emis}$) during the clean and the haze episodes after December 10th, respectively. The NO_2-to-HONO conversion frequency, ~~C_{HONO}~~ k_{HONO}, can be ~~expressed as~~ calculated using Eq. (7), by assuming that observed HONO comes from the conversion of NO_2 (Su et al., 2008a).

~~$$[\mathrm{HONO}]_{corr} = [\mathrm{HONO}] - [\mathrm{HONO}]_{emis} = [\mathrm{HONO}] - [\mathrm{HONO}] \times 0.511 \quad (3)$$~~

$$[HONO]_{corr} = [HONO] - [NO_x] \times 0.0078 \quad (6)$$

~~$$C_{HONO}^{X} = \frac{2\left(\frac{[HONO_{corr}]_{t_2}}{[X]_{t_2}} \times \overline{[X]} - \frac{[HONO_{corr}]_{t_1}}{[X]_{t_1}} \times \overline{[X]}\right)}{(t_2 - t_1)\left(\frac{[NO_2]_{t_2}}{[X]_{t_2}} + \frac{[NO_2]_{t_1}}{[X]_{t_1}}\right)\overline{[X]}}$$~~

~~$$= \frac{2\left(\frac{[HONO_{corr}]_{t_2}}{[X]_{t_2}} - \frac{[HONO_{corr}]_{t_1}}{[X]_{t_1}}\right)}{(t_2 - t_1)\left(\frac{[NO_2]_{t_2}}{[X]_{t_2}} + \frac{[NO_2]_{t_1}}{[X]_{t_1}}\right)} \quad (4)$$~~

~~$$C_{HONO} = \frac{1}{3}\left(C_{HONO}^{0} + C_{HONO}^{NO_2} + C_{HONO}^{BC}\right) \quad (5)$$~~

$$k_{HONO} = \frac{[HONO_{corr}]_{t_2} - [HONO_{corr}]_{t_1}}{(t_2 - t_1)[\overline{NO_2}]} \quad (7)$$

where ~~$[HONO_{corr}]_t$, $[NO_2]_t$, and $[X]_t$ represent mixing ratios of HONO, NO_2, and the reference gas at the sampling time t,~~ $[\overline{NO_2}]$ is the average NO_2 mixing ratio during the time interval of $t_2 - t_1$. ~~C_{HONO} is average conversion frequency, C_{HONO}^{X} is the conversion frequency scaled with species X,~~

~~and C^{0}_{HONO} is the conversion frequency which is not scaled.~~ The ~~average~~ conversion frequencies, ~~C_{HONO}~~ k_{HONO}, on ~~9, 10 and 11~~ December 9th, 10th, and 11th were ~~0.0039 h^{-1}, 0.0026 h^{-1}, and 0.0039 h^{-1}~~ 0.0082, 0.0060 and 0.0114 h^{-1}, respectively, corresponding to a HONO production rate by NO_2 (P_{NO_2}) of 0.25 ± 0.03, 0.28 ± 0.02, and 0.60 ± 0.02 ppb h^{-1} (i.e. $C_{HONO} \times \overline{[NO_2]}$), respectively. It is necessary to elaborate that the derived P_{NO_2} is the net HONO production, which means sources and sinks of HONO (aerosol and ground surface sources, deposition, etc.) have already been taken into account in the P_{NO_2}. The HONO conversion frequency obtained in this study is ~~which was~~ comparable to the observations by Hou et al. (2016) ~~in Beijing~~ (~~the~~ clean episode: 0.0065 h^{-1}, ~~the~~ haze episode: 0.0039 h^{-1}) and Zhang et al. (2018) in the Beijing region (haze episode: 0.058 h^{-1}, severe haze episode: 0.0146 h^{-1}), ~~and Lammel et al. (1999) in Mainz and Milan (0.0041 h^{-1} and 0.00491 h^{-1}), but much~~ However, they are lower than the observations made by Li et al. (2012) (0.024 ± 0.015 h^{-1}) and Su et al. (2008b) (0.016 ± 0.014 h^{-1}) at a rural site in southern China.

It was assumed that production of HONO on aerosol surface was insignificant compared to the ground surface during the clean episode, which has been suggested in other studies of HONO vertical gradient (VandenBoer et al., 2013; Wong et al., 2011; Zhang et al., 2009). Therefore, the HONO production (P_{NO_2}) could be considered as a net contribution of the surface production of HONO to the total column of HONO when HONO deposition is considered in P_{NO_2}. The surface production rate of HONO of 0.25 ± 0.03 and 0.28 ± 0.02 ppb h^{-1} were an order of magnitude higher than the maximum production rate of HONO on aerosol surface (0.047 and 0.062 ppb h^{-1}) on December 9th and 10th. This result suggests that ground surface dominated HONO production by heterogeneous conversion of NO_2 during the clean episode. In contrast, the production of HONO solely on aerosol surface can explain the HONO observations in the residual layer during E3, indicating that the aerosol surface production was an important nocturnal source of HONO during the haze episodes. The derived P_{NO_2} is the total HONO production rate of the aerosol and ground surfaces by heterogeneous conversion of NO_2. To compare the HONO heterogeneous production on aerosol and ground surfaces, a deposition velocity of NO_2 to the surface in the dark, V_{dep,NO_2}, of 0.07 cm s^{-1} (VandenBoer et al., 2013), in a boundary layer of height, *h* of 140 m, was used to estimate the HONO production rate by NO_2 on the ground surface. The nocturnal production of HONO by heterogeneous uptake of NO_2 on ground surface can be estimated by the following,

$$P_{HONO,ground} = \frac{1}{2}\frac{V_{dep,NO_2}}{h}\overline{[NO_2]} \quad (8)$$

The surface production rate of HONO ($P_{HONO,ground}$) was 0.47 ± 0.02 ppb h^{-1} on December 11th (E3), which was comparable to the HONO production rate on aerosol surface of 0.2 ppb h^{-1}. This result also suggests that the production of HONO on aerosols is an important nocturnal source of HONO during the haze episode. The higher production rates of HONO on the ground surfaces were consistent with the fact that the ground had a much greater surface area than the aerosol (i.e, the ground surface area was 7140 μm^2 cm^{-3} in a 140 m deep NBL, versus the average S_{aw} of 2255 μm^2 cm^{-3} during E3). However, the vertical transport of the surface production of HONO throughout the column was likely inhibited during E3. The column average concentration of HONO was independent of the mixing ratio of HONO observed between ground level and 10 m (Fig. 10a), which may have been due to a more stable nocturnal boundary layer structure during the haze episode.

~~As illustrated above, HONO production from the heterogeneous conversion of NO_2 on the aerosol surfaces cannot explain our HONO vertical measurements. The heterogeneous conversion from NO_2 to HONO on ground surfaces at nighttime was further evaluated,~~

~~$$C_{HONO} = \frac{P_{HONO}}{[NO_2]} = \frac{\phi_{NO_2\to HONO}\times v_{NO_2}^{ground}}{H} - \frac{v_{HONO}^{ground}}{H}\times\frac{[HONO_{corr}]}{[NO_2]} \quad (6)$$~~

~~where v_{HONO}^{ground} and $v_{NO_2}^{ground}$ are the dry deposition velocities of HONO and NO_2, which were expected to be similar since because the nocturnal controlling resistances were mainly the aerodynamic resistance and the quasi-laminar layer resistance (Su et al., 2008a; Stutz et al., 2002). $\phi_{NO_2\to HONO}$ is the HONO yield from deposited NO_2, which varies between 0 and 1, indicating that the deposited NO_2 molecule is not necessarily converted to HONO. H is the mixing depth height. Previous studies reported the value of v_{HONO}^{ground} between 0.077 and 3 cm s^{-1} (Harrison and Kitto, 1994; Harrison et al., 1996; Spindler et al., 1998; Stutz et al., 2002; Coe and Gallagher, 1992; Laufs et al., 2017). In the present study, we used a mean v_{HONO}^{ground} of 0.095 cm s^{-1} (Su et al., 2008a; Stutz et al., 2002; Coe and Gallagher, 1992) and assumed that boundary layer mixing depth H is 100 m high. The $\phi_{NO_2\to HONO}$ values on 9 (C2), 10 (C2) and 11 December (E3) were 0.10, 0.08, and 0.09, respectively, which means that every 10–13 deposited NO_2 molecules will result in one HONO being released into atmosphere. The value of deposited NO_2 molecules converted into gas phase HONO is within the range of published results (3–33) (Stutz et al., 2002; Su et al., 2008a; Li et al., 2012). The derived $\phi_{NO_2\to HONO}$ value is lower than calculation by Su et al (2008a) (0.34), which is caused by the differences in surface~~

~~environment between urban and rural areas. Similar $\phi_{NO_2 \to HONO}$ values were found during C2 and E3, suggesting that the potential of heterogeneous conversion from NO_2 to HONO on ground surface at night is consistent.~~

A budget equation of nighttime HONO (Eq. 9) was utilized to separate the contributions of the individual chemical processes involved in the nocturnal production and loss of HONO (Su et al., 2008b; Oswald et al., 2015).

$$\frac{d[HONO]}{dt} = P_{emis} + P_{aerosol} + P_{ground} + P_A - L_{dep} \pm T_h \pm T_v \quad (9)$$

The production terms of the HONO consist of the direct emission rate (P_{emis}); the heterogeneous production rate on aerosol ($P_{aerosol}$) and ground surfaces (P_{ground}); and the additional nighttime HONO source/sink (P_A). The loss process (L_{dep}) is the dry deposition rate at nighttime. T_h and T_v describe the horizontal and vertical transport processes, respectively. The horizontal transport, T_h, is negligible in a relative calm atmosphere with low wind speeds (<1.6 m s^{-1}) during vertical measurements. The vertical transport, T_v, acts as a sink close to the surface and as an additional source at elevated levels. However, it is difficult to quantify T_v without direct measurements of fluxes or using the chemical transport model, and its contribution is uncertain. Without explicitly considering T_v, the budget analysis is reasonable for relatively well-mixed conditions. Thus, the budget analysis is used for the measurements conducted on December 9th and 10th, when no shallow inversion layer was observed near the surface.

Simplifying Eq. (9), the $dHONO/dt$ was approximated by $\Delta HONO/\Delta t$, which is the difference in the observed HONO mixing ratios at two time points. An additional nocturnal production rate term (P_A) can be derived by Eq. (10). The emission ratio of HONO/NO_x (0.78%) and $HONO_{emis}$/HONO ratio (26% ± 11.3%) obtained in section 3.3 were used to estimate P_{emis}. The nocturnal production of HONO via NO_2 on aerosol and ground surfaces, and the production rate terms of $P_{aerosol}$ and P_{ground} in Eq. (4) and (8) were used as representations of the nocturnal production of HONO in Eq. (10). An upper limit uptake coefficient of γ_{NO_2} (1×10^{-5}) was assumed to estimate the HONO production rate on aerosol surface. For L_{dep}, the temperature-dependent deposition velocity of HONO ($V(HONO)_T = \exp(23920/T - 91.5)$) was used to estimate the $V_{dep,HONO}$, which decreased exponentially to non-significant values at 40 °C (Laufs et al., 2017). The average $V_{dep,HONO}$ calculated from the nocturnal measurements (00:00–06:00 LT) was 1.8 cm s^{-1}, with a range of values spanning 0.9

to 3 cm s^{-1}, which was within the range of previously reported values between 0.077 and 3 cm s^{-1} (Harrison and Kitto, 1994; Harrison et al., 1996; Spindler et al., 1998; Stutz et al., 2002; Coe and Gallagher, 1992; Laufs et al., 2017).

$$\frac{\Delta HONO}{\Delta t} = \frac{1}{2}\frac{V_{dep,NO_2}}{h}[NO_2] + \frac{1}{8}S_{aw}C_{NO_2}\gamma_{NO_2}[NO_2] + \frac{\Delta HONO_{emis}}{\Delta t} + P_A - \frac{V_{dep,HONO}}{h}[HONO] \quad (10)$$

Figure 11 shows the nocturnal HONO budgets from 18:00 to 06:00 LT on the 9th (C2) and 11th (E3) of December. The production rate of HONO on aerosol surface (0.04 ± 0.01 ppb h^{-1}) was insignificant compared to the ground surface (0.28 ± 0.03 ppb h^{-1}) during C2. However, an average $P_{aerosol}$ of 0.19 ± 0.01 ppb h^{-1} derived during E3 was comparable to the surface production rate of HONO (P_{ground}, 0.47 ± 0.03 ppb h^{-1}), which supported the preceding result that HONO production on aerosols was an important nocturnal source of HONO during the haze episode. For the source of direct HONO emissions, P_{emis} only provided a small portion of the HONO at a rate of 0.06 ± 0.07 and 0.10 ± 0.10 ppb h^{-1}. The loss of HONO due to surface deposition was the dominant sink for HONO during nighttime. The L_{dep} contributed 0.74 ± 0.31 and 1.55 ± 0.32 ppb h^{-1} to the nocturnal loss of HONO during C2 and E3, respectively, implying that significant amounts of HONO were deposited to the ground surface at night. This had been suggested in another study on the vertical gradient of HONO (VandenBoer et al., 2013).

4 Conclusions

High-resolution vertical profiles of HONO and NO_2 were measured using an IBBCEAS instrument during the APHH-Beijing winter campaign. ~~Although the data set of this study is rather limited in scope, encompassing only four nights in December 2016 with a limited set of ancillary data, it is unique because,~~ To the best of our knowledge, this is the first high-resolution vertical measurements of HONO and NO_2 in urban areas of China. The ~~observed~~ HONO concentrations observed during E1, C2, and E3 were 4.26 ± 2.08, 0.83 ± 0.65, and 3.54 ± 0.91 ppb, respectively. A relatively well-mixed boundary layer was observed after sunset, and the vertical distribution of HONO ~~is~~ was consistent with reduced mixing and stratification in the lower several hundred meters of the nocturnal urban atmosphere. The small-scale stratification of the nocturnal atmosphere and the formation of a shallow inversion layer affected the vertical distribution of HONO and NO_2. A near-steady state in HONO mixing ratio and HONO/NO_2 ratio was observed near midnight on December 11th to 12th, and an approximate balance was established between the production and loss of

HONO. ~~The $HONO_{emis}$/HONO ratio was 51.1% indicating that direct emissions from combustion processes have a great deal of influence on ambient HONO concentrations and is an important nocturnal HONO sources at the measurement site. In addition, high resolution vertical profiles of HONO, HONO production from the heterogeneous conversion of NO_2 on aerosol surfaces cannot explain HONO vertical measurements and the correlation between the integrated column of HONO and HONO measured from the surface to 10 m height, all suggesting that the heterogeneous conversion of NO_2 on the ground surface dominated the HONO production at night, and then transported throughout the column due to the vertical convection.~~

~~A relatively well mixed boundary layer was observed after sunset, and the △HONO fluctuated around zero. The small scale stratification of the nocturnal urban atmosphere and the formation of a shallow inversion layer affect the vertical distribution of HONO and NO_2. The high resolution vertical profiles showed that dry deposition loss of HONO to the ground surface and vertical mixing effects reached a near steady state on the nighttime of 11-12 December, which revealed (1) the ground surface is the dominant reaction surface on which HONO is formed from the heterogeneous conversion of NO_2; (2) significant quantities of HONO are deposited to the ground surface at night, which is an important nocturnal sink of HONO. The nocturnal HONO production from the heterogeneous reaction of NO_2 at ground level was evaluated, and the $\phi_{NO_2 \to HONO}$ values on 9 (C2), 10 (C2) and 11 December (E3) were 0.10, 0.08, and 0.09 0.04, 0.046 and 0.039, respectively. The similar values of $\phi_{NO_2 \to HONO}$ indicate that the potential of heterogeneous conversion from NO_2 to HONO at the ground level is consistent for both the clean and the haze episodes.~~ Direct HONO emissions contributed an average of 29.3% ± 12.4% to the ambient HONO levels at night. High-resolution vertical profiles of HONO revealed (1) the ground surface dominated HONO production by heterogeneous conversion of NO_2 during the clean episode, (2) the production solely on aerosols explained the HONO observations in the residual layer during E3, suggesting that the aerosols was an important nighttime HONO source during the haze episode. The column average HONO concentration was independent of the HONO observed between the ground level and 10 m during E3, implying that the aerosols presumably dominated the heterogeneous production of HONO aloft from NO_2 during the haze episode. The average dry deposition rates of 0.74 ± 0.31 and 1.55 ± 0.32 ppb h^{-1} were identified during the clean and haze episodes, respectively, implying that significant amounts of HONO were deposited to the ground surface at night. Overall, these results draw a picture of the nocturnal sources of HONO during

different pollution levels, and demonstrated the urgent need for ~~Because of the relatively few vertical measurement cases and the limited height of the meteorological tower, future~~ high-resolution vertical measurements of HONO to a high height (e.g., using tethered balloons) and more comprehensive vertical observations to improve our ~~measurements in the megacities, are urgently needed for a better~~ understanding of the vertical distribution and ~~the formation mechanisms~~ chemistry of HONO in the PBL ~~in megacities~~.

Data availability. The data used in this study are available from the corresponding author upon request (mqin@aiofm.ac.cn).

Supplement.

Author contributions. MQ and PX organized the field contributions from the Anhui Institute of Optics and Fine Mechanics group for the APHH-Beijing project. MQ and JD designed the ~~research~~ study. WF and JD built the IBBCEAS instrument. JD and KT ~~conducted the measurements~~ collected the HONO and NO_2 data. YS and CX provided the ancillary data. FM and MQ analyzed the data. FM wrote the paper and MQ revised it. ~~MQ, YS and CY revised and commented on the paper.~~ The contributions of FM and MQ are the same for this paper.

Competing interests. The authors declare that they have no conflict of interest.

Special issue statement. This article is part of the special issue "In-depth study of air pollution sources and processes within Beijing and its surrounding region (APHH-Beijing) (ACP/AMT inter-journal SI)". It is not associated with a conference.

Acknowledgements. We gratefully acknowledge Bin Ouyang from Cambridge University for providing HONO measurement data for inter-comparison.

~~*Acknowledgements.*~~ *Financial support.* This work was supported by the National Natural Science Foundation of China (41875154, 41571130023, 91544104), the National Key R&D Program of China (2017YFC0209400, 2016YFC0208204), and the Science and Technology Major Special Project of Anhui Province, China

(16030801120).

References

Acker, K., Febo, A., Trick, S., Perrino, C., Bruno, P., Wiesen, P., Möller, D., Wieprecht, W., Auel, R., Giusto, M., Geyer, A., Platt, U., and Allegrini, I.: Nitrous acid in the urban area of Rome, Atmos. Environ., 40, 3123-3133, https://doi.org/10.1016/j.atmosenv.2006.01.028, 2006.

Alicke, B., Platt, U., Stutz, J.: Impact of nitrous acid photolysis on the total hydroxyl radical budget during the Limitation of Oxidant Production/Pianura Padana Produzione di Ozono study in Milan, J. Geophys. Res., 107, LOP 9-1-LOP 9-17, https://doi.org/10.1029/2000jd000075, 2002.

Ammann, M., Kalberer, M., Jost, D. T., Tobler, L., Rossler, E., Piguet, D., Gaggeler, H. W., and Baltensperger, U.: Heterogeneous production of nitrous acid on soot in polluted air masses, Nature, 395, 157-160, https://doi:10.1038/25965, 1998.

An, J., Li, Y., Chen, Y., Li, J., Qu, Y., and Tang, Y. J.: Enhancements of major aerosol components due to additional HONO sources in the North China Plain and implications for visibility and haze, Adv. Atmos. Sci., 30, 57-66, https://doi.org/10.1007/s00376-012-2016-9, 2012.

Aubin, D. G., and Abbatt, J. P. D.: Interaction of NO_2 with Hydrocarbon Soot: Focus on HONO Yield, Surface Modification, and Mechanism, J. Phys. Chem. A., 111, 6263-6273, https://doi.org/10.1021/jp068884h, 2007.

Bao, F. X., Li, M., Zhang, Y., Chen, C. C., and Zhao, J. C.: Photochemical Aging of Beijing Urban $PM_{2.5}$: HONO Production, Environ. Sci. Technol., 52, 6309-6316, https://doi.org/10.1021/acs.est.8b00538, 2018.

Bartolomei, V., Alvarez, E. G., Wittmer, J., Tlili, S., Strekowski, R., Temime-Roussel, B., Quivet, E., Wortham, H., Zetzsch, C., Kleffmann, J., and Gligorovski, S.: Combustion Processes as a Source of High Levels of Indoor Hydroxyl Radicals through the Photolysis of Nitrous Acid, Environ. Sci. Technol., 49, 6599-6607, https://doi.org/10.1021/acs.est.5b01905, 2015.

Bejan, I., Abd-El-Aal, Y., Barnes, I., Benter, T., Bohn, B., Wiesen, P., and Kleffmann, J.: The photolysis of *ortho*-nitrophenols: a new gas phase source of HONO, Phys. Chem. Chem. Phys., 8, 2028-2035, https://doi.org/10.1039/b516590c, 2006.

Bond, T. C., Doherty, S. J., Fahey, D. W., Forster, P. M., Berntsen, T., DeAngelo, B. J., Flanner, M. G., Ghan, S., Kärcher, B., Koch, D., Kinne, S., Kondo, Y., Quinn, P.K., Sarofim, M.C., Schultz, M.G., Schulz, M., Venkataraman, C., Zhang, H., Zhang, S., Bellouin, N., Guttikunda, S.K., Hopke, P.K., Jacobson, M.Z., Kaiser, J.W., Klimont, Z., Lohmann, U., Schwarz, J.P., Shindell, D., Storelvmo, T., Warren, S.G., and Zender, C.S.: Bounding the role of black carbon in the climate system: A scientific assessment, J. Geophys. Res. Atmos., 118, 5380-5552, https://doi.org/10.1002/jgrd.50171, 2013.

Brigante, M., Cazoir, D., D'Anna, B., George, C., and Donaldson, D. J.: Photoenhanced Uptake of NO2 by Pyrene Solid Films, J. Phys. Chem. A, 112, 9503-9508, https://doi.org/10.1021/jp802324g, 2008.

Bröske, R., Kleffmann, J., and Wiesen, P.: Heterogeneous conversion of NO_2 on secondary organic aerosol surfaces: A possible source of nitrous acid (HONO) in the atmosphere?, Atmos. Chem. Phys., 3, 469-474, https://doi.org/10.5194/acp-3-469-2003, 2003.

Brown, S. S., Dubé, W. P., Osthoff, H. D., Wolfe, D. E., Angevine, W. M., and Ravishankara, A. R.: High resolution vertical distributions of NO_3 and N_2O_5 through the nocturnal boundary layer, Atmos. Chem. Phys., 7, 139-149, https://doi.org/10.5194/acp-7-139-2007, 2007.

Cai, R. L., Yang, D. S., Fu, Y. Y., Wang, X., Li, X. X., Ma, Y., Hao, J. M., Zheng, J., and Jiang, J. K.: Aerosol

surface area concentration: a governing factor in new particle formation in Beijing, Atmos. Chem. Phys., 17, 12327-12340, https://doi.org/ /10.5194/acp-17-12327-2017, 2017.

Coe, H., and Gallagher, M. W.: Measurements of Dry Deposition of NO_2 to A Dutch Heathland Using the Eddy-Correlation Technique, Q. J. Roy. Meteor. Soc., 118, 767-786, https://doi.org/10.1002/qj.49711850608, 1992.

Cui, L. L., Li, R., Zhang, Y. C., Meng, Y., Fu, H. B. and Chen, J. M.: An observational study of nitrous acid (HONO) in Shanghai, China: The aerosol impact on HONO formation during the haze episodes, Sci. Total Environ., 630, 1057-1070, https://doi.org/10.1016/j.scitotenv.2018.02.063, 2018.

Donaldson, M. A., Berke, A. E., and Raff, J. D.: Uptake of Gas Phase Nitrous Acid onto Boundary Layer Soil Surfaces, Environ. Sci. Technol., 48, 375-383, https://doi.org/10.1021/es404156a, 2014.

Du, W., Zhao, J., Wang, Y. J., Zhang, Y. J., Wang, Q. Q., Xu, W. Q., Chen, C., Han, T. T., Zhang, F., Li, Z. Q., Fu, P. Q., Li, J., Wang, Z. F., and Sun, Y. L.: Simultaneous measurements of particle number size distributions at ground level and 260 m on a meteorological tower in urban Beijing, China, Atmos. Chem. Phys., 17, 6797–6811, https://doi.org/10.5194/acp-17-6797-2017, 2017.

Duan, J., Qin, M., Ouyang, B., Fang, W., Li, X., Lu, K. D., Tang, K., Liang, S. X., Meng, F. H., Hu, Z. K., Xie, P. H., Liu, W. Q., and Häsler, R.: Development of an incoherent broadband cavity-enhanced absorption spectrometer for in situ measurements of HONO and NO_2, Atmos. Meas. Tech., 11, 4531-4543, https://doi.org/10.5194/amt-11-4531-2018, 2018.

Finlayson-Pitts, B. J., Wingen, L. M., Sumner, A. L., Syomin, D., and Ramazan, K. A.: The heterogeneous hydrolysis of NO_2 in laboratory systems and in outdoor and indoor atmospheres: An integrated mechanism, Phys. Chem. Chem. Phys., 5, 223-242, https://doi.org/10.1039/b208564j, 2003.

Finlayson-Pitts, B. J.: Reactions at surfaces in the atmosphere: integration of experiments and theory as necessary (but not necessarily sufficient) for predicting the physical chemistry of aerosols, Phys. Chem. Chem. Phys., 36, 7760-7779, https://doi.org/10.1039/B906540G, 2009.

~~Fu, X., Wang, T., Zhang, L., Li, Q. Y., Wang, Z., Xia, M., Yun, H., Wang, W. H., Yu, C., Yue, D. L., Zhou, Y., Zheng, J. Y., and Han, R.: The significant contribution of HONO to secondary pollutants during a severe winter pollution event in southern China, Atmos. Chem. Phys., 19, 1-14, https://doi.org/10.5194/acp-19-1-2019, 2019.~~

~~George, C., Strekowski, R. S., Kleffmann, J., Stemmler, K., and Ammann, M.: Photoenhanced uptake of gaseous NO_2 on solid organic compounds: a photochemical source of HONO?, Faraday Discuss., 130, 195-210, https://doi.org/10.1039/b417888m, 2005.~~

George, C., Strekowski, R. S., Kleffmann, J., Stemmler, K., and Ammann, M.: Photoenhanced uptake of gaseous NO2 on solid organic compounds: a photochemical source of HONO?, Faraday Discuss., 130, 195-210, https://doi.org/10.1039/b417888m, 2005.

Gómez Alvarez, E., Sörgel, M., Gligorovski, S., Bassil, S., Bartolomei, V., Coulomb, B., Zetzsch, C., and Wortham, H.: Light-induced nitrous acid (HONO) production from NO_2 heterogeneous reactions on household chemicals, Atmos. Environ., 95, 391-399, https://doi.org/10.1016/j.atmosenv.2014.06.034, 2014.

Han, C., Yang, W. J., Wu, Q. Q., Yang, H., and Xue, X. X.: Heterogeneous Photochemical Conversion of NO_2 to HONO on the Humic Acid Surface under Simulated Sunlight, Environ. Sci. Technol., 50, 5017-5023, https://doi.org/10.1021/acs.est.5b05101, 2016.

Han, C., Yang, W. J., Yang, H., and Xue, X. X.: Enhanced photochemical conversion of NO_2 to HONO on humic acids in the presence of benzophenone, Environ. Pollut., 231, 979-986, https://doi.org/10.1016/j.envpol.2017.08.107, 2017.

Hanst, P. L., Spence, J. W., and Miller, M.: Atmospheric Chemistry of N-nitroso Dimethylamine, Environ. Sci. Technol., 11, 403-405, https://doi.org/10.1021/es60127a007, 1977.

Harrison, R. M., and Kitto, A. M. N.: Evidence for a surface source of atmospheric nitrous acid, Atmos. Environ.,

28, 1089-1094, https://doi.org/10.1016/1352-2310(94)90286-0, 1994.
Harrison, R. M., Peak, J. D., and Collins, G. M.: Tropospheric cycle of nitrous acid, J. Geophys. Res., 101, 14429-14439, https://doi.org/10.1029/96JD00341, 1996.
Hendrick, F., Müller, J. F., Clémer, K., Wang, P., De Mazière, M., Fayt, C., Gielen, C., Hermans, C., Ma, J. Z., Pinardi, G., Stavrakou, T., Vlemmix, T., and Van Roozendael, M.: Four years of ground-based MAX-DOAS observations of HONO and NO_2 in the Beijing area, Atmos. Chem. Phys., 14, 765-781, https://doi.org/10.5194/acp-14-765-2014, 2014.
Hou, S. Q., Tong, S. R., Ge, M. F., and An, J. L.: Comparison of atmospheric nitrous acid during severe haze and clean periods in Beijing, China, Atmos. Environ., 124, 199-206, https://doi.org/10.1016/j.atmosenv.2015.06.023, 2016.
~~Huang, R. J., Zhang, Y. L., Bozzetti, C., Ho, K. F., Cao, J. J., Han, Y. M., Daellenbach, K. R., Slowik, J. G., Platt, S. M., Canonaco, F., Zotter, P., Wolf, R., Pieber, S. M., Bruns, E. A., Crippa, M., Ciarelli, G., Piazzalunga, A., Schwikowski, M., Abbaszade, G., Schnelle-Kreis, J., Zimmermann, R., An, Z. S., Szidat, S., Baltensperger, U., El Haddad, I., and Prévôt, A. S. H.: High secondary aerosol contribution to particulate pollution during haze events in China, Nature, 514, 218-222, https://doi.org/10.1038/nature13774, 2014.~~
Huang, R. J., Yang, L., Cao, J. J., Wang, Q. Y., Tie, X. X., Ho, K. F., Shen, Z. X., Zhang, R. J., Li, G. H., Zhu, C. S., Zhang, N. N., Dai, W. T., Zhou, J. M., Liu, S. X., Chen, Y., Chen, J., and O'Dowd, C. D.: Concentration and sources of atmospheric nitrous acid (HONO) at an urban site in Western China, Sci. Total Environ., 593-594, 165-172, https://doi.org/10.1016/j.scitotenv.2017.02.166, 2017.
Hao, N., Zhou, B., Chen, D., and Chen, L. M..: Observations of nitrous acid and its relative humidity dependence in Shanghai, J. Environ. Sci., 18, 910-915, https://doi.org/10.1016/S1001-0742(06)60013-2, 2006.
Karamchandani, P., Emery, C., Yarwood, G., Lefer, B., Stutz, J., Couzo, E., and Vizuete, W.: Implementation and refinement of a surface model for heterogeneous HONO formation in a 3-D chemical transport model, Atmos. Environ., 112, 356-368, https://doi.org/10.1016/j.atmosenv.2015.01.046, 2015.
Kirchstetter, T. W., Harley, R. A., and Littlejohn D.: Measurement of nitrous acid in motor vehicle exhaust, Environ. Sci. Technol., 30, 2843-2849, https://doi.org/10.1021/es960135y, 1996.
Kleffmanna, J., Beckera, K. H., and Wiesena, P.: Heterogeneous NO_2 conversion processes on acid surfaces: possible atmospheric implications, Atmos. Environ., 32, 2721-2729, https://doi.org/10.1016/S1352-2310(98)00065-X, 1998.
Kleffmann, J., Becker, K. H., Lackhoff, M., and Wiesen, P.: Heterogeneous conversion of NO_2 on carbonaceous surfaces, Phys. Chem. Chem. Phys., 1, 5443-5450, https://doi.org/10.1039/A905545B, 1999.
Kleffmann, J., Kurtenbach, R., Lörzer, J., Wiesen, P., Kalthoff, N., Vogel, B., and Vogel, H.: Measured and simulated vertical profiles of nitrous acid—Part I: Field measurements, Atmos. Environ., 37, 2949-2955, https://doi.org/10.1016/s1352-2310(03)00242-5, 2003.
Kleffmann, J.: Daytime Sources of Nitrous acid (HONO) in the Atmospheric Boundary Layer, Chemphyschem, 8, 1137-1144, https://doi.org/10.1002/cphc.200700016, 2007.
Kurtenbach, R., Becker, K. H., Gomes, J. A. G., Kleffmann, J., Lörzer, J., Spittler, M., Wiesen, P., Ackermann, R., Geyer, A., and Platt, U.: Investigations of emission and heterogeneous formation of HONO in a road traffic tunnel, Atmos. Environ., 35, 3385–3394, https://doi.org/10.1016/S1352-2310(01)00138-8, 2001.
~~Lammel, G.: Formation of Nitrous acid: Parameterisation and comparison with observations. Technical report, Max-Planck-Institute for Meteorology, Hamburg, Germany, 1999.~~
Laufs, S., Cazaunau, M., Stella, P., Kurtenbach, R., Cellier, P., Mellouki, A., Loubet, B., and Kleffmann, J.: Diurnal fluxes of HONO above a crop rotation, Atmos. Chem. Phys., 17, 6907-6923, https://doi.org/10.5194/acp-17-6907-2017, 2017.

Li, D. D., Xue, L. K., Wen, L., Wang, X. F., Chen, T. S., Mellouki, A., Chen, J. M., and Wang, W. X.: Characteristics and sources of nitrous acid in an urban atmosphere of northern China: Results from 1-yr continuous observations, Atmos. Environ., 182, 296-306, https://doi.org/10.1016/j.atmosenv.2018.03.033, 2018.

Li, S. P., Matthews, J., and Sinha, A.: Atmospheric Hydroxyl Radical Production from Electronically Excited NO_2 and H_2O, Science, 319, 1657-1660, https://doi.org/10.1126/science.1151443, 2008.

Li, X., Brauers, T., Häseler, R., Bohn, B., Fuchs, H., Hofzumahaus, A., Holland, F., Lou, S., Lu, K. D., Rohrer, F., Hu, M., Zeng, L. M., Zhang, Y. H., Garland, R. M., Su, H., Nowak, A., Wiedensohler, A., Takegawa, N., Shao, M., and Wahner, A.: Exploring the atmospheric chemistry of nitrous acid (HONO) at a rural site in Southern China, Atmos. Chem. Phys., 12, 1497-1513, https://doi.org/10.5194/acp-12-1497-2012, 2012.

Li, X., Rohrer, F., Hofzumahaus, A., Brauers, T., Häseler, R., Bohn, B., Broch, S., Fuchs, H., Gomm, H., Holland, F., Jäger, J., Kaiser, J., Keutsch, F. N., Lohse, I., Lu, K. D., Tillmann, R., Wegener, R., Wolfe, G. M., Mentel, T. F., Kiendler-Scharr, A., Wahner, A.: Missing Gas-Phase Source of HONO Inferred from Zeppelin Measurement in the Troposphere, Science, 334, 292-296, https://doi.org/10.1126/science.1248999, 2014.

Liang, Y. T., Zha, Q. Z., Wang, W. H., Cui, L., Lui, K. H., Ho, K. F., Wang, Z., Lee, S. C., and Wang, T.: Revisiting nitrous acid (HONO) emission from on-road vehicles: A tunnel study with a mixed fleet, J. Air Waste Manag., 67, 797-805, https://doi.org/10.1080/10962247.2017.1293573, 2017.

Liu, X., Cheng, Y., Zhang, Y., Jung, J., Sugimoto, N., Chang, S.Y., Kim, Y. J., Fan, S., and Zeng, L.: Influences of relative humidity and particle chemical composition on aerosol scattering properties during the 2006 PRD campaign, Atmos. Environ., 42, 1525–1536, https://doi.org/10.1016/j.atmosenv.2007.10.077, 2008.

Liu, Y. H., Lu, K. D., Li, X., Dong, H. B., Tan, Z. F., Wang, H. C., Zou, Q., Wu, Y. S., Zeng, L. M., Hu, M., Min, K. E., Kecorius, S., Wiedensohler, A., and Zhang, Y. H.: A Comprehensive Model Test of the HONO Sources Constrained to Field Measurements at Rural North China Plain, Environ. Sci. Technol., 53, 3517-3525, https://doi.org/10.1021/acs.est.8b06367, 2019.

Liu, Y. L., Nie, W., Xu, Z., Wang, T. Y., Wang, R. X., Li, Y. Y., Wang, L., Chi, X. G., and Ding, A. J.: Semi-quantitative understanding of source contribution to nitrous acid (HONO) based on 1 year of continuous observation at the SORPES station in eastern China, Atmos. Chem. Phys., 19, 13289-13308, https://doi.org/10.5194/acp-19-13289-2019, 2019.

Liu, Z., Wang, Y. h., Costabile, F., Amoroso, A., Zhao, C., Huey, L. G., Stickel, R., Liao, J., and Zhu, T.: Evidence of Aerosols as a Media for Rapid Daytime HONO Production over China, Environ. Sci. Technol., 48, 14386-14391, https://doi.org/10.1021/es504163z, 2014.

Liu, Z., Wang, Y., Gu, D., Zhao, C., Huey, L. G., Stickel, R., Liao, J., Shao, M., Zhu, T., Zeng, L., Amoroso, A., Costabile, F., Chang, C.-C., and Liu, S.-C.: Summertime photochemistry during CAREBeijing-2007:RO_x budgets and O_3 formation, Atmos. Chem. Phys., 12, 7737-7752, https://doi.org/10.5194/acp-12-7737-2012, 2012.

Lu, K. D., Rohrer, F., Holland, F., Fuchs, H., Bohn, B., Brauers, T., Chang, C. C., Häseler, R., Hu, M., Kita, K., Kondo, Y., Li, X., Lou, S. R., Nehr, S., Shao, M., Zeng, L. M., Wahner, A., Zhang, Y. H., and Hofzumahaus, A.: Observation and modelling of OH and HO_2 concentrations in the Pearl River Delta 2006: a missing OH source in a VOC rich atmosphere, Atmos. Chem. Phys., 12, 1541-1569, https://doi.org/10.5194/acp-12-1541-2012, 2012.

Ma, Q. X., Wang, T., Liu, C., He, H., Wang, Z., Wang, W. H., and Liang, Y. T.: SO_2 Initiates the Efficient Conversion of NO_2 to HONO on MgO Surface, Environ. Sci. Technol., 51, 3767-3775, https://doi.org/10.1021/acs.est.6b05724, 2017.

Mendez, M., Blond, N., Amedro, D., Hauglustaine, D. A., Blondeau, P., Afif, C., Fittschen, C., and Schoemaecker, C.: Assessment of indoor HONO formation mechanisms based on in situ measurements and modeling, Indoor Air, 27, 443-451, https://doi.org/10.1111/ina.12320, 2017.

Meusel, H., Kuhn, U., Reiffs, A., Mallik, C., Harder, H., Martinez, M., Schuladen, J., Bohn, B., Parchatka, U.,

Crowley, J. N., Fischer, H., Tomsche, L., Novelli, A., Hoffmann, T., Janssen, R. H. H., Hartogensis, O., Pikridas, M., Vrekoussis, M., Bourtsoukidis, E., Weber, B., Lelieveld, J., Williams, J., Pöschl, U., Cheng, Y. F., and Su, H.: Daytime formation of nitrous acid at a coastal remote site in Cyprus indicating a common ground source of atmospheric HONO and NO, Atmos. Chem. Phys., 16, 14475-14493, https://doi.org/10.5194/acp-16-14475-2016, 2016.

Michoud, V., Colomb, A., Borbon, A., Miet, K., Beekmann, M., Camredon, M., Aumont, B., Perrier, S., Zapf, P., Siour, G., Ait-Helal, W., Afif, C., Kukui, A., Furger, M., Dupont, J. C., Haeffelin, M., and Doussin, J. F.: Study of the unknown HONO daytime source at a European suburban site during the MEGAPOLI summer and winter field campaigns, Atmos. Chem. Phys., 14, 2805-2822, https://doi.org/10.5194/acp-14-2805-2014, 2014.

Michoud, V., Doussin, J.-F., Colomb, A., Afif, C., Borbon, A., Camredon, M., Aumont, B., Legrand, M., and Beekmann, M.: Strong HONO formation in a suburban site during snowy days, Atmos. Environ., 116, 155-158, https://doi.org/10.1016/j.atmosenv.2015.06.040, 2015.

Monge, M. E., D'Anna, B., Mazri, L., Giroir-Fendler, A., Ammann, M., Donaldson, D. J., and George, C.: Light changes the atmospheric reactivity of soot, P. Natl. Acad. Sci. USA, 107, 6605-6609, https://doi.org/10.1073/pnas.0908341107, 2010.

Neuman, J. A., Trainer, M., Brown, S. S., Min, K. E., Nowak, J. B., Parrish, D. D., Peischl, J., Pollack, I. B., Roberts, J. M., Ryerson, T. B., and Veres, P. R.: HONO emission and production determined from airborne measurements over the Southeast U.S, J. Geophys. Res. Atmos., 121, 9237-9250, https://doi.org/10.1002/2016JD025197, 2016.

Oswald, R., Behrendt, T., Ermel, M., Wu, D., Su, H., Cheng, Y., Breuninger, C., Moravek, A., Mougin, E., Delon, C., Loubet, B., Pommerening-Röser, A., Sörgel, M., Pöschl, U., Hoffmann, T., Andreae, M. O., Meixner, F. X. and Trebs, I.: HONO Emissions from Soil Bacteria as a Major source of Atmospheric Reactive Nitrogen, Science, 341, 1233-1235, https://doi.org/10.1126/science.1242266, 2013.

Oswald, R., Ermel, M., Hens, K., Novelli, A., Ouwersloot, H. G., Paasonen, P., Petäjä, T., Sipilä, M., Keronen, P., Bäck, J., Königstedt, R., Hosaynali Beygi, Z., Fischer, H., Bohn, B., Kubistin, D., Harder, H., Martinez, M., Williams, J., Hoffmann, T., Trebs, I., and Sörgel, M.: A comparison of HONO budgets for two measurement heights at a field station within the boreal forest in Finland, Atmos. Chem. Phys., 15, 799-813, https://doi.org/10.5194/acp-15-799-2015, 2015.

Pitts, J. N., Grosjean, D., Cauwenberghe, K. V., Schmid, J. P., and Fitz, D. R.: Photooxidation of aliphatic amines under simulated atmospheric conditions: formation of nitrosamines, nitramines, amides, and photochemical oxidant, Environ. Sci. Technol., 12, 946-953, https://doi.org/10.1021/es60144a009, 1978.

Bröske, R., Kleffmann, J., and Wiesen, P.: Heterogeneous conversion of NO_2 on secondary organic aerosol surfaces: A possible source of nitrous acid (HONO) in the atmosphere?, Atmos. Chem. Phys., 3, 469-474, https://doi.org/10.5194/acp-3-469-2003, 2003.

Rappenglück, B., Lubertino, G., Alvarez, S., Golovko, J., Czader, B., and Ackermann, L.: Radical precursors and related species from traffic as observed and modeled at an urban highway junction, J. Air Waste Manag. Assoc., 63, 1270-1286, https://doi.org/10.1080/10962247.2013.822438, 2013.

Reisinger, A. R.: Observations of HNO_2 in the polluted winter atmosphere: possible heterogeneous production on aerosols, Atmos. Environ., 34, 3865-3874, https://doi.org/10.1016/S1352-2310(00)00179-5, 2000.

Saastad, O. W., Ellermann, T., and Nielsen, C., J.: On the adsorption of NO and NO_2 on cold H_2O/H_2SO_4 surfaces, Geophys. Res. Lett., 20, 1191-1193, https://doi.org/10.1029/93GL01621, 1993.

Scharko, N. K., Martin, E. T., Losovyj, Y., Peters, D. G., and Raff, J. D.: Evidence for Quinone Redox Chemistry Mediating Daytime and Nighttime NO_2-to-HONO Conversion on Soil Surfaces, Environ. Sci. Technol., 51, 9633-9643, https://doi.org/10.1021/acs.est.7b01363, 2017.

Sleiman, M., Gundel, L. A., Pankow, J. F., Jacob III, P., Singer, B. C., and Destaillats, H.: Formation of carcinogens indoors by surface-mediated reactions of nicotine with nitrous acid, leading to potential thirdhand smoke hazards, P. Natl. Acad. Sci. USA, 107, 6576-6581, https://doi.org/10.1073/pnas.0912820107, 2010.

Sörgel, M., Regelin, E., Bozem, H., Diesch, J. M., Drewnick, F., Fischer, H., Harder, H., Held, A., Hosaynali-Beygi, Z., Martinez, M., and Zetzsch, C.: Quantification of the unknown HONO daytime source and its relation to NO_2, Atmos. Chem. Phys., 11, 10433-10447, https://doi.org/10.5194/acp-11-10433-2011, 2011.

Spataro, F., Ianniello, A., Esposito, G., Allegrini, I., Zhu, T., and Hu, M.: Occurrence of atmospheric nitrous acid in the urban area of Beijing (China), Sci. Total Environ., 447, 210-224, https://doi.org/10.1016/j.scitotenv.2012.12.065, 2013.

Spindler, G., Brüggemann, E., and Herrmann, H.: Nitrous acid (HNO_2) Concentration Measurements and Estimation of Dry Deposition over Grassland in Eastern Germany, Transactions on Ecology and Environment, 28, 223-227, 1999.

Stemmler, K., Ammann, M., Donders, C., Kleffmann, J., and George, C.: Photosensitized reduction of nitrogen dioxide on humic acid as a source of nitrous acid, Nature, 440, 195-198, https://doi.org/10.1038/nature04603, 2006.

~~Stemmler, K., Ndour, M., Elshorbany, Y., Kleffmann, J., D'Anna, B., George, C., Bohn, B., and Ammann, M.: Light induced conversion of nitrogen dioxide into nitrous acid on submicron humic acid aerosol, Atmos. Chem. Phys., 7, 4237-4248, https://doi.org/10.5194/acp-7-4237-2007, 2007.~~

Stutz, J., Alicke, B., Neftel, A.: Nitrous acid formation in the urban atmosphere: Gradient measurements of NO_2 and HONO over grass in Milan, Italy, J. Geophys. Res., 107, LOP 5-1-LOP 5-15, https://doi.org/10.1029/2001JD000390, 2002.

Stutz, J., Alicke, B., Ackermann, R., Geyer, A., Wang, S. H., White, A. B., Williams, E. J., Spicer, C. W., and Fast, J. D.: Relative humidity dependence of HONO chemistry in urban areas, J. Geophys. Res.-Atmos., 109, D03307, https://doi.org/10.1029/2003JD004135, 2004a.

Stutz, J., Alicke, B., Ackermann, R., Geyer, A., White, A., and Williams, E.: Vertical profiles of NO_3, N_2O_5, O_3, and NO_x in the nocturnal boundary layer: 1. Observations during the Texas Air Quality Study 2000, J. Geophys.l Res.-Atmos., 109, D12306, https://doi.org/10.1029/2003JD004209, 2004b.

Su, H., Cheng, Y. F., Cheng, P., Zhang, Y. H., Dong, S. F., Zeng, L. M., Wang, X. S., Slanina, J., Shao, M., and Wiedensohler, A.: Observation of nighttime nitrous acid (HONO) formation at a non-urban site during PRIDE-PRD2004 in China, Atmos. Environ., 42, 6219-6232, https://doi.org/10.1016/j.atmosenv.2008.04.006, 2008a.

Su, H., Cheng, Y. F., Shao, M., Gao, D. F., Yu, Z. Y., Zeng, L. M., Slanina, J., Zhang, Y. H., and Wiedensohler, A.: Nitrous acid (HONO) and its daytime sources at a rural site during the 2004 PRIDE-PRD experiment in China, J. Geophys. Res., 113, D14312, https://doi.org/10.1029/2007JD009060, 2008b.

Su, H., Cheng, Y. F., Oswald, R., Behrendt, T., Trebs, I., Meixner, F. X., Andreae, M. O., Cheng, P., Zhang, Y. H., and Pöschl, U.: Soil nitrite as a Source of Atmospheric HONO and OH Radicals, Science, 333, 1616-1618, https://doi.org/10.1126/science.1207687, 2011.

Sun, Y. L., Wang, Z. F., Fu, P. Q., Yang, T., Jiang, Q., Dong, H. B., Li, J., and Jia, J. J.: Aerosol composition, sources and processes during wintertime in Beijing, China, Atmos. Chem. Phys., 13, 4577-4592, https://doi.org/10.5194/acp-13-4577-2013, 2013.

Sun, Y. L., Jiang, Q., Wang, Z. F., Fu, P. Q., Li, J., Yang, T., and Yin, Y.: Investigation of the sources and evolution processes of severe haze pollution in Beijing in January 2013, J. Geophys. Res. Atmos., 119, 4380-4398, https://doi.org/10.1002/2014JD021641, 2014.

Tan, Z. F., Fuchs, H., Lu, K. D., Hofzumahaus, A., Bohn, B., Broch, S., Dong, H. B., Gomm, S., Häseler, R., He, L.

Y., Holland, F., Li, X., Liu, Y., Lu, S. H., Rohrer, F., Shao, M., Wang, B. L., Wang, M., Wu, Y. S., Zeng, L. M., Zhang, Y. S., Wahner, A., and Zhang, Y. H.: Radical chemistry at a rural site (Wangdu) in the North China Plain: observation and model calculations of OH, HO_2 and RO_2 radicals, Atmos. Chem. Phys., 17, 663–690, https://doi.org/10.5194/acp-17-663-2017, 2017.

Tang, K., Qin, M., Duan, J., Fang, W., Meng, F. H., Liang, S. X., Xie, P. H., Liu, J. G., Liu, W. Q., Xue, C. Y., and Mu, Y. J.: A dual dynamic chamber system based on IBBCEAS for measuring fluxes of nitrous acid in agricultural fields in the North China Plain, Atmos. Environ., 196, 10-19, https://doi.org/10.1016/j.atmosenv.2018.09.059, 2019.

Tang, Y., An, J., Wang, F., Li, Y., Qu, Y., Chen, Y., and Lin, J.: Impacts of an unknown daytime HONO source on the mixing ratio and budget of HONO, and hydroxyl, hydroperoxyl, and organic peroxy radicals, in the coastal regions of China, Atmos. Chem. Phys., 15, 9381-9398, https://doi.org/10.5194/acp-15-9381-2015, 2015.

Tong, S. R., Hou, S. Q., Zhang, Y., Chu, B. W., Liu, Y. C., He, H., Zhao, P. S., and Ge, M. F.: Exploring the nitrous acid (HONO) formation mechanism in winter Beijing: direct emissions and heterogeneous production in urban and suburban areas, Faraday Discuss., 189, 213-230, https://doi.org/10.1039/c5fd00163c, 2016.

Trinh, H. T., Imanishi, K., Morikawa, T., Hagino, H., and Takenaka N.: Gaseous nitrous acid (HONO) and nitrogen oxides (NO_x) emission from gasoline and diesel vehicles under real-world driving test cycles, J. Air Waste Manage. Assoc., 67, 412-420, https://doi.org/10.1080/10962247.2016.1240726, 2017.

VandenBoer, T. C., Brown, S. S., Murphy, J. G., Keene, W. C., Young, C. J., Pszenny, A. A. P., Kim, S., Warneke, C., de Gouw, J. A., Maben, J. R., Wagner, N. L., Riedel, T. P., Thornton, J. A., Wolfe, D. E., Dubé, W. P., Öztürk, F., Brock, C. A., Grossberg, N., Lefer, B., Lerner, B., Middlebrook, A. M., and Roberts, J. M.: Understanding the role of the ground surface in HONO vertical structure: High resolution vertical profiles during NACHTT-11, J. Geophy. Res.- Atmos., 118, 10155-110171, https://doi.org/10.1002/jgrd.50721, 2013.

Villena, G., Kleffmann, J., Kurtenbach, R., Wiesen, P., Lissi, E., Rubio, M. A., Croxatto, G., and Rappenglück, B.: Vertical gradients of HONO, NO_x and O_3 in Santiago de Chile, Atmos. Environ., 45, 3867-3873, https://doi.org/10.1016/j.atmosenv.2011.01.073, 2011.

Vogel, B., Vogel H., Kleffmann, J., and Kurtenbach, R.: Measured and simulated vertical profiles of nitrous acid—Part II. Model simulations and indications for a photolytic source, Atmos. Environ., 37, 2957-2966, https://doi.org/10.1016/S1352-2310(03)00243-7, 2003.

Wang, H. C., Lu, K. D., Chen, X. R., Zhu, Q. D., Wu, Z. J., Wu, Y. S., and Sun, K.: Fast particulate nitrate formation via N_2O_5 uptake aloft in winter in Beijing, Atmos. Chem. Phys., 18, 10483-10495, https://doi.org/10.5194/acp-18-10483-2018, 2018.

Wang, J. Q., Zhang, X. S., Guo, J., Wang, Z. W., and Zhang, M. G.: Observation of nitrous acid (HONO) in Beijing, China: Seasonal variation, nocturnal formation and daytime budget, Sci. Total Environ., 587-588, 350-359, https://doi.org/10.1016/j.scitotenv.2017.02.159, 2017.

Wang, S. S., Zhou, R., Zhao, H., Wang, Z. R., Chen, L. M., and Zhou, B.: Long-term observation of atmospheric nitrous acid (HONO) and its implication to local NO_2 levels in Shanghai, China, Atmos. Environ., 77, 718-724, https://doi.org/10.1016/j.atmosenv.2013.05.071, 2013.

Wong, K. W., Oh, H. -J., Lefer, B. L., Rappenglück, B., and Stutz, J.: Vertical profiles of nitrous acid in the nocturnal urban atmosphere of Houston, TX, Atmos. Chem. Phys., 11, 3595-3609, https://doi.org/10.5194/acp-11-3595-2011, 2011.

Wong, K. W., Tsai, C., Lefer, B., Haman, C., Grossberg, N., Brune, W. H., Ren, X., Luke, W., and Stutz, J.: Daytime HONO vertical gradients during SHARP 2009 in Houston, TX, Atmos. Chem. Phys., 12, 635-652, https://doi.org/10.5194/acp-12-635-2012, 2012.

Wong, K. W., Tsai, C., Lefer, B., Grossberg, N., and Stutz, J.: Modeling of daytime HONO vertical gradients

during SHARP 2009, Atmos. Chem. Phys., 13, 3587-3601, https://doi.org/10.5194/acp-13-3587-2013, 2013.
Xie, C. H., Xu, W. Q., Wang, J. F., Wang, Q. Q., Liu, D. T., Tang, G. Q., Chen, P., Du, W., Zhao, J., Zhang, Y. J., Zhou, W., Han, T. T., Bian, Q. Y., Li, J., Fu, P. Q., Wang, Z. F., Ge, X. L., Allan, J., Coe, H., and Sun, Y. L.: Vertical characterization of aerosol optical properties and brown carbon in winter in urban Beijing, China, Atmos. Chem. Phys., 19, 165–179, https://doi.org/10.5194/acp-19-165-2019, 2019.
Xu, W. Q., Sun, Y. L., Wang, Q. Q., Zhao, J., Wang, J. F., Ge, X. L., Xie, C. H., Zhou, W., Du, W., Li, J., Fu, P. Q., Wang, Z. F., Worsnop, D. R., and Coe, H.: Changes in Aerosol Chemistry From 2014 to 2016 in Winter in Beijing: Insights From High-Resolution Aerosol Mass Spectrometry, J. Geophys. Res.- Atmos., 124, 1132-1147, https://doi.org/10.1029/2018JD029245, 2019.
Xu, Z., Wang, T., Wu, J. Q., Xue, L. K., Chan, J., Zha, Q., Z., Zhou, S. Z., Louie, P. K. K., and Luk, C. W. Y.: Nitrous acid (HONO) in a polluted subtropical atmosphere: Seasonal variability, direct vehicle emissions and heterogeneous production at ground surface, Atmos. Environ., 106, 100-109, https://doi.org/10.1016/j.atmosenv.2015.01.061, 2015.
Yang, Q., Su, H., Li, X., Cheng, Y. F., Lu, K. D., Cheng, P., Gu, J. W., Guo, S., Hu, M., Zeng, L. M., Zhu, T., and Zhang, Y. H.: Daytime HONO formation in the suburban area of the megacity Beijing, China, Sci. China Chem., 57, 1032-1042, https://doi.org/10.1007/s11426-013-5044-0, 2014.
Ye, C. X., Zhang, N., Gao, H. L., and Zhou, X. L.: Photolysis of Particulate Nitrate as a Source of HONO and NO_x, Environ. Sci. Technol., 51, 6849-6856, https://doi.org/10.1021/acs.est.7b00387, 2017.
Ye, C. X., Zhou, X. L., Pu, D., Stutz, J., Festa, J., Spolaor, M., Tsai, C., Cantrell, C., Mauldin III, R. L., Weinheimer, A., Hornbrook, R. S., Apel, E. C., Guenther, A., Kaser, L., Yuan, B., Karl, T., Haggerty, J., Hall, S., Ullmann, K., Smith, J., and Ortega, J.: Tropospheric HONO distribution and chemistry in the southeastern US, Atmos. Chem. Phys., 18, 9107-9120, https://doi.org/10.5194/acp-18-9107-2018, 2018.
Yu, Y., Galle, B., Panday, A., Hodson, E., Prinn, R., and Wang, S.: Observations of high rates of NO_2-HONO conversion in the nocturnal atmospheric boundary layer in Kathmandu, Nepal, Atmos. Chem. Phys., 9, 6401-6415, https://doi.org/10.5194/acp-9-6401-2009, 2009.
Zhang, N., Zhou, X. L., Shepson, P. B., Gao, H. L., Alaghmand, M., and Stirm, B.: Aircraft measurement of HONO vertical profiles over a forested region, Geophys. Res. Lett., 36, L15820, https://doi.org/10.1029/2009GL038999, 2009.
Zhang, R., Wang, G., Guo, S., Zamora, M. L., Ying, Q., Lin, Y., Wang. W., Hu, M., and Wang, Y.: Formation of Urban Fine Particulate Matter, Chem. Rev., 115, 3303-3855, https://doi.org/10.1021/acs/chemrev.5b00067, 2015.
Zhang, W. Q., Tong, S. R., Ge, M. F., An, J. L., Shi, Z. B., Hou, S. Q., Xia, K. H., Qu, Y., Zhang, H. X., Chu, B. W., Sun, Y. L., and He, H.: Variations and sources of nitrous acid (HONO) during a severe pollution episode in Beijing in winter 2016, Sci. Total Environ., 648, 253-262, https://doi.org/10.1016/j.scitotenv.2018.08.133, 2018.

Table

Table 1. Classification of the meteorological conditions and corresponding concentrations of NR-PM_1, NO_2 and HONO from ~~7 to 12~~ December 7^{th} to 12^{th}.

Time period	Weather condition	NR-PM_1 ($\mu g \cdot m^{-3}$)	HONO (ppb)	NO_2 (ppb)	WS ($m \cdot s^{-1}$)	WD	*T* (°C)	RH (%)
7 Dec–8 Dec (10:00)	Haze (E1)	30–184	1.49–7.59	24.91–65.48	0.03–1.95	NW-ESE[a]	1.6–9.3	36–82
8 Dec (10:00)–11 Dec	Clean (C2)	3–97	0.05–3.75	3.33–47.84	0.01–6.24	NE-NW	-2.4–9.1	16–53
11 Dec–12 Dec	Haze (E3)	69–217	1.54–5.51	38.58–66.57	0.02–1.81	NE-NW	-1.6–6.9	40–69

[a] NE: Northeast; ESE: East-southeast; NW: Northwest;

Table 2. The nocturnal gradient of HONO and NO_2 throughout the vertical measurements. The linear least squares regression slope and correlation coefficient of HONO and NO_2 to altitude identified in each vertical profile measurement.

Date	Time period (hh:mm, LT)	Gradient-HONO ($ppt\ m^{-1}$)	R^2	Gradient-NO_2 ($ppt\ m^{-1}$)	R^2
9/12/2016	22:42–23:06	-4.49 ± 0.31	0.90	-14.38 ± 1.62	0.77
9/12/2016	23:15–23:40	-4.35 ± 0.70	0.62	-16.54 ± 1.85	0.77
10/12/2016	22:36–23:01	-1.08 ± 0.49	0.15	-2.97 ± 1.53	0.11
10/12/2016	23:01–23:25	-3.61 ± 0.50	0.60	-7.59 ± 1.24	0.62
11/12/2016	22:35–23:00	-6.91 ± 0.33	0.95	-9.53 ± 1.01	0.79
11/12/2016	23:04–23:29	-0.03 ± 0.43	0.0003	-5.32 ± 0.80	0.67
12/12/2016	00:00–00:26	0.23 ± 0.36	0.02	-5.21 ± 0.79	0.65
12/12/2016	00:45–01:09	-1.79 ± 0.28	0.64	-5.28 ± 0.84	0.63

Table 3. Emission ratios (△HONO/△NO_x) of the fresh direct emission plumes.

Date	Local Time	R^2	△NO/△NO_x	△HONO/△NO_x (%)
15/11/2016	18:05–18:15	0.97	0.99	1.07
16/11/2016	20:50–21:10	0.83	0.96	0.92
24/11/2016	20:50–21:10	0.92	1.13	1.12
26/11/2019	02:10–02:40	0.94	0.94	1.31
26/11/2016	22:15–22:30	0.95	1.00	1.73
28/11/2019	04:40–04:55	0.87	0.85	0.78
29/11/2016	03:30–03:50	0.95	0.98	1.60
2/12/2016	23:40–23:55	0.95	1.01	1.67
7/12/2016	02:25–02:35	0.87	0.90	1.67
10/12/2016	01:00–01:25	0.84	0.95	1.43
10/12/2016	02:40–02:55	0.86	0.93	0.79

Figures

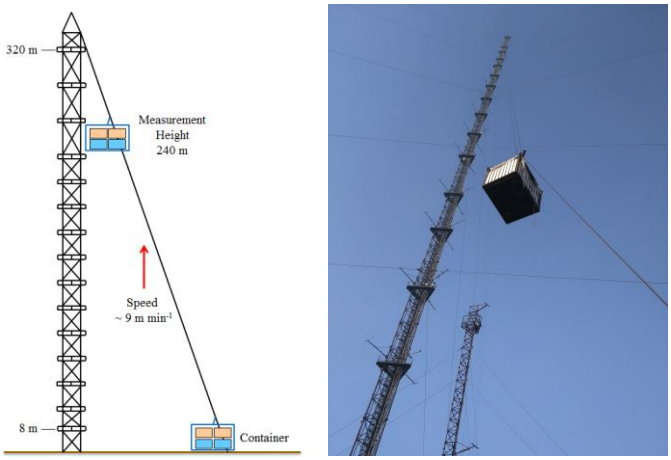

Figure 1. The Beijing 325-m meteorological tower (BMT) at the Institute of Atmospheric Physics (IAP).

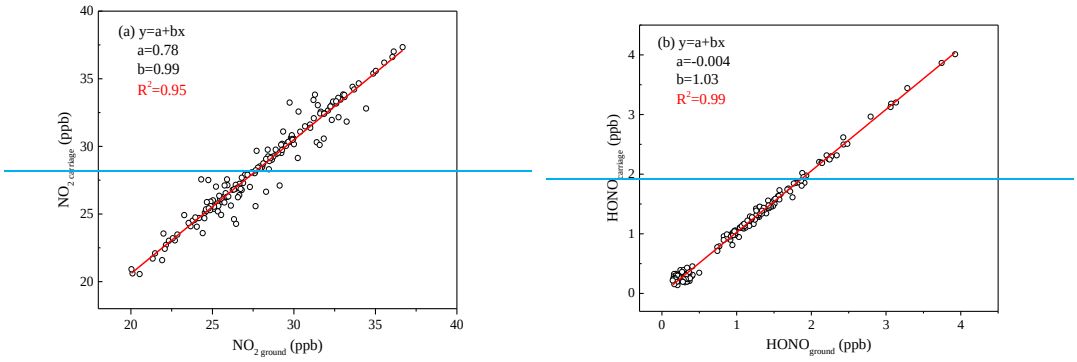

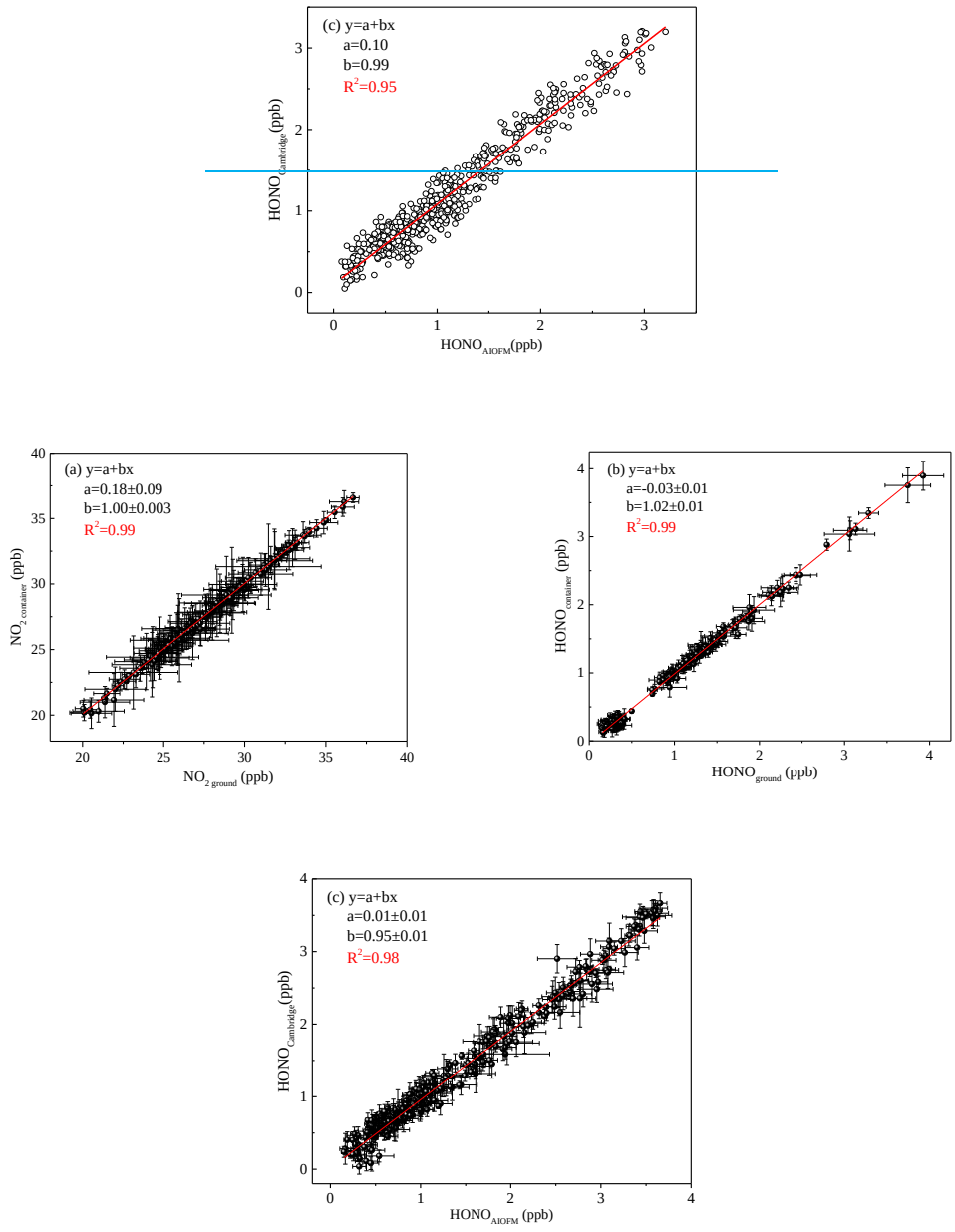

Figure 2. (a) Correlation of NO_2 concentration was measured ~~by~~ using the two IBBCEAS instruments; (b) correlation of HONO concentration was measured ~~by~~ using the two IBBCEAS instruments; (c) an inter-comparison between the IBBCEAS of Cambridge University and the IBBCEAS of the Anhui Institute of Optics and Fine Mechanics (AIOFM). The solid lines (red lines) show the orthogonal linear least squares regression between the two IBBCEAS instruments.

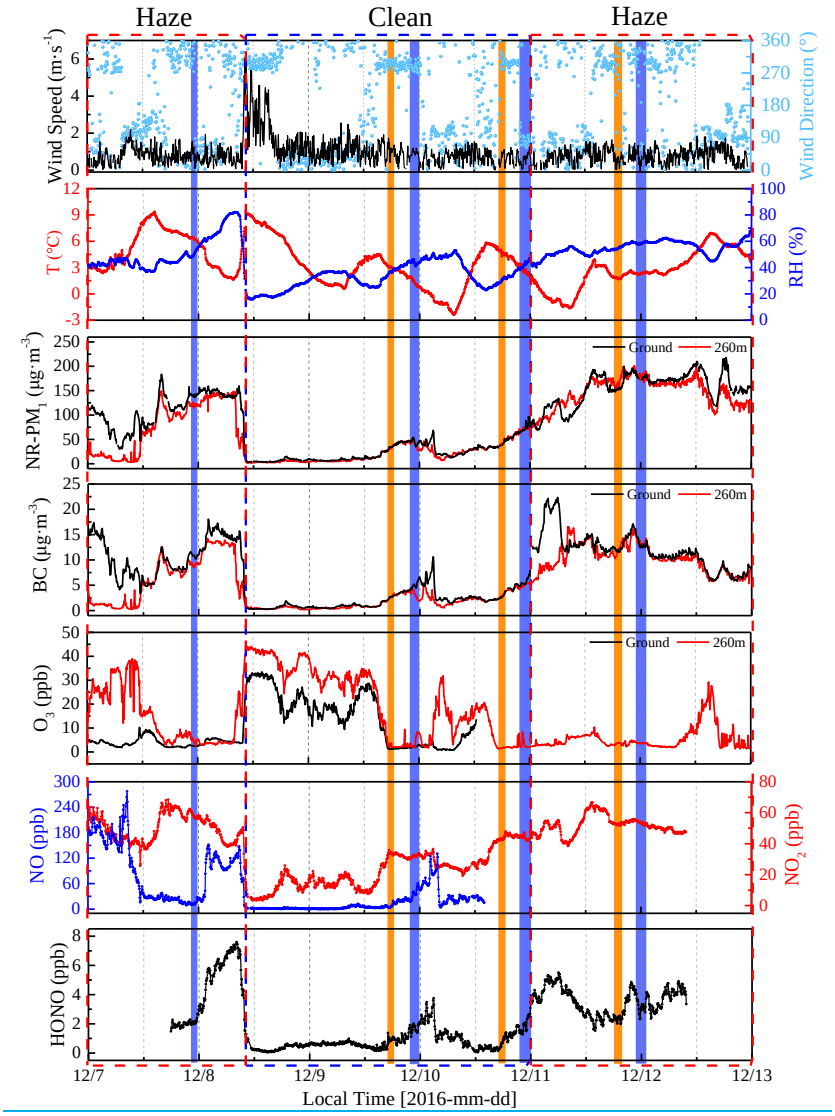
Haze
Clean
Haze
Wind Speed (m·s-1)
Wind Direction (°)
T (°C)
RH (%)
NR-PM1 (μg·m-3)
BC (μg·m-3)
O3 (ppb)
NO (ppb)
NO2 (ppb)
HONO (ppb)
Ground
260m
12/7
12/8
12/9
12/10
12/11
12/12
12/13
Local Time [2016-mm-dd]

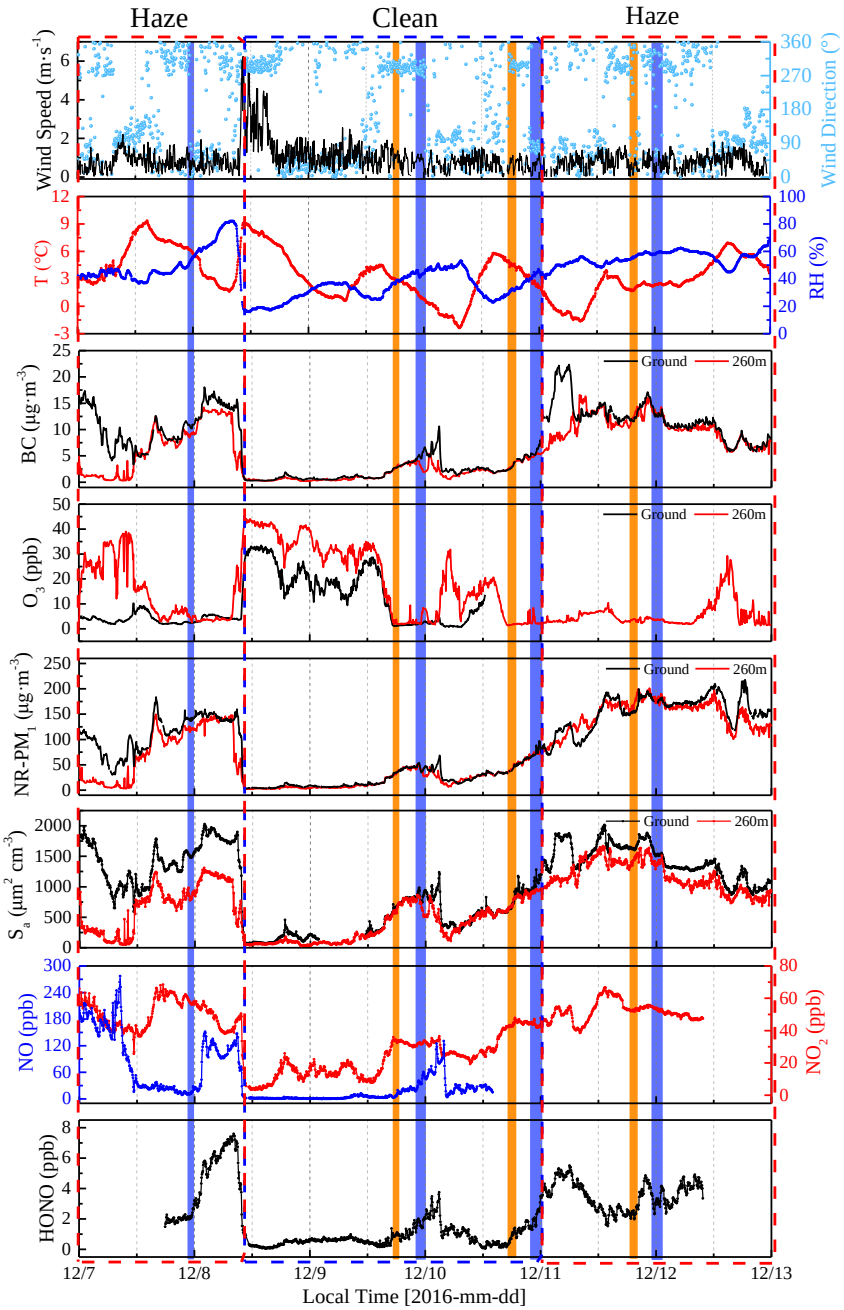

Figure 3. Time-series of wind speed (WS) and direction (WD), temperature (*T*), relative humidity (RH), ~~NR-PM$_1$,~~ BC, O_3, NR-PM$_1$, aerosol surface area (S_a), NO, NO_2, and HONO from ~~7 to 12~~ December 7th to 12th 2016 at the IAP-Tower Division in Beijing, China. The shaded region represents the eight vertical measurements (Table S1). The orange shaded region represents the vertical measurements after sunset, and the violet shaded region represents the vertical measurements at night and midnight.

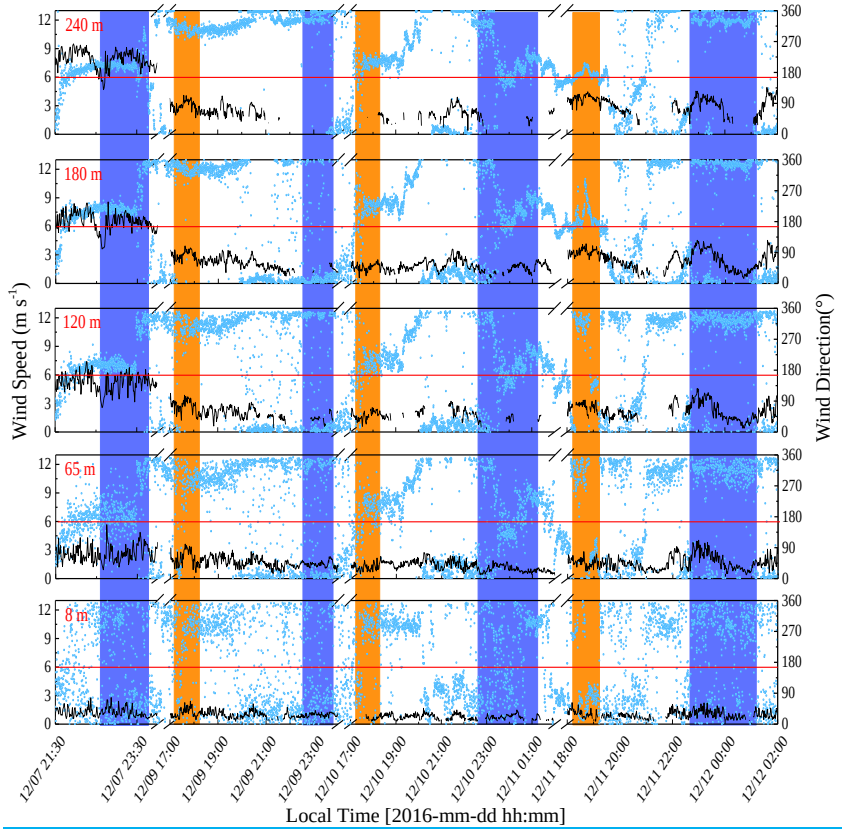

Figure 4. Temporal variations of the wind speed at fixed heights on the meteorological tower (8, 65, 120, 180, and 240 m) throughout the measurement period. Vertical measurements were conducted after sunset (orange shaded regions) and during nighttime (violet shaded regions). The red line denoted the wind speed is 6 m·s^{-1}.

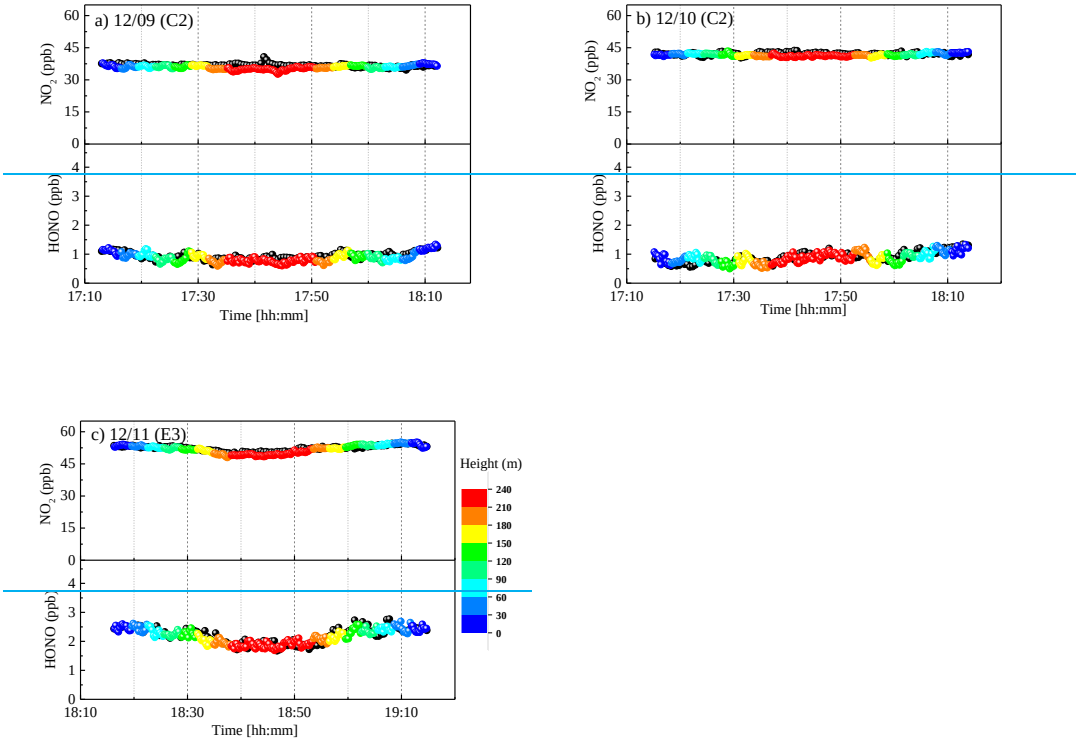

Figure 5. Temporal variations in the mixing ratios of HONO and NO_2 at ground level (black solid circles) and in the container (colored solid circles) during (a, b) the clean episode (C2) and (c) the haze episode (E3). The vertical measurements of HONO and NO_2 are color code by height.

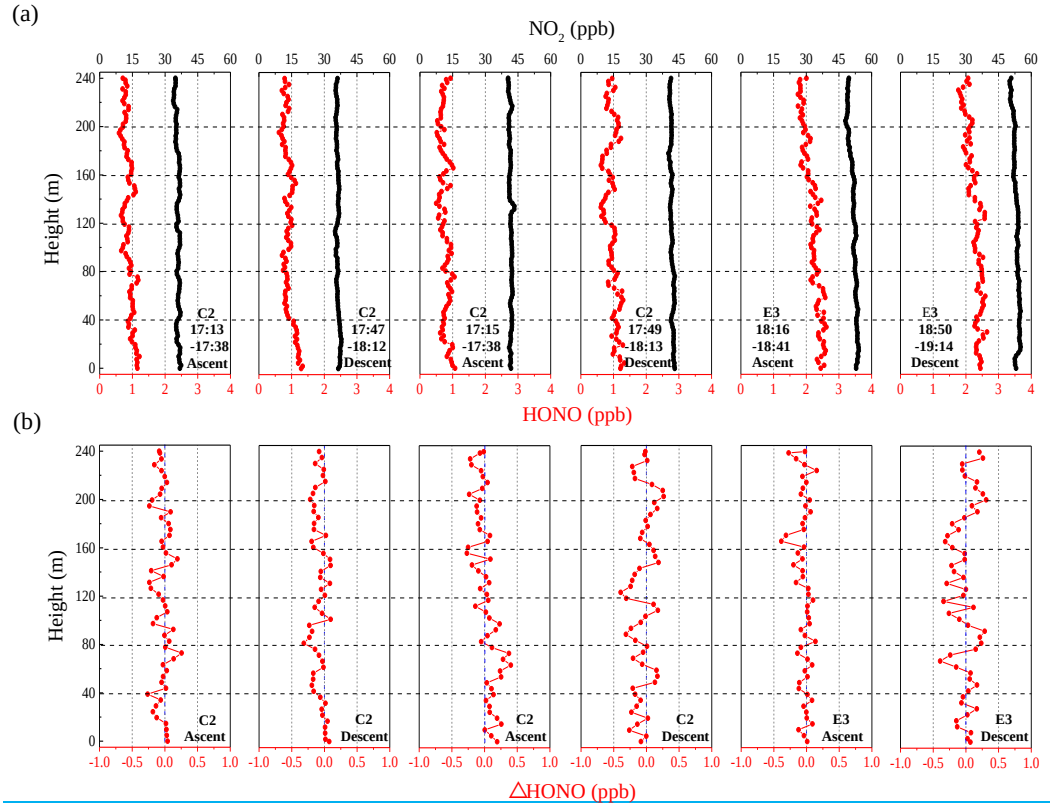

Figure 6. (a) Vertical profiles of HONO (red solid line) and NO_2 (black solid line) after sunset during the clean episode (C2) and the haze episode (E3). Each vertical measurement includes the ascent process and the descent process. The time on each plot corresponds to the measurement time of the vertical profile during the ascent or descent process. (b) Vertical profiles of △HONO (red dotted line) during C2 and E3 are also shown.

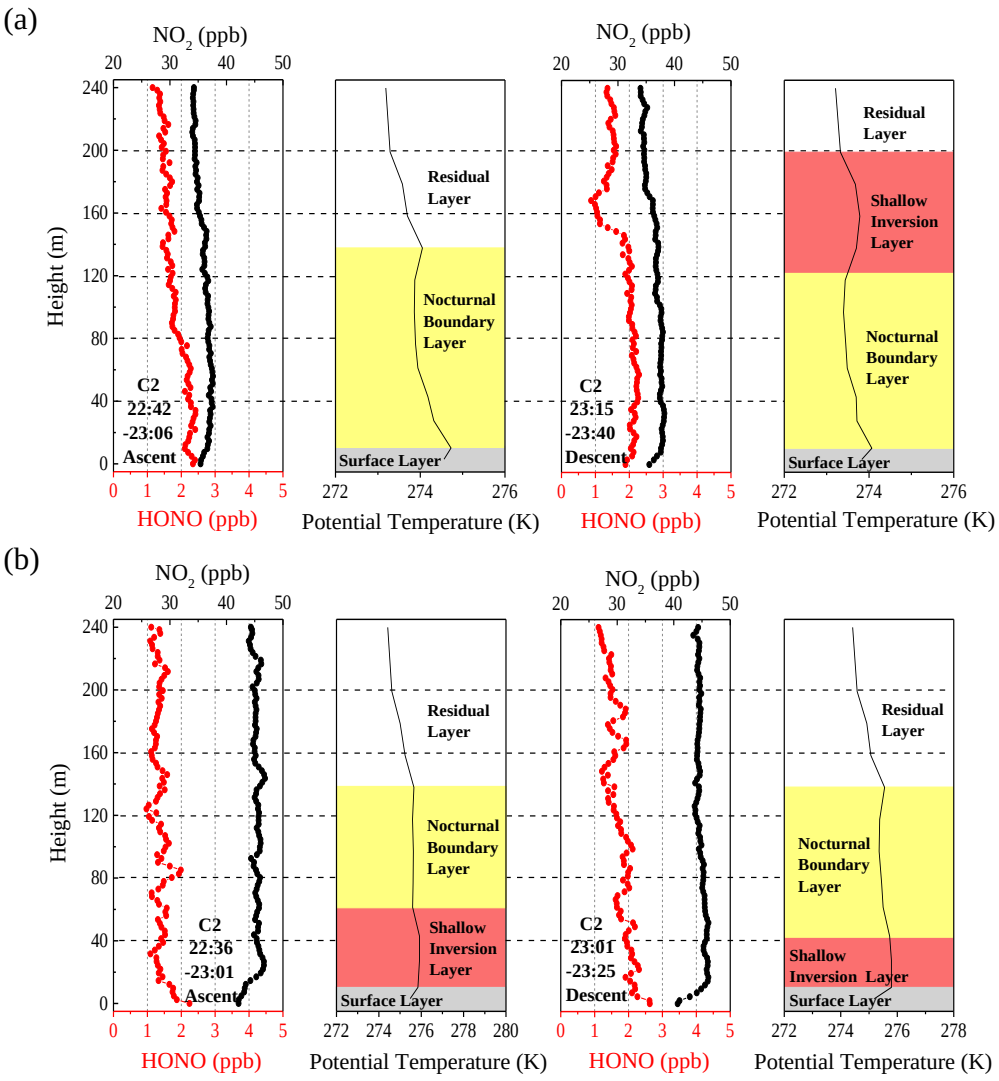

Figure ~~7~~ 4. Nocturnal vertical profiles of HONO, NO_2, and the potential temperatures during the ascent and descent of the container on the (a) 9th and (b) 10th of December. The time in the figure corresponds to the measurement time of the vertical profile of the HONO and NO_2. The different ~~colors~~ colored shaded region indicates the nocturnal small-scale stratification (surface layer, nocturnal boundary layer, shallow inversion layer, and residual layer). The heights of the surface layer, the shallow inversion layer, the nocturnal boundary layer, and the residual layer are denoted by grey shaded regions, pink shaded regions, yellow shaded regions, and white shaded regions, respectively.

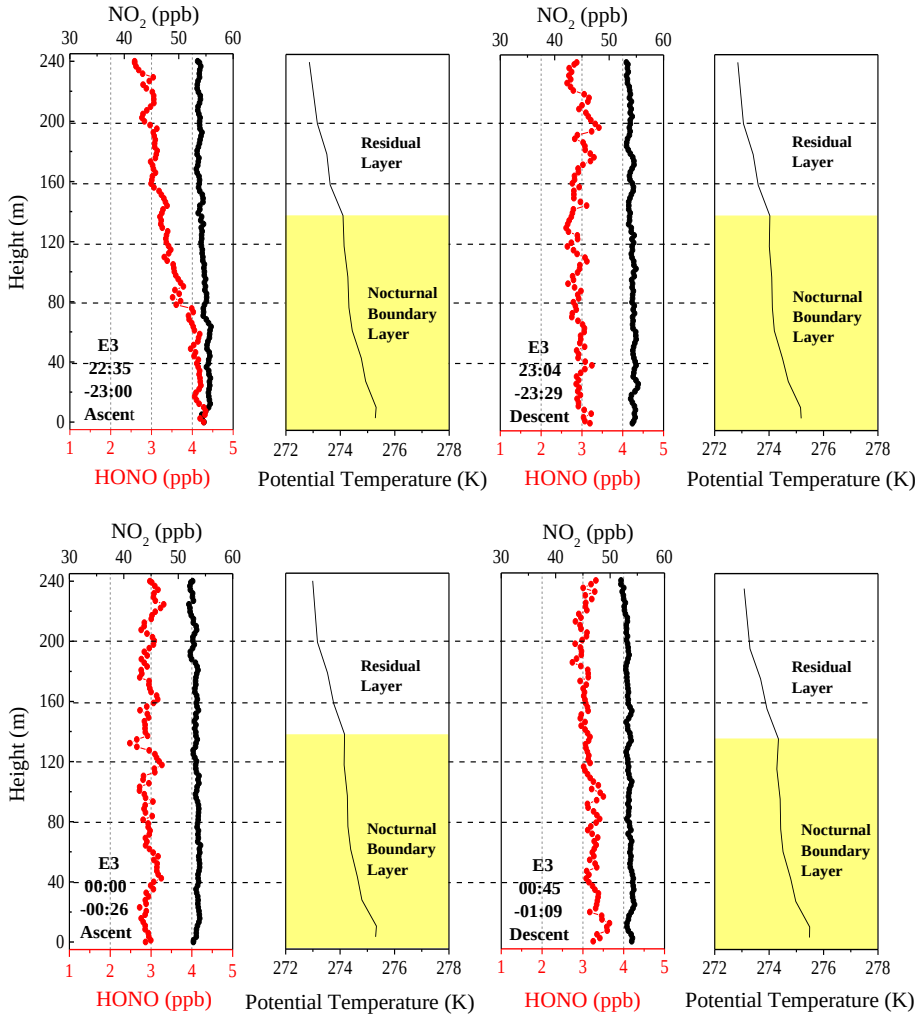

Figure ~~8~~ 5. Vertical profiles of HONO and NO_2 on the night of ~~11~~ December 11th and midnight of ~~12~~ December 12th. The potential temperature profiles indicate nocturnal small-scale stratification (a nocturnal boundary layer and a residual layer). The height of the nocturnal boundary layer (NBL) is denoted by the yellow shaded region. The time in the figure corresponds to the measurement time of the vertical profiles of HONO and NO_2.

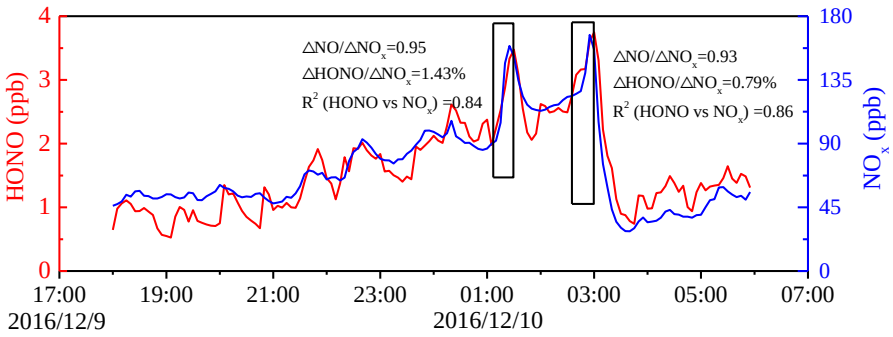

Figure 6. Temporal variation of nocturnal HONO and NO_x on December 9th to 10th, 2016. The HONO emission ratios were estimated using data collected in the black frame.

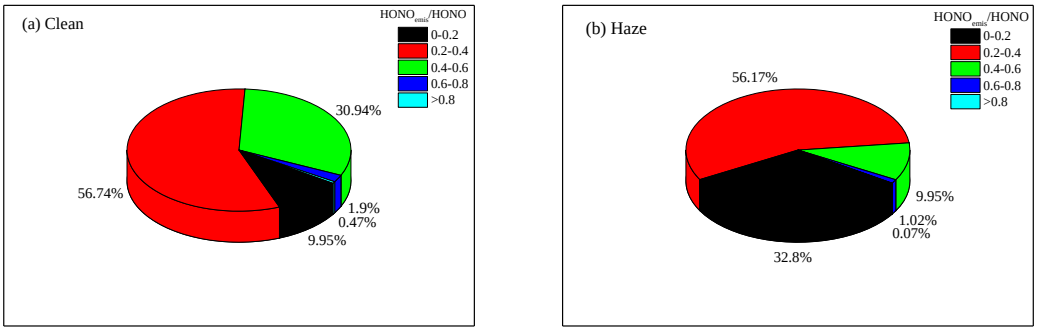

Figure 7. The nocturnal $HONO_{emis}$/HONO ratios frequency distribution during (a) clean and (b) haze episodes.

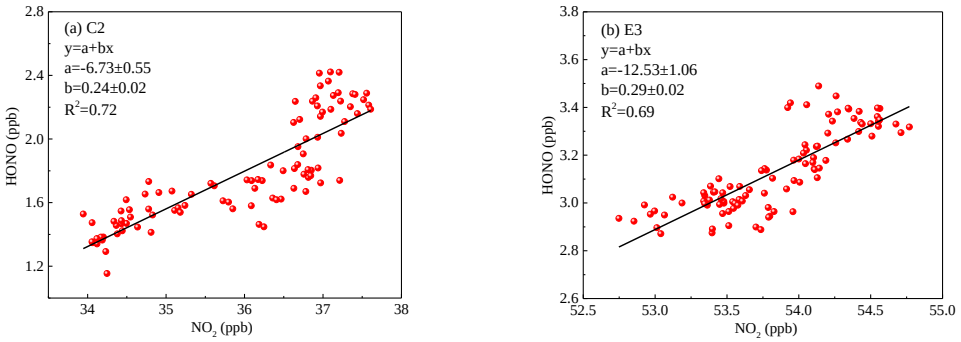

Figure ~~9~~ 8. The correlation of the vertical profiles between HONO and NO_2 during (a) the clean episode (C2) and (b) the haze episode (E3) using a linear least squares regression fit.

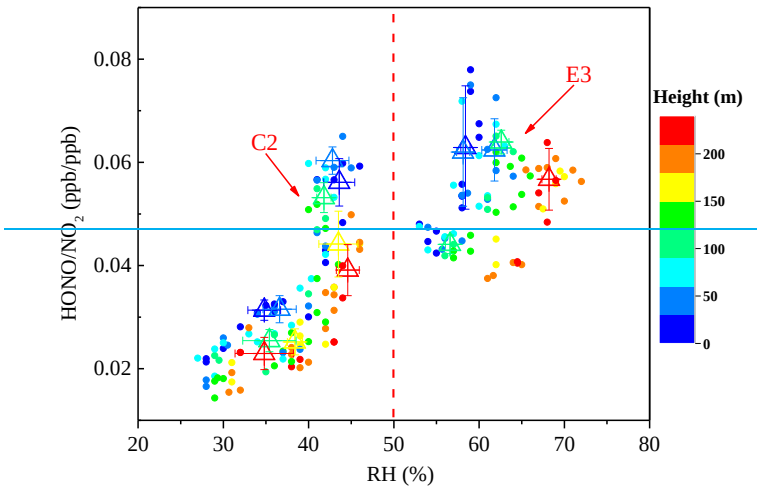

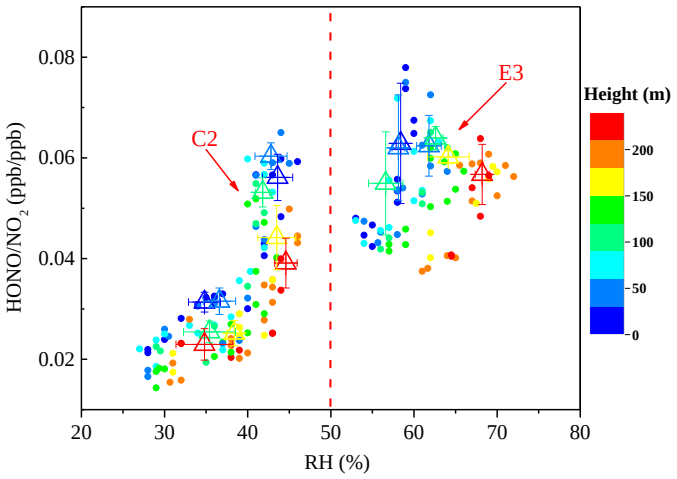

Figure ~~10~~ 9. Scatter plot of HONO/NO_2 against RH of all vertical profiles during the clean episode (C2) and the haze episode (E3). The HONO/NO_2 ratio is color coded by the heights. Triangles are the average of the first five HONO/NO_2 values in each 10% RH interval at different height intervals (8–65 m, 65–120 m, 120–180 m, and 180–240 m).

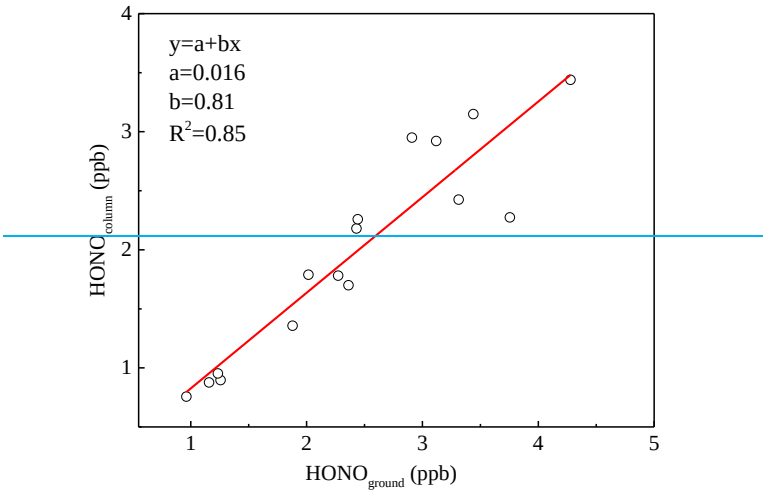

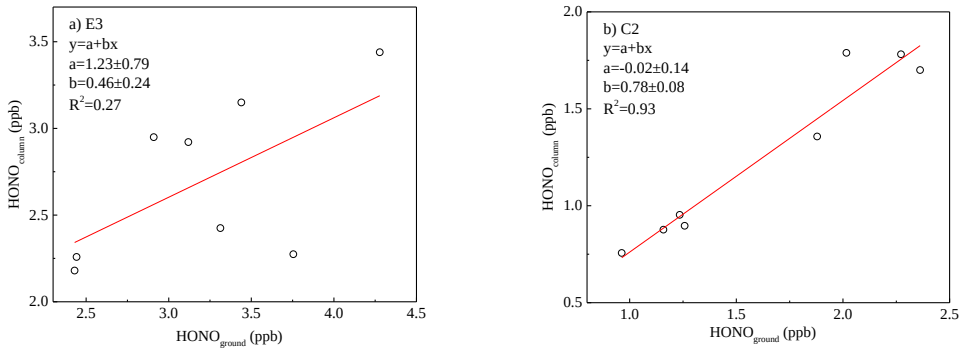

Figure ~~11~~ 10. Orthogonal linear least squares correlation between the ~~integrated~~ column average concentration of HONO (~~10–240 m~~ the average HONO column concentration from 10 to 240 m) and HONO measured from the ground level to 10 m above the ground level (AGL). Column values ~~of vertical measurements~~ were calculated for ~~9 to 12 December~~ (a) E3 and (b) C2.

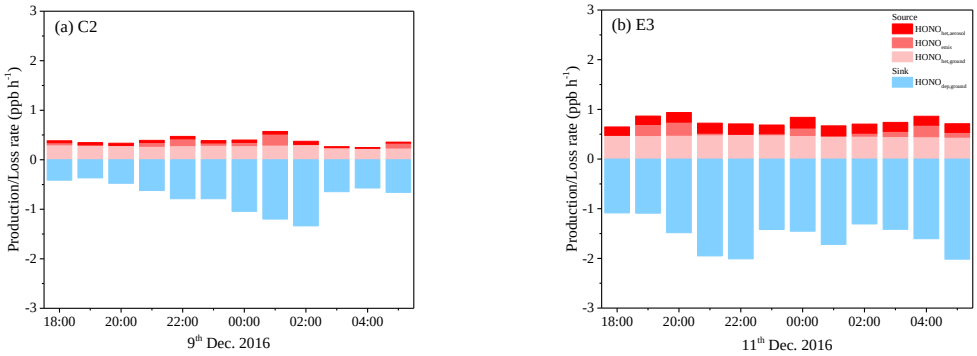

Figure 11. Separated contributions of production and loss terms (colored bars) of HONO on (a) the 9th (C2) and (b) 11th (E3) of December 2016. An upper limit uptake coefficient for NO_2 was adopted to calculate the HONO production rate on aerosol surface.